

Poster Abstracts: Clinical MRI—Ischemic Heart Disease

221. Gadolinium Pharmacokinetics of Viable and Injured Myocardium: Implications for MR Viability Imaging

James W. Goldfarb, PhD, Sunil T. Mathew, MD, Nathaniel Reichek, MD. *Research and Education, St Francis Hospital, Roslyn, NY, USA.*

Introduction: Recent studies have shown that images obtained after the administration of gadolinium-contrast material can accurately distinguish between reversible and irreversible myocardial ischemic injury. Other studies have shown discrepancies between enhancement region size with different imaging parameters and imaging times. Studies have been performed to dynamically measure contrast agent concentrations over time in blood and several organs, but those involving the myocardium have only provided a limited number of temporal measurements (e.g. 10 and 20 min).

Purpose: In this study, we sought to develop and show the feasibility of a method capable of dynamically measuring contrast agent concentrations in the blood pool of the left ventricle, injured myocardium and normal myocardium over a one hour time period. Recommendations for the optimal time to commence imaging after contrast agent administration and the necessary changes in inversion time for normal myocardial nulling can be specified. Also, the best sequence type (FLASH, True-FISP, phase-sensitive acquisition) can be chosen based on contrast-to-noise ratio predictions. Lastly, new information capable of discriminating between acute and chronic infarcts may be contained in the wash-in and wash-out data over an extended time period.

Methods: Eleven subjects (age: mean=63 years; range=43–84) with known chronic myocardial infarcts (mean age of infarct: 7 years) who had undergone a

previous positive MR or SPECT viability examination participated in the study. Imaging was performed using a 1.5T clinical scanner (Magnetom Sonata). A 2D multi-phase inversion recovery slice-selective segmented True-FISP sequences was used (TR=2.5, TE=1.1, FA=50, BW=965 Hz/pixel, voxel size=2.5 × 1.8 × 8.0 mm³). A single slice was positioned based on the previous MR/SPECT study to include regions with both injured and normal myocardium. Each breath-hold yielded 19–24 images with increasing inversion times at intervals of 37 ms. 0.2 mmol/kg of gadodiamide (Omniscan) was injected at 2 ml/s followed by a 15 ml saline flush. Imaging commenced directly after the administration of the contrast agent and continued for one hour with acquisitions occurring approximately every minute.

Images were transferred to a stand-alone SUN workstation and a custom JAVA computer program was used to segment the myocardial regions. For each

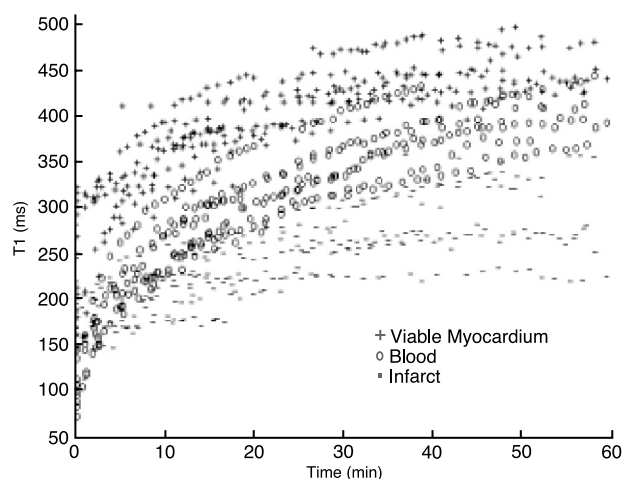


Figure 1. T1 versus time.

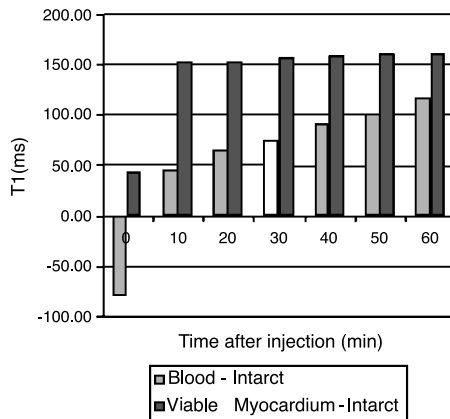


Figure 2. T1 difference. (View this art in color at www.dekker.com.)

acquisition, epicardial and endocardial myocardial borders were hand drawn and a signal intensity threshold was set for each image to segment normal and injured myocardium. The T1 for both types of myocardial regions and the left ventricular (LV) blood pool was calculated using a multidimensional unconstrained nonlinear minimization (Nelder-Mead) applied to the IR True-FISP signal intensity equation.

Results: Imaging was successfully performed in each case, but was terminated early in several cases. (Imaging time: mean=46 min range=20–60 min). Each breath-hold yielded a number of images with consecutive inversion times demonstrating the infarct. Quantitative results for all subjects are plotted in Figure 1. In five cases, the area of infarction could be identified before contrast administration as has been previously reported. T1 differences between the infarct, neighboring myocardium and blood are summarized in Figure 2.

Conclusions: Myocardial contrast-enhancement can be monitored with a temporal resolution of 1 minute. The use of a multi-phase IR True-FISP technique yields multiple images with increasing inversion times capable of calculating the T1 of regions in the heart. Images were of sufficient quality to locate and segment enhancing regions and calculate inversion times for optimal nulling of viable myocardial tissue.

After a delay of approximately 10 minutes, gadolinium concentrations continue to reduce in the blood and viable myocardium creating increased image contrast with infarcted myocardium. Data suggests that improved contrast between necrotic tissue and the LV blood pool is achieved at imaging times after 30 minutes. When data is available in a larger population, optimization can be performed with respect to contrast agent dose, imaging parameters and sequence types.

222. Myocardial Viability Assessment by Contrast-Enhanced MRI Compared to Low-Dose Dobutamine Stress Echocardiography

Peter Hunold, MD,¹ Holger Eggebrecht, MD,² Thomas W. Schlosser, MD,¹ Kai-Uwe Waltering, MD,¹ Thomas Bartel, MD,² Jörg F. Debatin, MD,¹ Jörg Barkhausen, MD.¹ ¹Department for Diagnostic and Interventional Radiology, University Hospital, Essen, Germany, ²Department of Cardiology, University Hospital, Essen, Germany.

Introduction: The presence of viable myocardium is a prerequisite for the recovery of regional and global function after revascularization in patients with ischemic heart disease and dysfunction of the left ventricle (LV). Different techniques have been applied to characterize viable myocardium and scar after infarction. Low-dose Dobutamine stress echocardiography has been used during the last decade, however, positron emission tomography using [¹⁸F]-FDG as a tracer has today been considered the standard of reference in this topic. In recent years, contrast-enhanced MR imaging using the "late enhancement" concept has emerged to offer new opportunities in viability assessment and seems to be superior to PET.

Purpose: To compare "late enhancement" (LE) in contrast-enhanced MRI with low-dose Dobutamine stress echocardiography (LD-DSE) in the characterization of viable myocardium in patients with CAD and impaired LV function.

Methods: In 19 patients (male/female, 15/4; age, 62±11 yrs) with proven occlusive CAD and impaired LV function (ejection fraction, 32±13%), contrast-enhanced MRI and LD-DSE were performed prior to coronary artery bypass surgery. MRI exams (1.5 T, Magnetom Sonata, Siemens Medical Systems, Erlangen, Germany) consisted of a cine study in long and contiguous short axis orientations of the entire LV using a SSFP sequence (TrueFISP; TR, 3 ms; TE, 1.5 ms; FA, 60°; slice thickness, 8 mm). 8–15 min after administration of 0.2 mmol/kg BW of Gd-DTPA (MagnevistTM, Schering, Berlin, Germany), the short axes were scanned with a segmented inversion-recovery TurboFLASH sequence (TR, 8 ms; TE, 4 ms; TI, 200–260 ms; slice thickness, 8 mm) to detect LE. LE was classified on a 4-point scale (score 1=no LE, 2=sub-endocardial LE of <50% of wall thickness, 3=non-transmural LE of >50%, 4=transmural LE). LD-DSE was performed at rest and under pharmacological stress during infusion of dobutamine (5 and 10 µg/kg/min). Regional wall motion was judged as normal, hypokinetic with recruitment under stress indicating myocardial hibernation, or hypokinetic without



change under stress indicating scar. Comparison was performed using the 17-segment model according to the AHA.

Results: A total of 323 myocardial segments were analyzed in both modalities. 168 segments (52%) showed no LE in MRI (score 1), non-transmural scars (score 2/3) were detected in 64/47 segments (20%/15%), and 44 segments (14%) showed transmural LE. 133 segments (41%) had normal wall motion in LD-DSE, 33 (10%) hypokinetic segments improved at stress, and 157 hypokinetic segments (49%) did not change at stress and were classified as scar tissue by LD-DSE. Only 95 (61%) of these 157 segments showed any kind of LE, whereas LE occurred in 46 (35%) of the 133 segments with normal wall motion in LD-DSE (MR score 2/3/4, 29/10/7). 29 (88%) of the 33 hypokinetic segments with improved function at stress (hibernation) had MRI score 1 or 2. Of 91 segments with LE score 3 or 4, which are not expected to improve function after revascularization, LD-DSE characterized only 70 (77%) as not viable.

Conclusions: In CAD patients with severely impaired LV function, low-dose Dobutamine stress echocardiography overestimates the extent of scar tissue compared to contrast enhanced MRI. On the other hand, about one third of segments without evidence of scar in MRI does not improve at low-dose stress. Those areas might contribute to the number of segments with lack of improvement after revascularization although anticipated viable. The combination of late enhancement imaging and low-dose Dobutamine in MRI might still improve the predictive value of this promising technique.

223. Delayed Enhancement Cardiac Magnetic Resonance Imaging and Electrocardiography Findings in Chronic Heart Failure Patients

Ramesh de Silva,¹ Klaus Witte,¹ Elena Lukaschuk,¹ Angela Lowe,² Andrew L. Clark,¹ Nikolay P. Nikitin,¹ John GF Cleland.¹ ¹Academic Cardiology, Hull CMR Research Group, Hull, United Kingdom, ²Lister In-Health, Leeds, United Kingdom.

Introduction: Delayed enhanced cardiac magnetic resonance imaging (deCMR) is an evolving technique used to delineate myocardial fibrosis. The technique allows identification of the transmural of infarcted tissue with high spatial resolution and is superior in identifying the region of infarct than conventional electrocardiography (ECG) in the presence of ischaemic

heart disease. It is unclear whether this applies to patients with chronic heart failure (CHF). Differences may be expected due to altered geometry that occurs as a result of remodelling in CHF and subsequent non-specific ST-T changes.

Purpose: To document ECG findings in CHF patients in the presence of deCMR.

Methods: CMR images from 76 patients with symptoms and signs of heart failure referred to a tertiary centre heart failure unit were acquired using a clinical 1.5 Tesla scanner (Signa CVi, General Electric, USA). 8–10 short axis delayed enhancement images were acquired 15 minutes after automated injection of 0.15 mmol/kg gadodiamide (Nycomed Amersham, UK). Regional late enhancement was scored based on the spatial extent of hyperenhancement (HE) using a 16-segment model similar to that proposed by the AHA. A five point scoring system was assigned based on the percentage of HE per segment (none=0, 1–25%=2, 26–50%=3, 51–75%=3 and 76–100%=4). ECG's were analysed for the presence or absence of pathological Q-waves and / or ST-T changes (T inversion, ST depression). These were documented for three areas defined as follows: anteroseptal V1–V4, lateral V5, V6, I, aVL and inferior II, III, aVL. Abnormalities in more than two contiguous leads were recorded as a positive score. Anteroseptal, lateral and inferior regions in the 16-segment model were identified according to the territories supplied by the coronary arteries as recommended by the AHA. A mean regional HE score (the sum of segmental HE scores in a region divided by the number of segments in the region) was used to quantify fibrosis in the corresponding areas.

Results: Based on the ECG findings, Q waves were present in the anteroseptal, lateral and inferior areas in 9, 1 and 10 patients and ST changes were present in 6, 27 and 9 patients respectively. Based on deCMR regional HE scores, the corresponding numbers were 29, 9 and 25 patients respectively. 9 patients had LBBB and 24 ECG's were within normal limits. There was no significant difference in the regional HE score in the presence of Q waves vs ST changes for anteroseptal (0.73 vs 0.61, p=0.7), lateral (0.66 vs. 0.31, p=0.2) or inferior (0.36 vs. 0.32, p=0.8) territories. Using deCMR as the gold standard for detecting the presence of infarcted tissue in any area, the sensitivity and specificity of the ECG was 76% and 55% respectively.

Conclusions: There are non-specific lateral changes in the ECG's of patients with CHF that do not relate to HE on deCMR. Whether this is due to the effects of left ventricular strain remains to be elucidated. A normal ECG is not a reliable indicator for the absence of myocardial scar tissue in CHF patients.



224. MR Imaging Evaluation for Urgical Ventricular Reconstruction (SVR)

Shunsuke Natori, MD,¹ John V. Conte, MD,² João A. C. Lima, MD,³ David A. Bluemke, MD, PhD.¹ ¹*Russell H. Morgan Department of Radiology and Radiological Science, Johns Hopkins University School of Medicine, Baltimore, MD, USA,* ²*Department of Surgery, Division of Cardiac Surgery, Johns Hopkins University School of Medicine, Baltimore, MD, USA,* ³*Department of Medicine, Division of Cardiology, Johns Hopkins University School of Medicine, Baltimore, MD, USA.*

Background: Congestive heart failure secondary to coronary artery disease is highly prevalent and is associated with a very high mortality rate. Surgical ventricular reconstruction (SVR) is an option for patients with a left ventricular dysfunction due to an ischemic and dilated ventricle.

Purpose: To quantitate left ventricular (LV) function, size, myocardial scar, and mass by magnetic resonance (MR) imaging before and after SVR.

Method and Results: 21 patients (19 males, 49–79 years old) with congestive heart failure were evaluated with cardiac MR imaging prior to planned SVR. The goal of SVR was to reconstruct the enlarged spherical ventricles to an elliptical shape and ventricular volume of 60 cc/m² body surface area using standardized ventricular manikins. (TR³ISVR™, Chase Medical, Richardson, Tx). MR examinations consisted of short and long axis cine images, perfusion images, and myocardial delayed enhancement (viability) imaging. Three patients were New York Heart Association function class II, twelve patients were class III, and five were class IV. MR images were analyzed using MASS software version 4.2 (Medis, Netherlands). The

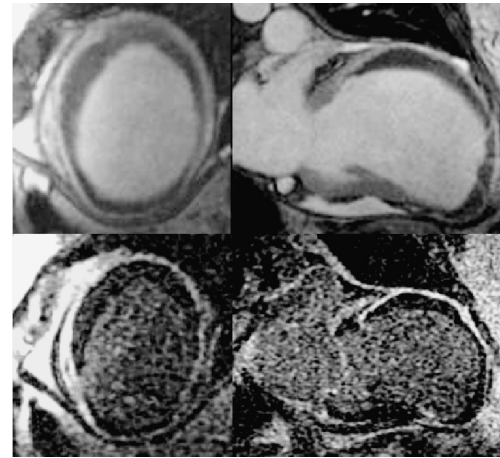


Figure 1.

Table 1 shows mean values for MR derived LV measurements before and after surgery. LV end diastolic volume (LVEDV) decreased in 302±149 to 221±72 ml and LV end systolic volume (LVSDV) decreased from 237±144 to 145±73 ml. LV ejection fraction (EF) increased from 24±12 to 37±12% (p<0.01), and cardiac output significantly increased from 4.48±1.8 to 5.86±1.4 (p<0.05). Postoperative LVEDV and LV mass were positively correlated (r=0.80, p<0.01). There was an inverse relationship between ejection fraction and the hyperenhanced region on myocardial delayed enhancement imaging (r=−0.49, p<0.05) (Fig. 1).

Conclusion: Ventricular remodeling surgery resulted in significant improvement in cardiac function and reduced LV volume as assessed by MR imaging. MR viability images are predictive of global LV function in this patient population.

Table 1. Left ventricular analysis LVEDV, left ventricular end diastolic volume, LVESV; left ventricular end systolic volume, LVSV; left ventricular stroke volume, LVEF; left ventricular ejection fraction; LV mass, left ventricular mass; HR, heart rate; CO, cardiac output; M/V, LV mass/LVEDV.

	Pre op		Post op		
	Mean	S.D.	Mean	S.D.	
ED volume	302.4	± 149.3	221.2	± 71.9	n.s.
ES volume	237.3	± 143.5	145.1	± 72.6	n.s.
St vol	65.0	± 26.1	76.0	± 16.7	n.s.
EF	23.9	± 11.5	37.4	± 11.7	p<0.01
LV mass ED	182.2	± 58.6	156.4	± 38.4	n.s.
HR	68.1	± 11.0	77.5	± 12.1	n.s.
CO	4.48	± 1.75	5.86	± 1.37	p<0.05
M/V	0.65	± 0.18	0.74	± 0.14	n.s.

225. Validation of Rapid High Resolution MRI Assessment of Left Ventricular Function

Mark Doyle, PhD, Geetha Rayarao, June Yamrozik, Ronald B. Williams, Diane A. Vido, Maria Jaksec, Robert W. W. Biederman, MD. *Allegheny General Hospital, Pittsburgh, PA, USA.*

Background: Currently, MRI applied to the LV requires acquisition of high-resolution cine images, which is time intensive. Typically, 10–15 slices are required to assess the entire LV, each slice acquired during a breath-hold. Generally, reduced scan time sequences compromise spatial or temporal resolution. We implemented a rapid cine imaging approach, Block Regional Interpolation Scheme for K-space (BRISK) that allows acquisition of three slices in a single breath-hold, yet might produce identical resolution.

Hypothesis: We hypothesize that BRISK cine MR imaging reduces the acquisition time for LV assessment without affecting image resolution, contrast or accuracy.

Methods: In 10 control subjects (2 female), cine imaging was performed on a 1.5 T GE CV/i MRI system. Contiguous cine images were acquired from base to apex. Conventional scan data were acquired using a single breath-hold per slice, while the BRISK data were acquired using three slices per breath-hold. All images were acquired with identical spatial and temporal resolution for the conventional and BRISK acquisitions (steady state free precession sequence, TR/TE/flip 3.7/1.8/45, matrix 256×192). Two independent readers analyzed cine data in a blinded manner.

Results: The scan time to acquire 10–15 slices using BRISK was less than half (44%) that required for the conventional scan (4.7 ± 1.0 min vs $10.8 \text{ min} \pm 2.1$, $p < 0.001$). The breath-hold duration for BRISK was well tolerated but was longer than the standard scan ($20.7 \text{ s} \pm 1.8$ vs. $15.9 \text{ s} \pm 1.0$, $p < 0.001$). Bland–Altman analysis comparing BRISK to the commercial scan data for ESV, EDV and LV mass showed excellent agreement with low bias and standard deviation compared to the mean. Correlations ranged from 0.88 to 0.98 ($p < 0.005$). Importantly, the contrast to noise ratio of LV blood was slightly higher for the BRISK set (8.9 ± 2.0 vs. 8.3 ± 1.9 , $p < 0.005$).

Conclusions: BRISK allows three high-resolution slices to be imaged in a single breath-hold. The entire LV was imaged in less than half the conventional time, with potential to improve patient compliance. The BRISK cine imaging approach, implemented on a commercial MRI scanner, generated LV cine images that were equivalent to commercial cine images with respect to contrast, spatial and temporal resolution.

226. Comparison of High Spatial and Temporal Resolution CE Myocardial Perfusion Using SSFP and Fast Gradient Echo Imaging: Inter-technique and Inter-observer Variability Using Semiquantitative Parameters of Contrast Kinetics

Jeffrey Goldman, MD,¹ Simone Hoffer,¹ Neescha Patel,¹ Niels Oesingman, PhD,² Javier Sanz,³ Teresa Rius, MD,³ Paola Kuschnir,³ Rafael Salguero,³ Michael Poon,³ Emil Cohen.¹ ¹Radiology, Mount Sinai Medical Center, New York, NY, USA, ²Siemens, Ehrlangen, Germany, ³Cardiology, Mount Sinai Medical Center, New York, NY, USA.

Introduction: Fast gradient echo (fgr) imaging remains the standard for myocardial perfusion MR. SSFP imaging is a newer technique which has some advantages over fast gradient imaging which makes it an attractive alternative for myocardial perfusion imaging. Concerns exist as to whether SSFP imaging can be used for quantitative evaluation of myocardial perfusion. Recent studies have suggested that the optimal technique for myocardial perfusion imaging needs to maintain reasonable spatial resolution while achieving temporal resolution close to 100 msec to decrease motion artifacts. We have optimized a myocardial perfusion protocol with temporal resolution of 120 msec maintaining an imaging matrix of 192 for both fast gradient echo and SSFP imaging techniques. We performed CE myocardial perfusion using fgr and SSFP on the same patients on separate days and compared semiquantitative measurements of contrast kinetics.

Purpose: The goal of our study was to: 1) determine the interobserver variability of our analysis tool for measuring seven semiquantitative parameters of myocardial perfusion, and 2) compare the inter-technique variability of myocardial perfusion using SSFP with fast gradient echo imaging as measured by semiquantitative parameters of contrast kinetics.

Methods: CE-myocardial perfusion MR was performed on five healthy volunteers using two techniques on two different days on a 1.5 T Siemens Sonata MRI. For perfusion imaging gadolinium was infused at a dose of 0.05 mmol/kg at a rate of 5 cc's/second. Both saturation recovery SSFP and fast gradient echo imaging technique were performed using similar parameters. A single slice was obtained through the mid left ventricle in the short axis plane. The acquisition time and TI time were kept the same for the two techniques at 120 msec and 200 msec respectively. In order to bring the acquisition time down both partial fourier (6/8) and parallel imaging (x2GRAPPA) were employed. In order to have



an equal minimal acquisition time of 120 msec the matrix for Flash was 192×132 and for TrueFISP was 192×102 . Semiquantitative analysis of perfusion was performed in each patient on six segments of the LV myocardium by two observers using the two techniques (total $n=120$ roi's). An analysis tool was employed which fits the SI/time curve to a gamma variate function providing 7 parameters of contrast uptake (time 0, time to peak, area under the curve, maximum slope, time to maximum slope, mean transit time and maximum signal intensity). Signal intensity, base line, and motion correction algorithms were employed in the analysis software.

Results: Interobserver variability (coefficient of covariance) ranged from 21–30% for 5 parameters (slope, time to peak, maximum SI, mean tranist time and time 0). Area under the curve and time to maximum slope had higher variability. No significant difference was observed for the interobserver variability between fgre and SSFP imaging. The inter-technique variability between fgre and SSFP imaging ranged between 19 and 31% between the same 5 parameters which had the least interobserver variability. This range was within the range of interobserver variability. No increased artifacts were found with either SSFP or fgre imaging.

Conclusion: The interobserver variability for our relatively high temporal and spatial resolution CE myocardial perfusion sequence ranged between 21–30% which was felt to be within acceptable limits given the difficulties inherent of placing an ROI within a given myocardial segment and not extending it into the blood volume. The inter-technique variability between fgre and SSFP imaging fell within the intra-observer variability supporting the supposition that SSFP imaging can be used for quantitative myocardial perfusion analysis. Future studies need to be performed to to determine whether semiquantitative parameters of contrast kinetics are accurate and reliable enough to identify myocardial ischemia and to determine relative advantages of fgre vs. SSFP imaging for myocardial perfusion.

227. Scar Volume as Measured by Contrast Enhanced-Magnetic Resonance Imaging Relates to Both Left Ventricular Geometry and Ejection Fraction in Chronic Myocardial Infarction

Casolo Giancarlo, MD,¹ Rega Luigi,² Del Meglio Jacopo,¹ Gensini Gian Franco,¹ Margheri Massimo.¹
¹Clinica Medica e Cardiologia, Azienda Universitaria Ospedaliera Careggi, Florence, Italy, ²Department of Radiology, Azienda Universitaria Ospedaliera Careggi, Florence, Italy.

Introduction: Contrast Enhanced Magnetic Resonance (CE-MRI) allows to differentiate viable from non-viable myocardium in coronary artery disease (CAD) patients. It is well known that left ventricular remodeling after myocardial infarction (MI) is strictly rekatel to infarct size. However only few data are available relating scar to left ventricular (LV) size and function due to the difficulties to detect and quantitate infarct size in-vivo.

Purpose: The aim of this study was to evaluate the relationship between the aumount of chronic scar and LV size and function. For this purpouse we studied a cohort of CAD patients with healed MI by using CE-MRI.

Methods: We studied 50 CAD patients (age 66 ± 9 years; 32 males and 18 females), with healed MI (>12 months after the acute event). We used a 1.5 Tesla scanner with a 5 element phased array surface coil (Philips Intera 1.5 T). After a scout scan to localize the heart, the left ventricle was fully covered by multiple breath-hold balanced FFE series. These data were used to measure both LV volumes and ejection fraction. Subsequently, all the patients received 0,2 mM/Kg Gd-DTPA intravenously. After 15 minutes patients were imaged again by using a 3D breath-hold IR-TFE sequence. The inversion time was adjusted to obtain optimal image quality and nulling of the signal from the normal myocardium. Images were then processed on a dedicated computer station (Easy Vision 4, Philips Eindhoven). The image quality was good in all the subjects while the examinations were usually completed within 30 min.

Results: In all the subjects a variable amount of CE areas were detected. Mean CE volume was 29 ± 16 mm³ (range 7–71 mm³). End-diastolic and end-systolic volumes (mean values 153 ± 37 cc and 96 ± 47 cc respectively) were significantly related to the amount of the CE volume ($r=0.52$ and 0.67 respectively, both $p < 0.0001$). Mean LV ejection fraction was $41 \pm 17\%$ and was significantly related to CE volume ($r=0.68$, $p < 0.0001$). LV mass was not related to CE volume (Fig. 1).

Conclusions: As CE-MRI regions have been found to represent scar in CAD patients after MI it is now available a very interesting method to explore new aspects of the physiopathology of CAD. We found that CE-MRI is able to detect regions of previous MI and

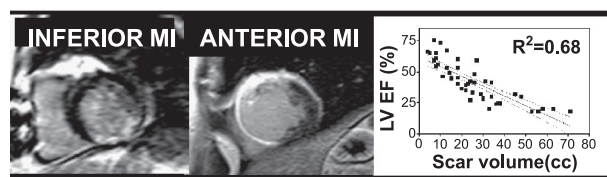


Figure 1.



quantitate the amount of scar present in a very short imaging time. The amount of CE volume detected relates to both LV geometry and function. Scar detected by CE-MRI may thus be an alternative and more important information with respect to LV ejection fraction. It is suggested that the information provided by CE-MRI may be an adjunctive important parameter to be collected in CAD patients with chronic MI. Scar volume as detected by MRI may possess unique and independent prognostic information.

228. Delayed Contrast Enhanced MRI Predicts Functional Recovery After Revascularization in Patients with Chronic Ischemic Left Ventricular Dysfunction: A Quantitative Analysis

Olga Bondarenko, MD,¹ Aernout M. Beek, MD,¹ Harald P. Kühl, MD,¹ Mark M. B. Hofman, PhD,² Jos W. R. Twisk, PhD,³ Willem G. van Dockum, MD,¹ Albert C. van Rossum, MD, PhD.¹ ¹Cardiology, VU University Medical Center, Amsterdam, Netherlands, ²Physics and Medical Technology, VU University Medical Center, Amsterdam, Netherlands, ³Clinical Epidemiology and Biostatistics, VU University, Amsterdam, Netherlands.

Introduction: Delayed contrast-enhanced (DCE) MRI has been shown to predict functional recovery after revascularization in patients with chronic ischemic left ventricular dysfunction. However, evidence is still limited and the full significance of DCE MRI remains to be established.

Purpose: To investigate whether DCE MRI predicts functional recovery after revascularization using quantitative assessment of myocardial enhancement and function.

Methods: Fifteen patients (age 64±9, 17 males) with left ventricular dysfunction (EF 40±10%) were imaged on a 1.5 MR scanner one month before and three months after surgical or percutaneous revascularization. Regional left ventricular function was assessed at base line and follow-up using cine gradient-echo MRI. Inversion-recovery turbo-FLASH images (TE 3.4 ms, TR 7.6 ms, TI 250–300 ms) were acquired at base line 20 minutes after i.v. administration of 0.2 mmol/kg gadolinium-DTPA. In each patient the segmental extent of hyperenhancement (SEH; expressed as percentage of total segmental area) and segmental wall thickening (SWT) were quantitatively analyzed in 6–8 contiguous short axis slices (12 segments/slice). Segments with SWT less than 3 mm were considered dysfunctional.

Percentage of the left ventricle that was dysfunctional but viable was calculated as the total number of dysfunctional segments with SEH of <33% divided by the total number of segments in the left ventricle.

Results: Of 420 initially dysfunctional segments 123 (29%) regained normal SWT at follow-up. The likelihood of functional recovery at follow-up decreased with increasing SEH: segments with 1–33%, 34–66%, 67–100% SEH respectively, were 8, 9 and 22 times less likely to recover than segments without hyperenhancement, (multilevel analysis, $p < 0,005$). There was also a strong correlation between the percentage of the left ventricle that was dysfunctional but predominantly viable at baseline and improvement of the ejection fraction at follow-up (regression coefficient 0,60, $p < 0,05$).

Conclusions: Using quantitative analysis we found an inverse relation between segmental extent of hyperenhancement and recovery of segmental wall thickening after revascularization. This study supports the previous qualitative evidence that DCE MRI is predictive in assessing the likelihood of functional recovery after revascularization in patients with chronic ischemic left ventricular dysfunction.

229. Left Ventricular Thrombus Detection with MRI: Delayed Enhancement is More Sensitive than BOLD

Ralf Wassmuth, MD, Rainer Dietz, MD, Matthias G. Friedrich, MD. *Franz-Volhard-Clinic, Humboldt-University Berlin, Berlin, Germany.*

Introduction: Transthoracic echocardiography is often not sufficient to depict left ventricular (LV) thrombus. Delayed enhancement (DE) MRI has been suggested to depict thrombi adjacent to a LV scar. Blood oxygen level dependent (BOLD) imaging is sensitive to structures rich in hemoglobin metabolites.

Purpose: We tested the sensitivity of BOLD and delayed enhancement images for LV thrombus imaging.

Methods: We prospectively scanned patients suspicious for LV thrombus based on echo or history in a 1.5 T clinical MRI. Steady state free precession (SSFP) cine images, blood oxygen level dependent (BOLD) images and delayed enhancement images were acquired with a typical in-plane resolution of 2,0×1,5 mm², 3×3 mm² and 1,7×1,2 mm², respectively. Thrombus was defined as a prominent endocardial mass within an akinetic segment in SSFP images. Thrombus size was measured in SSFP images.



Results: In 25 subjects SSFP cine MRI confirmed the presence of LV thrombus adjacent to an apical infarction scar. In BOLD thrombus was hypointense within bright blood. In DE thrombus appeared as a hypointense mass between infarct scar and blood pool. Sensitivity was 54% for BOLD and 96% for DE. Thrombi not detected in BOLD were smaller (4 mm vs. 12 mm, $p < 0.01$) than the others.

Conclusion: DE was superior to BOLD for LV thrombus detection. BOLD failed in very small thrombi, probably due to reduced spatial resolution.

230. Myocardial First-Pass Stress Perfusion MRI with Dipyridamole in the Clinical Setting: Evaluation of a Stress Perfusion-First Protocol

Marcelo Hadlich,¹ João L. Petriz,¹ Clerio F. Azevedo,¹ Luís A. Mendonça,¹ Thatiana Souza Hadlich,¹ Jorge Moll,¹ Carlos E. Rochitte.² ¹Cardiac MRI, Rede D'Or & Labs, Rio de Janeiro, Brazil, ²Cardiac MRI, Heart Institute (InCor) University of São Paulo Medical School, São Paulo, Brazil.

Introduction: Myocardial First-Pass perfusion MRI (MPI) has been shown to detect obstructive coronary artery disease. MPI has shown good accuracy for the diagnosis of CAD. However these results were reached by highly controlled research protocols and not in clinical routine with patients referred directly from cardiologists' office. Several schemes have been used to perform rest and stress perfusions on the same MR exam. Because the gadolinium is not completely eliminated of the circulation between the first and second injection of the contrast, our center routinely performs stress perfusion first, followed by rest perfusion. This is based on the concept that pre to

post-contrast mean myocardial signal intensity differences would be greater on the first injection and that this fact would help on the optimization of image quality and ultimately on the diagnosis. However, this concept has not yet been verified objectively.

Purpose: Our objectives were: To describe our initial clinical experience with MPI, to evaluate safety and usefulness of myocardial perfusion during stress with dipyridamole and rest in the clinical setting and; To measure pre-contrast to post-contrast myocardial signal intensity differences (SID) during first (stress) and second (rest) gadolinium injections in the same dipyridamole stress perfusion MR study.

Methods: Thirty-one consecutive patients underwent MRI exam in a 1.5 T ACS-NT Powertrack 6000 Philips scanner. All patients were referred to MR with suspected CAD by clinical cardiologists. Dipyridamole dose was 0.56 mg/kg/4 minutes. MPI used a gradient-echo EPI pulse sequence with a saturation pre-pulse, with the following parameters: TR 3.2 ms, TE 1.6 ms, FA30, TFE 5, EPI 11, TI 100–150, matrix 112 × 128, FOV350–380, ST 8, Gap to cover LV, 1RR, 4 short-axis slices. A 0.05 mmol/kg bolus IV gadolinium-based contrast injection was performed in each myocardial perfusion (stress and rest). Additional 0.2 mmol/kg was injected to acquire myocardial delayed enhanced images. Cine-MRI was performed between stress and rest perfusion. Figure 1 depicts the MR protocol. We measured the mean signal intensity in a myocardium ROI at pre-contrast and at peak myocardial enhancement during the first pass on first (stress) and second injection (rest). The comparison of pre and post-contrast SID was done by paired Student t test.

Results: Fifteen patients were referred to MPI as the first diagnostic screening. Sixteen patients were referred due to inconclusive results of other noninvasive diagnostic tests (7 nuclear medicine, 5 treadmill tests and 4 rest echocardiography). We observed a

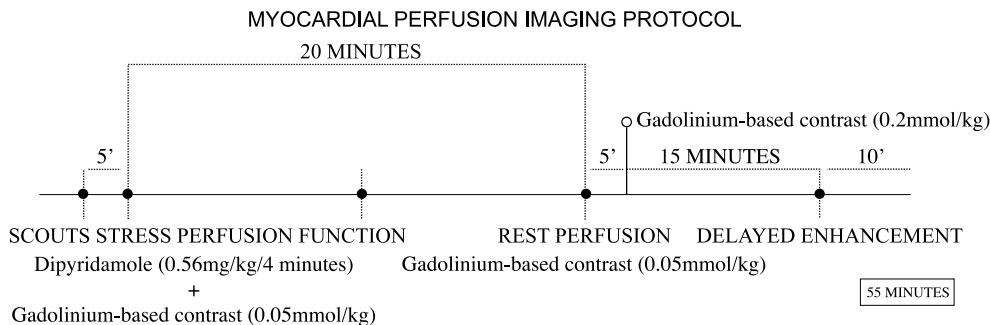


Figure 1.

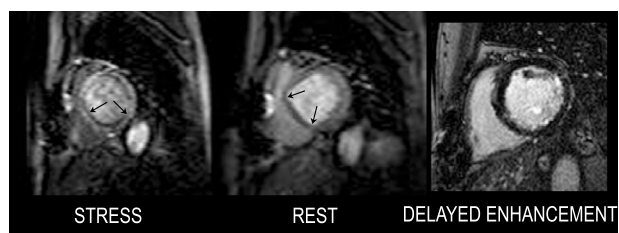


Figure 2.

mean 36% increase in heart rate during stress, and few symptoms (51% asymptomatic), most frequently headache and hot chest sensation. MPI was positive for ischemia in 9 cases (29%). In 2 patients the MPI disagreed with previous noninvasive tests, and correctly predicted the coronary angiography. The SID between pre and post-contrast during stress perfusion (first injection) was 541.7 ± 38.8 and SID during rest perfusion (second injection) 335.1 ± 29.8 , $p < 0.001$. The mean difference between stress and rest SID was 206.6 ± 37.3 , or 61.7% higher for the first injection. Figure 2 shows an example of these results. The mean time between stress and rest perfusion was 20.9 ± 1.3 minutes. Therefore, our results are supportive of the concept that in the range of 20 minutes period a second injection for myocardial perfusion generates a significant smaller increase in myocardial signal intensity, which could damage its ability to detect small perfusion defects.

Conclusions: Myocardial perfusion by MRI during stress with dipyridamole can be safely performed and provided additional information valuable for the routine clinical patient management. The protocol first performing stress perfusion seems to be a better option for optimizing myocardial enhancement during the most critical part of myocardial ischemia detection.

231. Myocardial Perfusion and Function Imaging by Contrast-Enhanced Cine Magnetic Resonance Imaging in Acute Myocardial Infarction

Gilbert L. Raff, MD, Ralph E. Gentry, RT, James A. Goldstein, MD. *Cardiology, William Beaumont Hospital, Royal Oak, MI, USA.*

Analysis of first-pass perfusion using contrast-enhanced magnetic resonance imaging (MRI) can assess adequacy of reperfusion in patients with acute myocardial

infarction (AMI), while dynamic cine MRI can measure LV function. This study was designed to determine whether a novel method, contrast-enhanced cine MRI, could determine both myocardial function and perfusion in a single exam.

Methods: Seventy-seven patients with enzyme-documented AMI were studied within 36 hours of admission. FFP was performed by an independent parallel acquisition technique turbo-FLASH pulse sequence (Siemens) in 3 simultaneous 8mm short axis slices with a 200% gap. An I.V. bolus of 0.075 mmol/kg of Gd-DTPA contrast was given. Afterwards, an additional 0.125 mmol/kg of contrast was given, followed by an EKG-gated segmented k-space true-FISP cine pulse sequence acquired in identical slices. Two blinded readers analyzed 8 radial segments in each slice for hypoenhancement. In 18 patients, short axis cine studies from apex to base were acquired before and after contrast, for analysis of global function parameters: ejection fraction, mass, end diastolic volume and end systolic volume.

Results: Regional hypoenhance on CEC was 77% sensitive and 95% specific for the presence of perfusion abnormalities by FFP. There was no significant difference in global LV function before and after gadolinium contrast.

Conclusions: This study demonstrates that a novel method, contrast-enhanced cine MRI, can determine both myocardial function and perfusion in a single exam. CEC may facilitate evaluation of patients with acute coronary syndromes.

232. Relationship of Regional Wall Parameters to the Transmural Extent of Infarct in Patients with Acute and Chronic Myocardial Infarction

Cory Swingen, PhD,¹ Ralph Gentry, RT,² Michael Jerosch-Herold, PhD,¹ Gil Raff, MD.² ¹*Radiology, University of Minnesota, Minneapolis, MN, USA,* ²*Cardiology, Beaumont Hospital, Royal Oak, MI, USA.*

Introduction:

Purpose: The aim of this study was to examine the relationship of several quantitative regional parameters to the regional transmural extent of infarct (TEI) in patients with acute (AMI) and chronic infarct (CMI).

Methods: We studied global and regional function by cine MRI and infarction by contrast-enhanced MRI in 10 patients acutely (2 ± 1 day) and chronically (99 ± 21 days) after reperfused first MI. Epicardial and endocardial contours were manually drawn and the



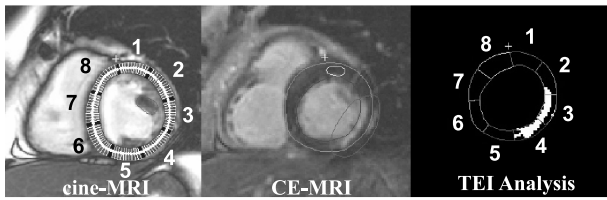


Figure 1. Image of diastolic cine image showing centerline segments (left), corresponding delayed contrast-enhanced image (middle) and quantified TEI (right). (View this art in color at www.dekker.com.)

quantitative parameters (ED thickness, ES thickness, Wall Motion, Wall Thickening) determined in 8 segments per slice on a computer using the centerline method. The TEI was quantified in matching slices and segments using the centerline method with infarcted pixels defined as those with signal intensities greater than 2 standard deviations above a remote region in the same slice (Figure 1). The TEI was calculated as the ratio of infarcted pixels and the total segment area. Linear regression analysis was used to compare the relationships between the regional wall parameters and segments with a TEI > 0%.

Results: Correlations between all parameters and the transmural extent of infarct in the AMI and CMI setting: ED wall thickness ($r=0.09$ AMI, 0.20 CMI); ES wall thickness ($r=0.42$ AMI, 0.50 CMI); Wall Motion ($r=0.48$ AMI, 0.60 CMI); Wall Thickening ($r=0.42$ AMI, 0.54 CMI) (Figure 2).

Conclusions: In the setting of reperfused AMI, endocardial wall motion correlated the closest with infarcted segments followed by wall thickening and ES thickness. ED thickness showed no trend. In the setting of CMI, all quantitative function parameters had a higher correlation than in the AMI setting. For the CMI cases wall motion still revealed the best correlation to the transmural extent of infarct, followed again by wall

thickening and ES thickness. ED thickness in the CMI patients showed a negative trend with increasing infarct transmural extent. These data highlight the relationship between different regional wall parameters to the transmural extent of infarct as well as their difference in the acute and chronic setting.

233. Remodeling After Acute Myocardial Infarction and Reperfusion Therapy Assessed by Cardiovascular Magnetic Resonance Imaging

Burkhard Sievers, MD, Marvin Addo, Binu John-Puthenveetil, Asli Bakan, Stefan Zimmermann, Simon Kirchberg, Kai Tintrup, Hans-Joachim Trappe, MD. *Cardiology and Angiology, University of Bochum, Herne, Germany.*

Purpose: To evaluate, whether contrast enhancement (CE) and wall motion abnormalities (WMAs) change over time in patients with acute myocardial infarction (AMI) and reperfusion therapy.

Methods: 17 patients (12 men and 5 women, mean age 64 ± 9.6 years) with AMI underwent either thrombolytic therapy (thrombolysis) or acute coronary artery intervention (PCI). They were examined 3 days and 7.1 ± 1.2 months after AMI using a 1.5 Tesla MR-imager. Cine imaging was performed with TrueFISP, CE-MRI with a segmented turbo FLASH sequence. A total of 289 segments was analyzed according to a 17-segment model. WMAs were scored visually (grade 0–4). CE was outlined for each slice, the area per segment (%) was calculated and the transmural extent (TE) of CE divided into 4 groups (1–25%, 26–50%, 51–75%, 76–100%). Analysis was performed by two different and blinded observers using a commercially available software.

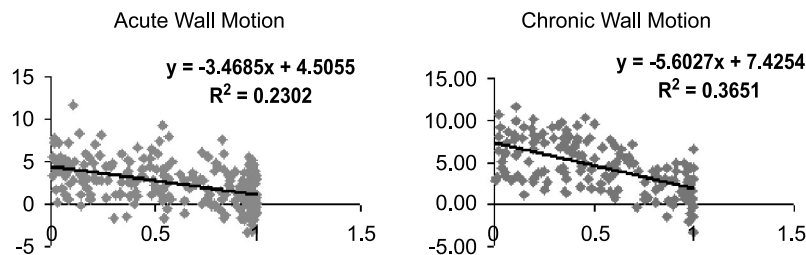


Figure 2. Plots of wall motion vs. TEI for all segments in the AMI (left) and CMI (right) setting. These graphs show a greater number of dyskinetic segments (wall motion less than zero) in the acute setting compared to chronic for TEI values less than 1. (View this art in color at www.dekker.com.)

Results: CE decreased significantly over time ($p \leq 0.001$). Regarding the TE of CE per segment, CE decreased (91%), increased (8%) or did not change (1%) over time. The less the TE of CE was, the greater was the likelihood of disappearance of the CE ($p = 0.0005$) and vice versa ($p \leq 0.001$). The correlation between the TE of CE and the change of WMA was not significant ($p = 0.427$), but segments with CE > 75% of the myocardial wall did show less improvement of WMAs than segments with a TE of CE < 75%. ($p = 0.089$). Changes of the TE of CE and the changes of the WMA did not correlate significantly ($p = 0.806$). There was a trend towards a greater decrease of CE in the PCI group compared to the thrombolysis group ($p = 0.0787$). A complete regression of CE was seen more in the PCI group (27%) than in the thrombolysis group (17%, $p = 0.229$). Interobserver variability was good ($\kappa \geq 0.84$). The global left ventricular function was not significantly different in both examinations ($p = 0.1359$).

Conclusions: CE can decrease, increase or stay the same over time in patients with AMI. TE of CE does not influence either the severity nor the likelihood of improvement of wall motion abnormalities over time. Remodeling in patients with PCI seems to be superior than in patients undergoing thrombolysis therapy.

234. First Pass Rest Cardiac Perfusion Imaging at 3T

Josh Socolow,¹ Puneet Sharma,² Stam Lerkais,¹ Roderic Pettigrew,³ John Oshinski.³ ¹Medicine (Cardiology), Emory University, Atlanta, GA, USA, ²Biomedical Engineering, Emory University, Atlanta, GA, USA, ³Radiology, Emory University, Atlanta, GA, USA.

Introduction: Gadolinium based contrast agents have been used in 1.5 T systems to measure first-pass myocardial perfusion and identify areas of myocardium which are supplied by stenotic or occluded coronary arteries. The use of this technique with the newer 3T systems has not been reported.

Purpose: This study investigates rest perfusion imaging in normal volunteers and in a patient with known coronary artery disease. We investigate whether a perfusion defect can be seen in a 3T system and whether the contrast uptake will be qualitatively different from results obtained in normal volunteers.

Methods: Four normal patients ranging in age from 22–37 and one patient with a known myocardial infarction were scanned in a Siemens Trio 3T scanner using a cardiac phased array coil. Perfusion imaging



Figure 1.

was performed with a, saturation recovery TrueFisp sequence, TI=110 ms, FOV 320 mm, matrix 128*96, TE=0.96 mm, flip angle=31, slice thickness 7 mm, TR 200 ms, 3 slice per RR interval. Each subject was given either 0.1 mmol/kg or 0.2 mmol/kg of Gd-DPTA-BMA (Omniscan). Myocardial segments in the anterior, lateral, inferior and septal walls as well as the LV cavity were traced using OSIRIS and signal intensity (SI) was measured in each of these segments for each time point. Upslope of the SI/time curves were calculated by linear fit. The upslopes for the myocardial segments were corrected by dividing by the upslope of the LV cavity SI/time curve to correct for difference in contrast bolus volume and injection rate. Perfusion was also judged qualitatively by visual assessment.

Results: 20 normal segments had mean slopes of 0.22 ± 0.127 . The segment from the patient which was known to be abnormal (by history, abnormal perfusion at 1.5 T and evidence of infarct by delayed hyperenhancement at 1.5 T) had a slope of 0.03. The figure below shows the perfusion defect in the septal wall (Fig. 1).

Conclusions: First pass rest perfusion imaging is possible at 3T. We were able to detect both qualitatively and quantitatively a perfusion defect in a segment known to be abnormal by other tests.

235. Delayed Contrast Enhancement and No-Reflow Phenomenom in Acute Myocardial Infarction

Oliver Bruder,¹ Kai-Uwe Waltering,² Markus Jochims,¹ Markus Hollenhorst,² Georg V. Sabin,¹ Jörg Barkhausen.² ¹Department of Cardiology and Angiology, Elisabeth Hospital, Essen, Germany, ²Department of Diagnostic and Interventional Radiology, University Clinic, Essen, Germany.

Introduction: After injection of paramagnetic contrast a dark zone in the center of the necrotic tissue has been



reported by several authors in patients with acute myocardial infarction (MI). The extent of this no-reflow area indicating microvasculature occlusion is associated with an increased number of cardiac events and poor prognosis. However, no studies about the optimum time-point for imaging after contrast administration and the early changes of the volume of the no-reflow area have been conducted so far.

Method: 12 patients with first acute myocardial infarction (7 male, 5 female, mean 66 years, range 40 to 76) were included into this study in accordance with the regulations of the local ethics committee. All patients had acute PCI (percutaneous coronary intervention) resulting in TIMI grade 3 flow. Patients with a history of PCI, CABG (coronary artery bypass grafting) and previous myocardial infarction were not included. All imaging was performed using a 1.5 T MR-scanner (Siemens, Magnetom Sonata) within the first 5 days after acute ST-elevation myocardial infarction (STEMI). One, 2, 3, 4, 5, 10, 15 and 20 minutes after i.v. administration of Gadodiamid (0,2 mmol/kg, Omniscan, Amersham) MR-imaging was performed using a single shot inversion recovery steady-state free precession sequence (TR 2.4 ms, TE 1.08 ms, TI 180–280 ms, FA 50°) covering the entire ventricle in a single breath-hold. For each data set the inversion time (TI) was set to null the signal of normal myocardium. The area of late enhancement and the area of the no-reflow zone were measured by planimetry for the different time points after contrast injection.

Results: The inversion recovery SSFP sequence demonstrated late enhancement of the anterior myocardial wall in 7 patients, and inferior myocardial infarction was seen in 5 patients. Immediately after contrast injection a no-reflow area was detected in 9 patients (anterior MI n=5, inferior MI n=4, mean infarct size $34 \pm 11\%$ of the LV mass). Only 3 patients with smaller infarction size ($9 \pm 13\%$ of the LV mass) showed no area of microvascular obstruction. In all patients the area of late enhancement remained unchanged from 5 to 20 minutes after contrast injection, whereas there was a significant reduction of the extend of the no-reflow area ($17,5 \pm 3,5\%$ LV mass at min 5 versus $9,1 \pm 2,2\%$ LV mass at min 15–20).

Discussion: Several case reports and studies with a small number of patients demonstrated the potential of contrast-enhanced CMR to visualize microvascular occlusion in patients with acute myocardial infarction. Compared to other studies our data show a higher incidence of no-reflow zones, because we used a fast single shot inversion recovery TrueFISP sequence, covering the entire left ventricle in a single breathhold immediately after contrast injection. Techniques covering only a limited number of slices or techniques covering

the entire ventricle within several minutes after contrast injection will underestimate the extent of the no-reflow area because it continuously declines over time, whereas the total area of late enhancement remains constant.

Conclusion: In patients with acute myocardial infarction the area of late enhancement remains unchanged over time within the first 20 minutes after contrast injection, whereas the extent of the no-reflow zone continuously decreases. Therefore, measurements of the no-reflow area to assess patients prognosis should be performed immediately after contrast injection with techniques covering the entire ventricle.

236. A Novel Rotational Long-Axis MRI Myocardial Perfusion Technique Is Superior to the Standard Short-Axis Approach

Yi Wang, DSc, Khurran Moin, MD, Sunil T. Mathew, MD, Olakunle Akinboboye, MD, Nathaniel Reichek, MD. *Cardiac Research, St. Francis Hospital, SUNY Stony Brook, Roslyn, NY, USA.*

Introduction: Conventional MR first-pass perfusion imaging covers myocardium in several parallel short axis (PSA) slices per heartbeat. However, through-plane motion of the basal myocardium, thin apical myocardium, fat-induced field inhomogeneity and apical location remote from surface coils limit PSA perfusion imaging. We evaluated a long axis perfusion imaging method, such that slices are distributed rotationally (RLA) around a left ventricular centroid. This method was compared to PSA acquisition in 15 volunteers in terms of contrast to noise ratio (CNR), relative signal upslope and myocardial coverage. The results demonstrate that compared to PSA, RLA perfusion images exhibit 31% improvement in total myocardial area with similar CNR and relative upslope. This new perfusion-imaging scheme provides more comprehensive coverage over the myocardium and better delineation of the true apical and basal region without any compromise in temporal or spatial resolution. Combining rotational long axis cines, delayed enhancement imaging and adenosine stress perfusion, we can potentially provide myocardial viability and cardiac function in one examination over a reasonable scan time.

Methods: Fifteen volunteers (ages: 57 to 74, 5 females) without known coronary artery disease were studied with IRB approval and informed consent. RLA slices were prescribed orthogonal to a mid-ventricular short axis slice with evenly spaced angular separation



and displayed on a short-axis reference image (Figure 1). A 1.5 T Siemens Sonata scanner (Siemens Medical Solutions, Malvern, PA) with a CP body array flex coil was used. A Imaging was performed using a partial Fourier saturation recovery TrueFISP sequence with the following parameters for both RLA and PSA imaging: TR/TE/TI/FA=2.9 ms/1.3 ms/90 ms/50°, data matrix 78×192, and usual voxel spatial resolution 3.5×1.9×8 mm³ dependent on the size of the volunteer. Contrast dose was 0.05 mmol/kg (Omniscan, Amersham). PSA and RLA were acquired in random order with a 20-minute washout period between contrast injections. The number of slices available was cycle length dependent with both techniques. Using Siemens Argus software for CNR analysis, regions of interest (ROI) were placed on the septum, lateral, anterior and inferior wall. The ratio of the signal difference between baseline (pre-contrast) and maximal contrast signal in that ROI was used as the CNR. MASS software (Medis, Leiden, The Netherlands) was used to measure the myocardial area and the contrast signal upslope relative to ventricular cavity of six myocardial segments in each slice.

Results: Both RLA and PSA perfusion images demonstrated good image quality and contrast between myocardium and blood, as shown in 5 RLA slices at contrast arrival in the left ventricle (Figure 1). The total myocardial area imaged differed between the two techniques, consistently favoring RLA (Figure 2). The mean myocardial area imaged on RLA was 60.37±18.5 cm², 31% more than PSA (46.01±14.6 cm², p<0.01). The mean relative upslope was similar on RLA and PSA imaging (RLA was 8.9±3.56, Versus 9.19±3.57 PSA, p=ns). Mean CNR was also similar (RLA 156.9±55.2, versus 140.9±44.8 PSA, p=ns).

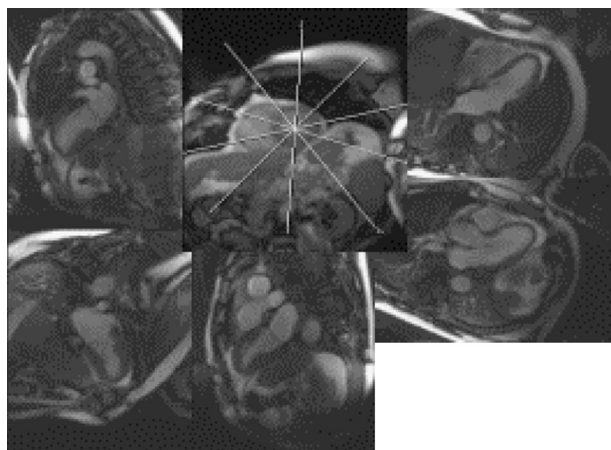


Figure 1. Five long-axis myocardial perfusion slices prescribed on a short-axis image.

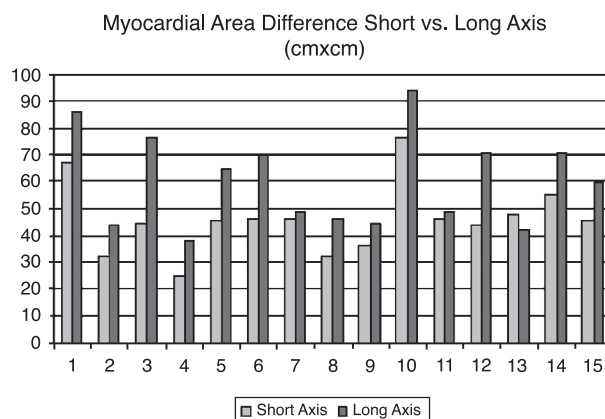


Figure 2. The imaged myocardial area differences between PSA and RLA. (View this art in color at www.dekker.com.)

Conclusions: Compared to short-axis imaging, rotational long axis perfusion images showed a substantial improvement in myocardial coverage with good depiction of true basal and apical myocardium and no change in CNR or tissue perfusion indices.

237. Rapid Quantitation of Myocardial Infarction

Andressa Borges, MD, Yi Wang, Sc.D., Roger Grimson, PhD, William Schapiro, Nathaniel Reichel, MD. *Research, St. Francis Hospital, Stony Brook University, Roslyn, NY, USA.*

Introduction: Delayed hyperenhancement (DE) imaging using inversion recovery TurboFLASH (IRTFL) CMR accurately depicts and quantitates myocardial scar or necrosis. However, each image slice requires a breath-hold. When combined with volumetric ventricular function imaging and other potentially relevant study components (e.g. assessment of mitral regurgitation, first pass rest-stress perfusion or contrast MRA), study duration may exceed patient stamina in patients with advanced heart disease. TrueFISP imaging (TFi) permits acquisition of multiple DE slices on a single breath-hold with good temporal and spatial resolution, markedly reducing imaging time, but is known to show smaller DE regions than TFL.

Purpose: We hypothesized that DE area using TFi correlates well with TFL DE area, with narrow limits of agreement, so that fast TFi can be substituted for slower TFL if required.



Methods: Contrast-enhanced (CE) MRI was performed in 20 patients (age 63.4±9.7 yrs, 14 men) with history of documented myocardial infarction (MI) using a Siemens Sonata. Contiguous short axis slices covering the entire left ventricle (LV) were obtained 10 to 20 minutes following contrast using TFL and TFi in random order. TI scout imaging was used to determine optimal inversion time prior to each type of imaging. In all, 165 DE regions were planimeted in Siemens Argus. Infarct area, LV myocardial area and % infarct were calculated. Mean signal intensity in the hyperenhanced and remote myocardium were determined on each slice and signal-to-noise(SNR) and contrast-to-noise (CNR) determined.

Results: Total DE area/pt by TFL and TFi were 41.7±27.7 and 34.8±24.8 cm² (p=0.0001) representing 24.0±14.3 and 20.3±13.4% of the LV (p<0.005). As expected, TFi area was less than TFL DE area on individual slices (m=4.6±2.9 cm² TFi vs. 5.3±3.2, TFL, p<0.05). However, DE areas by TFL and TFi correlated well (r=0.92, p<0.001, TFL=0.712+1.008(TFi). Bland–Altman analysis revealed a mean difference of 0.748±2.48 cm²(2SD). Predicted TFL, derived from TFi data, differed from actual TFL area by 0.0±2.48 cm²(2SD). Despite higher SNR (25.2±8.7, TFL vs. 31.4±12.4, TFi, p<0.01), CNR was lower with TFi (TFL: 4.5±3.4 vs. TFi: 3.4±1.9, p<0.0005).

Conclusions: TFi correlates well with TFL DE area and can be used to predict it. Thus, to avoid excessive study duration, TFi can be used as a fast DE method to quantitate infarct size. Differences between TFi and TFL infarct areas are probably due to lower CNR with TFi, which would increase partial volume effects at the periphery of infarct regions.

238. Cardiac Magnetic Resonance Imaging (cMRI) Detects Subclinical Myocardial Ischemia and Infarction in Asymptomatic End Stage Renal Disease Patients (ESRD)

Nagesh S. Anavekar, MD,¹ Marcus A. Averbach, MD,¹ Valerie Luyckx, MD,² Peter Chuang, MD,² Ming Hui Chen, MD,¹ Ajay K. Singh, MD,² Raymond Y. Kwong, MD.¹ ¹Cardiology, Brigham and Womens Hospital, Boston, MA, USA, ²Renal Medicine, Brigham and Womens Hospital, Boston, MA, USA.

Introduction: Individuals with ESRD have a high burden of coronary artery disease (CAD) and this is

the leading cause of death amongst these patients. Conventional methods for screening CAD may not be applicable amongst this cohort, as they are often asymptomatic, present atypically, have limited exercise tolerance and frequently have non-specific baseline ECG abnormalities. We determined the utility of cMRI in detecting subclinical CAD in a group of ESRD, compared to conventional clinical parameters of history, ECG and cardiac enzymes.

Methods: 12 patients with ESRD on hemodialysis (6M, 6F) at a mean age of 65±14 years were studied by cMRI. 2 studies were incomplete due to claustrophobia and/or obesity. 2 of the remaining 10 patients had a history of CAD with 1 a history of prior MI. EKG and serum troponin were performed at the time of the MRI. ST depression of 1 mm or abnormal T waves and significant q waves were used as EKG criteria for ischemia and MI respectively. Regional myocardial function and perfusion during progressive stages of dobutamine stress and delayed hyperenhancement imaging to detect MI were performed in all patients. Myocardial ischemia was defined by deterioration of regional function or perfusion during dobutamine stress; MI or scar was indicated by the presence of delayed hyperenhancement by cMRI. Regional myocardial function and perfusion during progressive stages of dobutamine stress and delayed hyperenhancement imaging were used to detect ischemia and MI respectively. All results were interpreted in a blinded fashion based on the consensus of two cardiologists. Differences between the two methods were analyzed using the χ^2 test.

Results: Our results demonstrated that none of the 10 pts demonstrated evidence of ischemia or infarction by clinical parameters despite 2 pts having a history of CAD (Table 1). Both patients with a history of CAD had cMRI evidence of MI with significant ischemia detected in 1 of the 2 pts (Figure 1). Among the 8 pts without a history of CAD, cMRI detected MI and ischemia in 5 pts. Troponin was abnormal in only 2 pts, both of which had MI by cMRI.

Conclusions: cMRI detects CAD in asymptomatic ESRD pts by detecting evidence of MI and ischemia missed by EKG, past cardiac history, and serum troponin. This supports the potential use of cMRI as

Table 1. Percentage detection of abnormalities (n=10).

Myocardial ischemia or infarction	EKG and troponin	cMRI	p value
Yes	20%	70%	<0.001
No	80%	30%	<0.001



Figure 1.

a diagnostic tool in this population but also underscores the large burden of CAD in the ESRD population.

239. Reliable Detection of Coronary Stenoses with Contrast Enhanced, 3D Free Breathing Coronary MR Angiography Using a Gadolinium-Based Intravascular Contrast Agent

Ingo Paetsch, MD,¹ Michael E. Huber, PhD,² Axel Bornstedt, PhD,¹ Friedrich Cavagna, PhD,³ Bernhard Schnackenburg, PhD,¹ Peter Boesiger, PhD,² Matthias Stuber, PhD,⁴ Eike Nagel, MD,¹ Eckart Fleck, MD.¹
¹Cardiology, German Heart Institute, Berlin, Germany, ²ETH Zurich, Zurich, Switzerland, ³Bracco Imaging SpA, Milan, Italy, ⁴Johns Hopkins University, Baltimore, MD, USA.

Background: Coronary MRA is useful for detection of stenoses in proximal and mid segments. Flow-dependent MRA techniques are hampered by signal loss from the coronary lumen. We determined the value of gadocoletic acid (B-22956; Bracco Imaging SpA, Milan, Italy), a bloodpool agent with high intravascularity (half life >4 hrs) for detection of coronary stenoses.

Methods: 10 patients with CAD underwent imaging of the left and right coronary system before and after application of a single dose of gadocoletic acid. For precontrast scanning a previously published coronary MRA standard protocol (T2Prep) and for postcontrast scanning an inversion recovery, 3D gradient echo sequence were used, both combined with real-time navigator correction. Inversion times were determined individually to ensure complete suppression of myocardium. Pre- and postcontrast we assessed parameters of image quality (signal-to-noise, contrast-to-noise ratio (CNR), vessel sharpness (VSh)), and quantitative MR angiographic parameters (number of assessable coronary segments, number of visible side branches) with a dedicated analysis tool. Sensitivity and specificity for detection of stenosis >50% were calculated on a segment-to-segment basis in pre- and postcontrast scans with x-ray coronary angiography as the standard of reference. Significance level: *p<0.05 or **p<0.01.

Results: In postcontrast scans image quality (e.g. CNR+91%**, Vsh+21%**), MR angiographic parameters and the number of assessable segments (78 vs. 92%**) increased significantly. Sensitivity and specificity for stenosis detection in precontrast vs. postcontrast scans were 65 vs. 87% and 79 vs. 90%, respectively (Fig. 1).

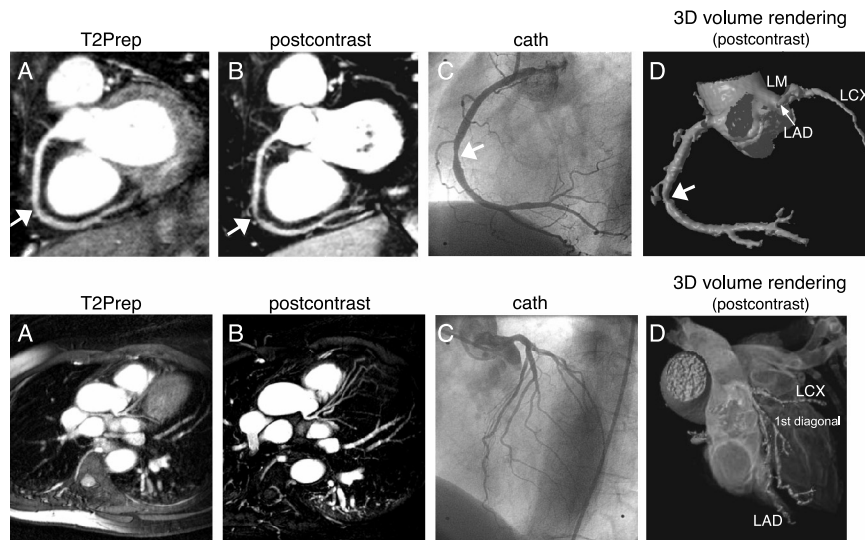


Figure 1.

Conclusions: Intravascular contrast enhancement in coronary MRA significantly improves image quality, MR angiographic measurements and diagnostic accuracy.

240. Severe Tako-Tsubo Cardiomyopathy in a Healthy Female: A Cardiac MRI Study

Ludington J. Katherine, MD, Raghu Gollapudi, MD, Nourani Sam, MD, Guy P. Curtis, MD, Robert J. Russo, MD. *Cardiology, Scripps Clinic, La Jolla, CA, USA.*

Introduction: Tako-Tsubo Cardiomyopathy is a newly recognized, stress-induced cardiomyopathy first described in Japan with unusual LV dysfunction that spares the base of the heart. The cardiomyopathy was so named by the Japanese (tako=octopus, tsubo=pot) for the dilated and akinetic appearance of the mid to distal left ventricle and sparing of the left ventricular base. The etiology of this transient syndrome of apical ballooning and its underlying pathophysiology is unknown and has not been previously characterized by the novel techniques of cardiac MRI.

Purpose: The purpose of this study was to delineate the microvascular perfusion and delayed contrast enhancing characteristics of this disorder with cardiac MRI.

Methods: A 56 year old, otherwise healthy female was admitted with 2 hours of severe, retrosternal chest pain radiating to the neck and associated with nausea, diaphoresis, and dyspnea. The chest pain began suddenly while the patient was on the witness stand for her daughter's rape trial. She had no previous history of heart disease, diabetes, hypertension, hyperlipidemia, smoking or family history of premature coronary disease. On physical examination, her jugular venous pressure was 10 centimeters, the lungs were clear, an S3 gallop was present and there was no peripheral edema. Electrocardiogram demonstrated 2 mm J-point elevation in the anterolateral leads. Cardiac enzymes were elevated with a CKMB of 12.1 units/L and a troponin I of 3.8 ng/mL. Coronary angiogram revealed normal coronary arteries without evidence of vasospasm upon nitroglycerin administration. Left ventriculogram revealed mid to distal akinesis of the heart and an LVEDP of 28 mmHg. Echocardiogram demonstrated an EF of 35% and akinesis of the anterior, lateral, inferior, septal walls in the mid to distal segments and hypercontractile function of the base of the heart. RV systolic pressure was 44 mmHG.

Results: Cardiac MRI using a 1.5 T Siemens Symphony system using steady state free precision cines during 8 second breath holds (TE/TR 1.6/3.2 ms, flip angle 60°) in long-axis planes and 3, 8-mm short-axis

slices (base, mid-ventricle and distal ventricle) revealed akinetic wall motion in the distal 2/3 portion of the heart and dyskinesis of the apex. Ejection fraction was calculated to be 27.8%. A circumferential band of hypercontractile muscle at the base was noted. First pass perfusion with Gadolinium administration of 0.05 mgmol/kg revealed global microvascular slow flow and no perfusion deficit. Delayed Gd enhanced cardiac MRI with 0.2 mmol/kg Gd showed no uptake in the myocardium. The patient remained in cardiogenic shock for 3 days requiring dopamine pressure support. Cardiac markers normalized prior to discharge and EKG changes resolved. Cardiac MRI repeated 3 weeks following hospital admission revealed normalization of the LV dysfunction with EF calculated at 43.6%. Perfusion analysis showed rapid microvascular flow in the myocardium compared to the previous study and no Gd hyperenhancement was seen on delayed imaging. Follow up echocardiogram confirmed the normalization of LV function. The patient has remains asymptomatic.

Conclusions: This is the first characterization by cardiac MRI of Tako-Tsubo cardiomyopathy, a rare and unusual form of stress-induced cardiomyopathy mimicking acute MI that spares the base of the heart and results in severe apical hypokinesis. Cardiac MRI with first pass perfusion demonstrates global microvascular dysfunction and delayed ceMRI shows no infarction despite elevated cardiac markers. The lack of delayed Gd uptake is similar to that of acute myocarditis described by McCrohon et al (*Circulation* 2003; 108:54). Novel cardiac MRI techniques of first pass and delayed contrast-enhanced MRI help further characterize this unusual form of cardiomyopathy with microvascular dysfunction that normalizes with time. 2 other cases at our institution reveal similar MRI patterns.

Delayed enhanced Gd SAX image:

241. A "One-Stop-Shop" Method of Assessing Ischemic Heart Disease Using CMR

Javier Sanz, MD, Paola Kuschnir, MD, Teresa Rius, MD, Rafael Salguero, MD, Michael Poon, MD. *Cardiology, Mount Sinai School of Medicine, New York, NY, USA.*

Introduction: Evaluation of patients with ischemic heart disease (IHD) often requires multiple tests and is time consuming. CMR is particularly well suited for the evaluation of IHD in one single setting. We report our experience on the feasibility of a "one-stop-shop" approach.



Purpose: To assess the feasibility of a rapid, efficient method of evaluating IHD with CMR.

Methods: We performed a comprehensive evaluation of IHD in a clinical magnet (1.5 T). The protocol included perfusion under pharmacologic stress with adenosine (140 µg/kg/min), resting biventricular function, rest perfusion, delayed hyperenhancement (cumulative gadolinium dose of 0.2 mmol/kg) and stress function with dobutamine (increasing doses of 5, 10, 20, 30 and 40 µg/kg/min±atropine). We employed a steady-state free precession sequence for rest and stress function (TrueFISP), a modified trueFISP sequence with partial Fourier acquisition for perfusion analysis and a phase-sensitive inversion-recovery prepared fast gradient-echo sequence for the detection of infarction.

Results: In one year, 49 individuals (34 males, mean age=64.8) were evaluated. 12 were referred to rule out coronary artery disease and 37 had some evidence of IHD (21.6% abnormal noninvasive tests, 40.5% with prior infarction and 56.7% with percutaneous or surgical revascularization). Mean study duration was 68.9 minutes (range: 45–96). Mean dobutamine dose achieved was 31.4±9.2 µg/kg/min. No major complications were observed. 8 patients had chest pain, 2 had multiple extrasystole and 1 paroxysmal atrial fibrillation. CMR detected IHD in 22 (44.9%) subjects: myocardial infarction in 15 by delayed hyperenhancement (6 with viability as determined by low-dose dobutamine) and ischemia in 14 (7 by perfusion, 2 by high-dose dobutamine and 5 with both). In 22 patients (44.9%) additional tests (within 12 months of the CMR) were available. CMR agreed with coronary angiography in all the cases (11 studies) and with other non-invasive tests in 12 cases. Of the 10 cases where there was disagreement between CMR and other non-invasive modalities, only 5 of them had angiography and the angiogram was in agreement with CMR.

Conclusions: This “one-stop-shop” ischemic protocol with CMR is feasible and safe. Initial results in comparison with other diagnostic tests are highly promising. On-going study is in progress to assess the sensitivity and specificity of this rapid and efficient method of evaluating IHD.

242. Peak Total CPK Correlates with Cardiac MR Infarct Size in Reperfused Acute ST Elevation Myocardial Infarction

Appelbaum Evan, MD, Ganesh Venkataraman, MD, Kraig V. Kissinger, RT, Thomas Hauser, MD, Susan

Yeon, MD, Warren J. Manning, MD. *Division of Cardiology, Beth Israel Deaconess Medical Center, Boston, MA, USA.*

Introduction: Peak total creatine phosphokinase (CPK) has been shown to be both an accurate estimate of radionuclide estimated infarct size and a strong predictor of prognosis following acute myocardial infarction. The ability of cardiovascular magnetic resonance (CMR) to accurately assess infarct size, as compared with peak total CPK, has not been fully studied.

Purpose: To compare peak total CPK with CMR infarct size after ST-elevation MI.

Methods: We studied 9 patients (7 males, ages 42–82) presenting to our institution with acute ST-elevation MI treated with primary angioplasty and stenting. Serial CPK (IU/L) was measured q6–8 hours for the first 48 hours after admission. CMR (1.5 T, Philips ACS-NT, Best, NL) was performed within 4–7 days after presentation using a 2-D contiguous, short-axis stack (10 mm slice thickness) of images using a segmented inversion-recovery (IR) TFE sequence obtained 10 minutes after an intravenous injection of 0.1 mmol/kg of gadolinium. Volumetric image analysis was performed on a separate workstation to measure total LV myocardial volume and the regional volume of delayed hyperenhancement (infarct). Infarct size was expressed as a % total LV mass (mass of hyperenhanced region/total LV mass).

Results: CMR infarct mass ranged from 4–91 grams. Infarct size ranged from 3–37% total LV mass. Peak CPK ranged from 582–4218 IU/L. There was a significant correlation between peak CPK and %LV infarct mass (R^2 0.86, $p=0.05$ (see Figure 1)).

Conclusions: CMR infarct size correlates strongly with peak total CPK in any patient with reperfused ST-elevation MI. These data may extend our understanding of the relationship between total CPK and LV remodeling.

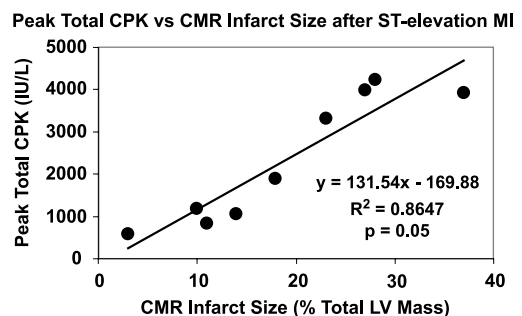


Figure 1.

243. Prediction of Left Ventricular Systolic Dysfunction and Dilatation by Contrast Enhanced Cardiac Magnetic Resonance in Patients with Myocardial Infarction

Paola Kuschnir, Javier Sanz, MD, Teresa Rius, MD, Rafael Salguero, MD, Frank Macaluso, RT, Paul Wisdom, RT, Michael Poon, MD. *Cardiology, Mount Sinai School of Medicine, New York, NY, USA.*

Introduction: Larger infarctions are clinically associated with depressed systolic function, more remodeling and poor prognosis. Cardiac magnetic resonance (CMR) is the gold standard for the evaluation of ventricular volumes and ejection fraction (EF). Delayed hyperenhancement (DH) can accurately detect and quantify myocardial infarction (MI).

Purpose: To analyze the correlation between infarct size and left ventricular parameters as determined with CMR.

Methods: Patients undergoing CMR in a 1.5 clinical magnet with coronary artery disease and positive DH were identified. Left ventricular (LV) end-diastolic volume (EDV), end-systolic volume (ESV), EF and myocardial volume were calculated from cine images obtained with a steady-state free precession sequence (*TrueFISP*). DH was assessed with a phase-sensitive inversion-recovery prepared fast gradient-echo sequence (*turboFLASH*) covering the LV with contiguous short-axis images. The total volume of scar tissue was quantified and expressed as a percentage of the total LV myocardial volume. Correlation with LV volumes and EF was estimated with Pearson's correlation coefficient and linear regression analysis.

Results: 15 patients were included (13 males, mean age=68.37, range=51–85). Mean and standard deviations for EF, EDV, ESV, MI volume and MI percentage were 46.3±11.3%, 173.4±5.4 ml, 99.1±44.5 ml, 22.7±5.5 ml and 16.5±10.8% respectively. MI volume and MI percentage showed a strong negative correlation with LVEF and ($r=-0.82$ and -0.87 respectively) and positive correlation with LV ESV ($r=0.78$ and 0.67 respectively) and ESV index ($r=0.76$ and 0.64 respectively). Correlations with EDV an EDV index were only moderate to poor ($r=0.29-0.50$). The percentages of infarcted LV associated with any (EF<50%) or severe (EF<35%) LV dysfunction were 12.4% (9.4%–18.8%; 95% confidence interval) and 29% (22%–43.8%, 95% confidence interval) respectively.

Conclusions: The extent of myocardial infarction identified with DH CMR is strongly correlated with LV systolic dysfunction and increased ESV. In this study a loss of at least 12% and 29% of total LV

myocardial volume were predictors of mild or severe systolic dysfunction.

244. A Simple Approach for Reproducible Slice Positioning of Short-Axis Cine MRI

Daniel R. Messroghli, MD, Gavin J. Bainbridge, MSc, Khaled Alfakih, MBBS, Tim R. Jones, MSc, Sven Plein, MD, John P. Ridgway, PhD, Mohan U. Sivananthan, MD. *Cardiac MRI Unit, Leeds General Infirmary, Leeds, United Kingdom.*

Introduction: The same properties which make cardiac MR an excellent tool for the assessment of global left ventricular function come into play when regional wall motion is to be addressed. For comparison between different patients and for follow-up studies it is necessary to identify corresponding areas of the left ventricle (LV). A consensus statement has established guidelines for the definition of standard segments of the LV, but has not provided guidance for the practical assessment of these segments.

Purpose: To study accuracy and robustness of a simple approach for the positioning of standard short-axis (SAX) slices for cine MRI.

Methods: Steady-state free precession cine MR studies were performed in 29 healthy volunteers (15 male, age 29±10 years) and in 20 infarct patients (18 male, age 57±12 years) with regional and global wall motion abnormalities. In systolic long axis images of the heart, 5 slices were positioned with an inter-slice gap chosen to cover the LV from apex to base (Figures 1 and 2). The middle 3 slices were selected for actual imaging of SAX cine studies ("3-of-5"). In the resulting basal, mid-cavity and apical slices, agreement with criteria for standard slices (Table 1) was tested and compared to the results from conventional multi-slice SAX ("multi-SAX") images (n=39). All volunteers underwent a second 3-of-5 study performed by a different radiographer. Inter-slice gap and end-diastolic diameters were determined as markers for positioning. End-diastolic wall thickness (EDW), end-systolic wall thickness (ESW), and absolute wall thickening (WTN) were measured for all 3 slices. All parameters were compared between the 2 set-ups using Pearson's correlation and Bland-Altman analysis.

Results: Slices derived from 3-of-5 met the criteria by 91.1% in volunteers and 85.8% in patients (multi-SAX: 91.2% and 90.0%, respectively). There was very



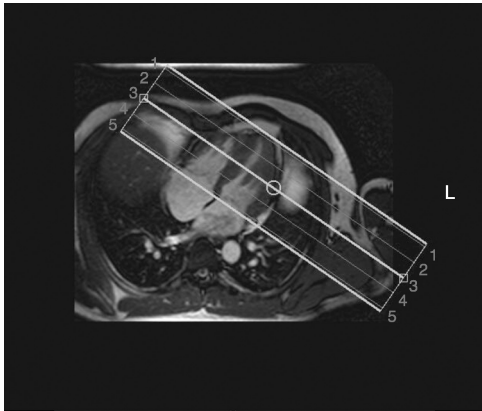


Figure 1. (View this art in color at www.dekker.com.)

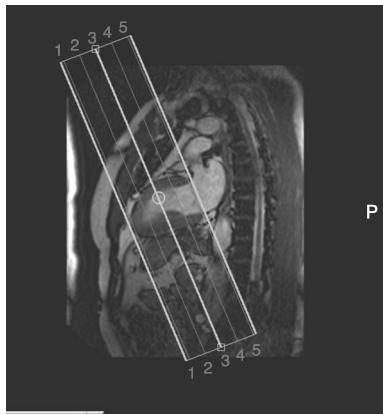


Figure 2. (View this art in color at www.dekker.com.)

good agreement of inter-slice gap and LV diameters in the 2 set-ups ($r > 0.83$). Good inter-study, inter-observer, and intra-observer agreement were found for EDW, ESW and WTN in basal, mid-cavity, and apical slice.

Conclusions: The 3-of-5 approach provides standard SAX slices for the evaluation of regional wall motion in an uncomplicated and highly robust fashion.

245. Evaluation of Myocardial Ischemia by Myocardial Stress Perfusion with Dipyridamole in Renal Transplant Candidates—Comparison with SPECT and Coronary Angiography

Joalbo M. Andrade, MD,¹ Luiz H. Gowdak, MD,¹ Flávio J. Paula, MD,² José R. Parga, MD,¹ Luiz F. Ávila, MD,¹ José A. F. Ramires, MD,¹ José J. G. Lima, MD,¹ Carlos E. Rochitte, MD.¹ ¹Heart Institute-InCor—University of São Paulo Medical School, São Paulo, Brazil, ²Nephrology, University of São Paulo Medical School, São Paulo, Brazil.

Introduction: Myocardial first-pass perfusion imaging by magnetic resonance (MPI) during pharmacological stress has been shown to detect coronary artery disease (CAD) and to have good correlation with coronary angiography (CA) and nuclear medicine techniques (NM). This technique has been used in patients with suspected CAD, but few data is available on the application of MPI in specific populations, as renal transplant candidates (RTC). Moreover, the noninvasive diagnosis of CAD on this population has been shown to be a challenge by traditional methods.

Purpose: The aim of this study was to determine the efficacy of dipyridamole MPI in the detection of significant CAD in RTC that are considered at high-risk for CAD.

Table 1. Criteria for definition of representative short-axis slices; specifications in italics.

Slice	Criteria
Basal	Tips of the mitral valve leaflets visible. <i>Moving structure between anterior and posterior papillary muscles, attributable to fish-mouth configuration, different from pure flow artefacts in other slices.</i> Tips of the papillary muscles visible at end-diastole. <i>More than 50% area of tips of papillary muscles must disappear in systole.</i> Myocardium present in 360° of LV circumference (no outflow tract visible). <i>Systolic thickening must be present in all segments (except if infarcted).</i>
Mid-cavity	Papillary muscles clearly visible throughout the cardiac cycle. <i>Papillary muscles must be separated from LV wall.</i>
Apical	No papillary muscles included. <i>Papillary muscles differ from anterior or posterolateral trabeculations by being thicker than septal trabeculations in the same slice.</i> Cavity present throughout the cardiac cycle.

Methods: Fifty-two patients, 41 (78.8%) males, mean age 58.1 years, were studied prospectively with stress SPECT sestamibi-Tc^{99m} and MPI. All patients were referred for CA as routine pre-surgical evaluation for renal transplant. High-risk for CAD was defined by at least one of the following criteria: 1) insulin-dependent diabetes mellitus, 2) age >50 years, 3) history of angina, 4) history of congestive heart failure, and 5) abnormal electrocardiogram (excluding LV hypertrophy). MPI was performed on a 1.5 T SIGNA CV/i GE system with a phased-array coil and a hybrid sequence to acquire LV short-axis slices. MPI temporal resolution was 1RR, except if at least 4 short-axis slices were unable to be prescribed. Then, a 2RR acquisition was prescribed. The parameters were: TR 6.3 ms, TE 1.2 ms, matrix 128 × 128, and FOV 34–38 cm. Dipyridamole was administered intravenously (0.56 mg/kg/4 min). Gadolinium dose was 0.05 mmol/kg, injected intravenously at a 5 ml/sec rate by a power injector. The short-axis MPI images were analyzed visually by 2 observers blinded to the CA and SPECT results. Each patient was classified as with or without significant CAD based on the presence of significant myocardial perfusion defect. Data analysis was done considering as significant CAD, a CA with at least one main coronary artery branch with an obstructive lesion of more than 50%; and a second analysis considering lesions with more than 70% obstruction. Sensitivity, specificity, predictive values, and accuracy were defined for SPECT and MPI studies using CA as the reference method (Marwick et al., 1990).

Results: The prevalence of significant CAD by CA was 63.5% (33/52) for lesions more than 50% and 55.8% (29/52) for lesions more than 70%. The NM showed a sensitivity of 50.0% and specificity of 84.2% in patients with lesions more than 50.0% and a sensitivity of 53.6% and specificity of 82.6% in patients with lesions more than 70%. The MPI had a sensitivity of 69.7% and specificity of 84.2% for lesions more than 50% and a sensitivity of 69.0% and specificity of 73.9% in patients with lesions more than 70%. Table 1 depicts the

Table 1. Results of MPI and SPECT compared to CA with both thresholds (50 and 70% coronary lesions).

	CA >50%		CA >70%	
	MPI	SPECT	MPI	SPECT
Sensitivity	69.7	50.0	69.0	53.6
Specificity	84.2	82.6	84.2	73.9
Accuracy	75.0	62.7	71.2	66.7
Positive predictive value	88.5	84.2	76.9	79.0
Negative predictive value	61.5	50.0	52.5	59.4

sensitivity, specificity, predictive values and accuracy for both methods. Figure 1 depicts an agreement between MPI with 2 perfusion defects (anterior and inferior segments) and CA with 2 stenotic lesions (LAD and RCA) in the same patient.

This is the first investigation directly comparing MPI and SPECT studies in high-risk RTC. In our study, MPI sensitivity and specificity were better than SPECT, in both analyses, for the detection of significant CAD. However, the overall results have shown that the noninvasive diagnosis of CAD on this subgroup of patients remains a difficult task. Possible interfering factors may be the presence of microvascular disease, the functional significance of the angiographic lesion and the effectiveness of the pharmacological agent in this population.

Conclusions: Myocardial perfusion imaging by magnetic resonance is a useful alternative to evaluate high-risk renal transplant candidate and probably may help to reduce the need of pre-surgical evaluation by coronary angiography.

REFERENCE

Marwick, T. H., et al. (1990). *Transplantation* 49(1):100–103.

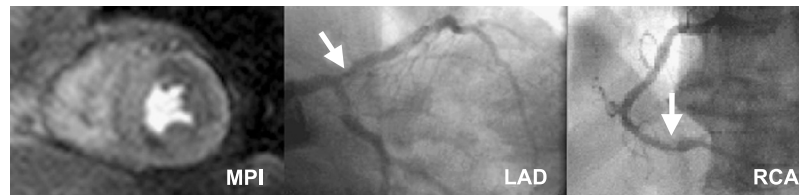


Figure 1.

246. Alteration of the β -Adrenoceptor Axis in Human Hibernating Myocardium Detected by CMR

Anna S. John,¹ Christophe Depre,² Ornella E. Rimoldi,³ Jadwiga Markiewicz,² John R. Pepper,⁴ Gilles D. Dreyfus,⁵ Dorothy E. Vatner,² Dudley J. Pennell,¹ Paolo G. Camici³. ¹CMR Unit, Royal Brompton Hospital, London, United Kingdom, ²Cardiovascular Research Institute, University of Medicine and Dentistry, Newark, NJ, USA, ³PET Cardiology, Hammersmith Hospital, London, United Kingdom, ⁴Cardiothoracic Surgery, Royal Brompton Hospital, London, United Kingdom, ⁵Cardiothoracic Surgery, Harefield Hospital, London, United Kingdom.

Background: Chronic left ventricular dysfunction in patients with coronary artery disease (CAD) may improve after revascularisation (hibernating myocardium). The mechanisms of ventricular dysfunction in these patients remain poorly understood. We hypothesised that the β -adrenoceptor (β AR) axis is abnormal in patients with hibernating myocardium. We therefore we measured on human biopsies ex vivo the expression and function of regulators of the β -AR pathway and correlated the results with functional measurements by CMR and PET in vivo.

Methods: Six patients with severe CAD awaiting bypass surgery underwent CMR for hibernation studies on a Siemens Sonata 1.5T scanner using standard trueFISP cines in long and short axis orientations to assess wall motion followed by late enhancement studies with a standard inversion recovery sequence after 0.1 mmol/kg gadolinium to assess viability. FDG-PET was performed on a Siemens ECAT 931 scanner to confirm viability. Myocardial pre-synaptic norepinephrine reuptake (volume of distribution, ml/g) was measured using PET with C11-labelled hydroxyephedrine, and C11 labelled CGP-12177 was used to measure β AR density (pmol/g). PET data for norepinephrine reuptake and β AR density in our patient population were compared with those in a group of normal controls (n=30). CMR wall motion and viability data as well as PET data were analysed using a 16 segment model. Dysfunctional, but viable segments (by CMR and FDG-PET) subtended by a significantly stenosed coronary artery were defined as hibernating. Myocardial biopsies were taken during bypass surgery from hibernating and remote control myocardium and processed for RNA extraction. Transcripts encoding β 1AR, β 2AR, Gs- α , and adenylylase-6 (AC) were specifically measured by quantitative PCR and normalised per cyclophilin (cph) used as housekeeping gene.

Table 1.

Values are mean \pm SD	Hibernating	Remote	p Value
C11-hydroxyephedrine (ml/g)	47.3 \pm 24.4	43.1 \pm 18.9	ns
C11-CGP-12177 (pmol/g)	6.4 \pm 2.2	6.7 \pm 1.3	ns
beta-AR1 (per cph)	6.0 \pm 2.0	1.5 \pm 1.0	<0.05
beta-AR2 (per cph)	0.5 \pm 0.2	1.5 \pm 0.5	<0.05
Gs-alpha (per cph)	6 \pm 2	26 \pm 6	<0.01
AC (per cph)	0.05 \pm 0.01	0.2 \pm 0.1	<0.01

Results: Both norepinephrine re-uptake and β AR density in vivo were globally reduced (p<0.05) in patients compared to controls, with no difference between hibernating and remote myocardium. β 1AR and β 2 AR mRNAs were reciprocally regulated, with no change in global β AR expression. By contrast, intracellular mediators of the β AR axis (Gs- α and AC mRNAs) were markedly reduced (Table 1).

Conclusion: Pre-synaptic norepinephrine re-uptake, β AR density and expression between hibernating and remote myocardium as detected by CMR are similar, but the intracellular signalling pathway of β -adrenergic stimulation is reduced in hibernating myocardium. This may explain contractile dysfunction of hibernating myocardium at rest in the presence of a maintained response to dobutamine stress. These data also demonstrate that the molecular adaptation in hibernation is different from that of heart failure.

247. Comparison of Dobutamine Stress MR, Adenosine Stress MR and Adenosine Stress Perfusion

Ingo Paetsch, MD,¹ Cosima Jahnke, MD,² Rolf Gebker, MD,¹ Michael Neuss, MD,¹ Andreas Wahl, MD,³ Eike Nagel, MD,¹ Eckart Fleck, MD.¹ ¹Cardiology, German Heart Institute, Berlin, Germany, ²Cardiology, University of Freiburg, Freiburg, Germany, ³Cardiology, Cardiovascular Center, Bern, Switzerland.

Background: Dobutamine stress MR (DSMR) is highly accurate for the detection of inducible wall motion abnormalities (WMA). Adenosine has a more favourable safety profile and is well established for the assessment of myocardial perfusion. We evaluated the diagnostic

value of inducible WMA during DSMR and adenosine stress compared to adenosine stress perfusion.

Methods: 40 consecutive pts (previous revascularization, no prior myocardial infarction) scheduled for cardiac catheterization underwent cardiac MR (1.5 T MR, Intera, Philips). After 4 min of adenosine infusion (140 µg/kg/min, 6 min infusion duration) wall motion scans were acquired (steady-state free precession) and, subsequently, perfusion scans (3 slice-TFE-EPI; resolution 2.6×2.6 mm, 0.05 mmol/kg Gd-BOPTA i.v. bolus). After a 15 min break, rest perfusion scanning was performed, followed by DSMR using a standard high-dose regime (up to 40 µg/kg/min plus atropine). Wall motion was analyzed by 2 observers based on a segment-to-segment approach, classified as pathologic if ≥2 segments showed inducible WMA. The transmural extent of inducible perfusion defects (<25%, 25–50%, 51–75% and >75%) was used to grade perfusion scans. Quantitative coronary angiography was performed with significant stenosis defined as >50% diameter stenosis (Figure 1).

Results: 28 pts (67%) had coronary artery stenoses >50%, sensitivity and specificity for detection by dobutamine and adenosine as well as adenosine perfusion are shown in the Table 1. Adenosine inducible WMA were only seen in segments with >75% transmural perfusion deficit.

Table 1.

	DSMR	Adenosine wall motion	Adenosine perfusion
Sensitivity in %	86	39	86
Specificity in %	83	83	67

Conclusions: In patients after revascularization dobutamine is superior to adenosine stress for the induction of WMA. Visual assessment of adenosine perfusion is highly sensitive with a low specificity. DSMR yields the highest diagnostic accuracy.

248. Elective Angioplasty Induces Resting Microvascular Perfusion Abnormalities Detectable by Magnetic Resonance Imaging

Andrew J. Taylor, F.R.A.C.P.,¹ Nidal Al-Saadi, MD,² Hassan Abdel-Aty, MD,² Jeannette Schulz-Menger, MD,² Daniel R. Messroghli, MD,² Michael Gross, MD,² Matthias G. Friedrich, MD². ¹Baker Heart Research Unit, Melbourne, Australia, ²Helios-Klinikum Berlin, Kardiologie, Franz-Volhard-Klinik, Berlin, Germany.

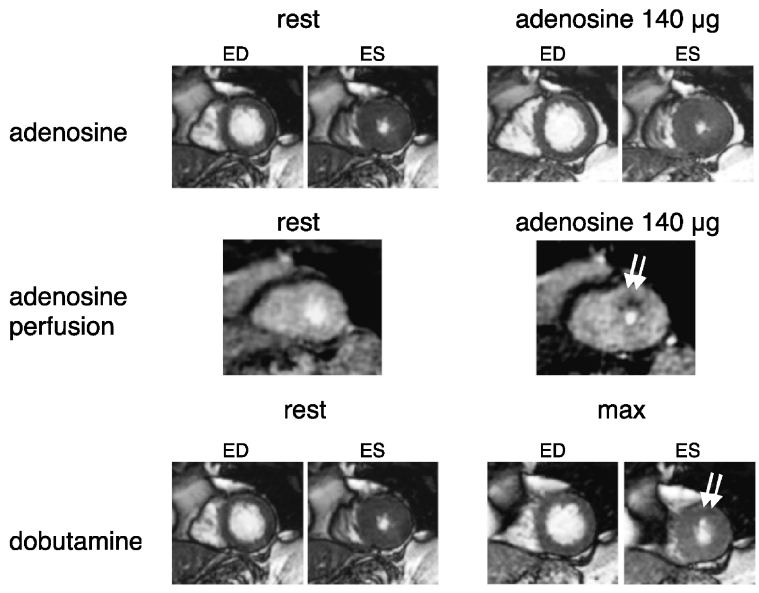


Figure 1. Example of a false negative examination regarding adenosine inducible wall motion abnormality. Upper row: the adenosine stress and rest scan are both normal with a hypercontractile response in all myocardial segments. Middle row: the adenosine perfusion scan shows a perfusion deficit with a 50% transmural extent in the anterior segment. Bottom row: dobutamine stress MR confirms an ischemic reaction in the anterior segment showing akinesia. Coronary angiography revealed an in-stent restenosis of the proximal LAD (QCA: 56%).

Introduction: Percutaneous coronary intervention (PCI) is known to induce atherosclerotic plaque rupture, which may have an effect on distal microvascular perfusion, mediated through either microembolisation or microvascular constriction.

Purpose: We utilised cardiac magnetic resonance imaging (CMR) to assess the impact of PCI on resting microvascular perfusion.

Methods: CMR was performed on 15 patients with stable coronary artery (CAD) disease prior to and within 24 hours following PCI, and also in 10 control patients utilising a clinical 1.5T CMR scanner. Microvascular perfusion was evaluated at rest by first-pass perfusion CMR (saturation recovery, gradient echo/echo planar-readout sequence, TR/TE 113–134 ms/1.3–1.7 ms, flip angle 25°, slice thickness 15 mm) following a bolus of Gadolinium-DTPA (0.1 mmol/kg) by calculating the time to 50% maximum myocardial enhancement ($T_{50\%max}$). The relative contrast delay in the region of myocardium subtended by the treated artery post-PCI was calculated by subtracting the $T_{50\%max}$ in this region from a remote region, which was then compared with its corresponding pre-PCI value. Left ventricular function was assessed by a steady state free precession pulse sequence (TR3.8 ms, TE 1.6 ms, 30 phases, slice thickness 15 mm) and percent myocardial systolic thickening was calculated.

Results: In control subjects, contrast wash-in was slower in the myocardium supplied by the left circumflex (mean delay 0.5 ± 0.2 seconds, 95% confidence interval 0.9–0.1 seconds) and right coronary arteries (mean delay 1.1 ± 0.3 seconds, 95% CI 0.6–1.6 seconds) compared with the left anterior descending coronary artery territory. In CAD subjects, PCI resulted in a significant increase in the relative contrast delay in the region of myocardium subtended by the treated artery post-PCI (mean delay 0.6 ± 0.2 seconds vs. 0.0 ± 0.2 seconds pre-angioplasty, $P < 0.05$), consistent with reduced resting microvascular perfusion. There was no change in mean systolic thickening in the region of myocardium subtended by the treated artery post-PCI ($54 \pm 7\%$ pre-PCI vs. $53 \pm 5\%$ post PCI, $P = NS$).

Conclusions: CMR detects subtle variations of resting microvascular perfusion in health, with contrast wash-in delays corresponding to the left circumflex and right coronary artery territories, presumably due to the initial atrioventricular course these vessels run prior to perfusing the myocardium. In CAD, contrast wash-in is delayed in the area of myocardium subtended by the treated artery following PCI, consistent with impairment of microvascular perfusion induced by plaque rupture.

249. Cut-off Values for CMR Flow Parameters to Detect Significant Stenoses in Saphenous Vein Coronary Artery Bypass Grafts

Liesbeth P. Salm,¹ Hubert W. Vliegen,¹ Susan E. Langerak,¹ Jeroen J. Bax,¹ Wouter Jukema,¹ Aeilko H. Zwinderman,² Hildo J. Lamb,³ Albert De Roos,³ Ernst E. Van der Wall.¹ ¹Cardiology, Leiden University Medical Center, Leiden, Netherlands, ²Medical Statistics, Academic Medical Center, Amsterdam, Netherlands, ³Radiology, Leiden University Medical Center, Leiden, Netherlands.

Introduction: In the evaluation of stenoses in saphenous vein coronary artery bypass grafts, coronary angiography is considered the gold standard. However, this is an invasive procedure with a small risk of serious complications. Cardiovascular magnetic resonance (CMR) with flow mapping is a potential noninvasive method to measure flow in vein grafts.

Purpose: To evaluate vein graft disease by CMR with flow mapping, and to formulate cut-off values to maximally separate normal from diseased grafts.

Methods: A total of 69 patients underwent coronary angiography due to recurrent chest pain, late after bypass surgery. In order to determine the stenosis severity objectively quantitative coronary arteriography (QCA) was performed. CMR with flow mapping at rest and during adenosine stress was performed. Rest and stress volume flow, systolic and diastolic peak flow (SPF; DPF) were derived from flow maps and coronary flow reserve (CFR) and diastolic-to-systolic flow ratio (DSFR) were calculated. ROC and logistic regression analysis was performed to calculate the sensitivity and specificity to determine the diagnostic performance of CMR flow parameters for the detection of stenoses=50% in vein grafts and optimal cut-off values for CMR flow parameters were formulated.

Results: A total of 125 vein grafts were studied. Stenoses as measured by QCA ranged from 0–100% with a mean stenosis severity of $46 \pm 39\%$. For single vein grafts ($n=81$) sensitivity and specificity of 87% (80–94%) and 79% (70–88%) were found for the detection of stenoses=50% ($p < 0.001$). For sequential vein grafts ($n=44$) sensitivity and specificity of 94% (87–100%) and 62% (48–76%) were demonstrated ($p=0.001$). Optimal cut-off values for CMR flow parameters are shown in Table 1.

Conclusion: CMR with flow mapping has a good performance in the detection of stenoses=50% in single and sequential vein grafts. Cut-off values can be used to accurately interpret flow maps of bypass grafts.

Table 1. Optimal cut-offs for CMR flow parameters.

Single vein grafts		Sequential vein grafts	
Volume flow baseline (ml/min)	24.2 [†]	Volume flow baseline (ml/min)	40.9*
Volume flow stress (ml/min)	48.7 [†]	Volume flow stress (ml/min)	93.6*
SPF baseline (ml/s)	0.83 [†]	SPF baseline (ml/s)	1.17*
SPF stress (ml/s)	1.49 [†]	SPF stress (ml/s)	2.28*
DPF baseline (ml/s)	1.18 [†]	DPF baseline (ml/s)	1.48
DPF stress (ml/s)	2.03 [†]	DPF stress (ml/s)	3.60*
CFR	1.56 [†]	CFR	1.87
DSFR baseline	0.93 [†]	DSFR baseline	0.99
DSFR stress	1.08 [†]	DSFR stress	1.41

[†]p<0.005.

*p<0.05.

250. Effects of Off Pump Versus on Pump Coronary Surgery on Early and Late Post-Operative Left Ventricular Function: A Randomised Trial Using Cardiovascular Magnetic Resonance Imaging

Joseph B. Selvanayagam,¹ Jane M. Francis,¹ Steffen E. Petersen,¹ Frank Wiesmann,¹ Matthew D. Robson,² Attila Kardos,¹ David P. Taggart,³ Stefan Neubauer.¹
¹Department of Cardiovascular Medicine, University of Oxford Centre for Clinical Magnetic Resonance Research, John Radcliffe Hospital, Oxford, United Kingdom, ²Department of Biochemistry, University of Oxford Centre for Clinical Magnetic Resonance Research, John Radcliffe Hospital, Oxford, United Kingdom, ³Department of Cardiothoracic Surgery, John Radcliffe Hospital, Oxford, United Kingdom.

Introduction & Aim: There is biochemical evidence that off pump coronary artery bypass grafting (OPCABG) reduces myocardial injury when compared to the use of cardiopulmonary bypass (ONCABG), but the functional significance of this is uncertain. We hypothesized that OPCABG surgery would result in improved early and late left ventricular function compared with ONCABG surgery.

Methods: In a single centre randomised trial, 30 patients undergoing multi-vessel total arterial revascularization were randomly assigned to OPCABG and 30 patients to ONCABG surgery. Patients underwent pre-operative, early (day 6) and late (6 months) post-operative cine MRI for global left ventricular function and regional wall motion assessment.

Results: The two surgical groups were well matched in terms of pre-operative (age, cardiopulmonary risk factors, pre-operative medication use) and peri-operative

(number of distal anastomoses, inotropic requirements) factors. The mean pre-operative cardiac index was similar in the two surgical groups (2.9±0.7 ONCABG; 2.9±0.8 OPCABG; p=0.9). Early post-operatively, the cardiac index was significantly higher in the OPCABG group (2.7±0.6 ONCABG; 3.2±0.8 OPCABG; p=0.04). The mean pre-operative ejection fraction was 62%±12% in the ONCABG group and 62%±11% in the OPCABG group (p=0.9). In the early post-operative period this decreased to 59%±11% in the ONCABG group and increased to 65%±12% in the OPCABG group (p=0.03 for the change in EF). When assessed at 6 months, the mean cardiac index was 3.1±0.6 in the ONCABG group and 3.1±0.8 in the OPCABG group (p=0.7). Ejection fraction at 6 months was significantly improved compared with pre-operative measurements for both groups (p>0.05 for each), but not significantly different between the two surgical groups (p=0.5).

Conclusion: In patients undergoing isolated coronary artery grafting, OPCABG surgery results in significantly better left ventricular function early after surgery, but at 6 months both surgical groups show a similar benefit in left ventricular function from revascularization.

251. Reliability of Cardiac Magnetic Resonance for Prediction of Systolic Function Recovery After First Acute Myocardial Infarction With Open Artery

Ma Pilar Lopez-Lereu, MD,¹ Jordi Estornell,¹ Vicente Bodi, MD,² Alicia Maceira, MD,¹ Begoña Igual, MD,¹ Joaquin Martin.¹ ¹Cardiology, ERESA, Valencia, Spain, ²Cardiology, Clinic University Hospital, Valencia, Spain.

Introduction: Assessment of systolic function and infarct size is essential for establishing patient prognosis after an acute myocardial infarction (MI).

Purpose: To assess the usefulness and diagnostic accuracy of early cardiac magnetic resonance (CMR) markers for prediction of systolic function recovery and ventricular remodelling after first MI with open infarct related artery (IRA).

Methods: 17 patients with first ST elevation MI were prospectively studied. All of them had Q waves in at least 2 leads and open IRA. Coronary angiography was carried out (median 5 days postMI), and PCI (PTCA±stent) was done when a significant lesion was found. The CMR study was done (median 7 days postMI) with a 1.5T unit (Sonata Magnetom; Siemens, Erlangen, Germany) and the initial protocol included: 1) left ventricular volumes and global systolic function assessment, 2) regional assessment with a 16 segment model, measuring wall thickness in diastole (DW, mm), wall thickening at baseline (BWT, mm) and at low dose (10 mcg/K/min) dobutamine infusion (Δ dob, mm), 3) myocardial perfusion study after gadolinium-DTPA 0.1 mmol/kg (Perf: 0=absence of perfusion, 1=preserved perfusion), and 4) gadolinium inversion-recovery sequences to assess transmural enhancement (Trans, %). 6 months later a new coronary angiography in which IRA patency was documented was done, and a second CMR study was performed including 1) assessment of left ventricular volumes (ml/m²) and ejection fraction (%), 2) regional wall motion and wall thickening (Δ 6 m, mm).

Results: 272 segments were analyzed, 73 segments (27%) with at least severe hypokinesia (BWT<2 mm) were furtherly assessed in order to analyse sensitivity, specificity and diagnostic accuracy (area under the ROC curve (AUCROC)) of the above mentioned indexes to predict improvement of regional myocardial contractility (Δ 6 m \geq 2 mm), systolic function recovery and ventricular remodelling at 6 months. 25 of the initially dysfunctional 73 segments (WM<2 mm) (34%) showed functional improvement at follow-up (Δ 6 m \geq 2 mm). Multivariate analysis showed that gadolinium enhancement <50% of wall thickness was the only independent predictor of regional function improvement (R=0.88, p<0.0001), end-diastolic volumes (R=0.61, p=0.009) and ejection fraction (R=0.72, p=0.001) at 6 months (Table 1).

Conclusions: Wall thickness <5 mm indicates absence of viability, but it is an infrequent finding. Low-dose dobutamine response is highly specific for functional recovery, but not sensible enough. Preserved microcirculation has acceptable sensitivity. The assessment of gadolinium enhancement has the best

Table 1. Improvement of contractility at 6 months.

	Sensitivity	Especificity	AUCROC	p
DW>5 mm	100%	11%	0.62	0.1
Δ dob>2 mm	41%	87%	0.65	0.02
Perf=1	80%	62%	0.71	0.001
Trans<50%	84%	86%	0.85	<0.0001

diagnostic accuracy for predicting systolic function recovery and remodelling after first MI with open IRA, the absence of late enhancement or enhancement affecting <50% wall thickness is an accurate indicator of viability.

252. Adenosine Stress MRI for Detection of Coronary Artery Disease: Validation of Qualitative Analysis with Invasive Coronary Angiography

Anwer Qureshi, MD,¹ Arun Kalyanasundaram, MD,¹ Khan Siddiqui, MD,² Frederick Emge, MD,³ Dennis Go, MD,² Cathleen Woomert, MD,² G. Craig Wood, MS,⁴ Louis A. Nassef, MD.¹ ¹Cardiology, Geisinger Medical Center, Danville, PA, USA, ²Radiology, Geisinger Medical Center, Danville, PA, USA, ³Pediatric Cardiology, Geisinger Medical Center, Danville, PA, USA, ⁴Biostatistician, Clinical Research Department, Geisinger Health System, Danville, PA, USA.

Introduction: Adenosine stress MRI is a promising new technique for the detection of coronary artery disease (CAD). Earlier studies have reported perfusion abnormalities using time consuming computer based analysis of regional myocardial perfusion.

Purpose: There is limited information regarding assessment of CAD utilizing adenosine stress MRI with rapid qualitative analysis of regional myocardial perfusion. We present our initial results with the clinical application of this method.

Methods: Of 158 patients undergoing adenosine stress MRI, 50 had invasive coronary angiography without revascularization within six months of the MRI. In these 50 patients, 24 had MRI for evaluation of chest pain prior to the heart catheterization and 26 had MRI after the heart catheterization to determine the significance of known CAD. Qualitative MRI analysis was based on a 17-segment model. Patients were considered to have CAD by MRI if two or more myocardial segments had reduced myocardial perfusion

Table 1. Accuracy of qualitative analysis of adenosine MRI in detecting CAD: diagnostic test measures and 95% confidence.

	Sensitivity	Specificity	PPV	NPV	Accuracy
Patients (n=50)	92% (78%, 98%)	77% (46%, 95%)	77% (46%, 95%)	92% (78%, 98%)	88% (76%, 95%)
Coronary territories (n=149)	88% (78%, 95%)	87% (78%, 93%)	90% (81%, 96%)	84% (73%, 92%)	87% (81%, 92%)

or one or more segment had delayed enhancement. Patients were considered to have significant CAD by coronary angiography if one or more major coronary artery had $\geq 50\%$ stenosis. MRI studies were performed on Signa CV/I 1.5T (GE Medical Systems).

Results: Results were analyzed in two ways: patient analysis to determine the accuracy of adenosine MRI in identifying patients with one or more significant coronary stenosis, and by coronary territory analysis to recognize the accuracy of MRI in correctly identifying significant stenosis in the left anterior descending, right, and circumflex coronary territories. MRI was adequate for interpretation in all 50 patients except one in whom apical images were inadequate. Results are in Table 1.

Patient level analysis showed no difference in the accuracy of adenosine MRI when performed either before or after the heart catheterization. In addition individual coronary territory analysis for the three different coronary territories was also quite accurate in both groups. In both instances the lack of difference may be due to a small sample size.

Conclusions: Qualitative estimation of myocardial ischemia using adenosine MRI is accurate in the non-invasive diagnosis of coronary artery disease. Larger prospective studies are, however, required to validate our findings.

253. Can Assessment of RV Function Using MRI Before LVAD Placement Help Predict Post-Implantation RV Failure?

Veronica V. Lenge, MD,¹ Margit A. Nemeth, MD,² John Ho, MD,² Reynolds Delgado, MD,³ Mercedes Pereyra, MD,⁴ Raja Muthupillai, PhD,⁵ Scott D. Flamm, MD⁶. ¹Departments of Diagnostic Radiology, St. Luke's Episcopal Hospital/THI, Houston, TX, USA, ²Departments of Cardiology, St. Luke's Episcopal Hospital, THI, Houston, TX, USA, ³Cardiology, St. Luke's Episcopal Hospital, THI, Houston, TX, USA, ⁴Departments of Diagnostic Radiology, St. Luke's Epi-

cospal Hospital, THI, Houston, TX, USA, ⁵Radiology, St. Luke's Episcopal Hospital/THI, Department of Radiology, Baylor College of Medicine, Houston, Texas, Philips Medical Systems, Cleveland, OH, Houston, TX, USA, ⁶Departments of Cardiology and Diagnostic Radiology, St. Luke's Episcopal Hospital/Texas Heart Inst, St. Luke's Episcopal Hospital/THI, Houston, TX, USA.

Introduction: Right ventricular failure (RVF) after implantation of a left ventricular assist device (LVAD) is associated with high morbidity and mortality, even if these patients ultimately receive a right ventricular assist device (RVAD). Invasive hemodynamic predictors of RV failure have been evaluated, but a method for non-invasive assessment of RV failure prior to LVAD implantation would be desirable. Early detection of frank or impending RV failure prior to LVAD placement may alter clinical decision-making, possibly leading to initial biventricular assist device placement. Recently MRI has been shown to measure RV volumes and RV function accurately (Figure 1).

Purpose: The purpose of this study was to assess RV volume and function using cine MRI as potential predictors of RV failure in patients prior to LVAD implantation.

Methods: Patient Population—Fifteen patients with impending LVAD implantation were imaged with cine MRI (14 male, age 55±12 years). **MRI data acquisition**—All images were acquired at 1.5T using a commercial MRI scanner (Gyrosan NT Intera, Philips Medical Systems). A series of contiguous 10 mm thick short axis slices of the entire right

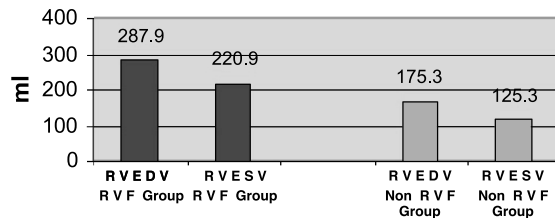


Figure 1. Right ventricular volumes. (View this art in color at www.dekker.com.)

ventricle were acquired using a steady state free precession based cine MRI sequence (balanced FFE). Specific acquisition parameters were as follows: TR/TE/flip: 3.4 msec/1.7 msec/60 deg; temporal resolution: 35 msec; breath-hold duration/slice: 6–8 sec. In addition, a four chamber long axis view was acquired using a long TE cine EPI technique for qualitative assessment of atrio-ventricular valve regurgitation with following acquisition parameters: TR/TE/flip: 31 msec/8 msec/7 deg; EPI factor: 7; temporal resolution: 30 msec. **Post processing**—The short axis slices were transferred to a post-processing workstation (EasyVision, Philips Medical Systems). An experienced reader manually traced RV and LV endocardium on diastolic and systolic images. From these tracings, RV end-diastolic volume (RVEDV), RV end-systolic volume (RVESV), RV ejection fraction (RVEF), RV stroke volume (RV SV), and RV cardiac output (RV CO) were calculated. In similar fashion, from the left ventricular (LV) endocardial contours drawn in diastole and systole, LVEDV, LVESV, and LV EF were computed. **Clinical Criteria for RVF**—RVF was defined as requirement of inotropes for 14 days or more, liver dysfunction (SGOT and SGPT > 100 U/L), renal dysfunction (creatinine > 3 mg/dl), right atrial pressure (RAP) 15 mm Hg or the need for RVAD support.

Results: Based on clinical criteria, 8/15 patients had RVF. The RVF group had a greater proportion of non-ischemic cardiomyopathy compared to the non-RVF group (86% vs. 50%). The RVEDV, RVESV, and LVEDV were significantly larger in the RVF group (all $p < 0.05$). Although statistically not significant there was a trend toward greater tricuspid regurgitation (TR), and larger RV SV in the RVF group (Table 1). The LVEF, RVEF and RV CO of the RVF group was not statistically different from the non-RVF group. Using a threshold of RVEDV > 250 cc, the sensitivity and specificity for identifying RVF was 75% and 86%,

respectively. Using a threshold of LVEDV > 300 cc identified RVF with sensitivity and specificity of 88% and 86%, respectively.

Conclusions: Neither RV EF nor LV EF is a useful predictor of RV failure after LVAD implantation. However, the dilation of the RV reflected by large RVEDV and RVESV correlates significantly with RVF following LVAD placement. Interestingly, LVEDV was also significantly larger in patients with RV failure suggesting that these patients suffer more severely from global cardiac dysfunction. Thus, pre-operative MR assessment of RV function may yield prognostic indicators for RVF after LVAD implantation. Larger trials are necessary to confirm these initial findings.

254. Papillary Muscle Hyperenhancement in Acute Myocardial Infarction is Associated with Mitral Valve Regurgitation

Hassan Abdel-Aty, Philipp Boye, Rainer Dietz, Matthias G. Friedrich. *Cardiology, Franz-Volhard Klinik, Berlin, Germany.*

Introduction: Mitral valve regurgitation complicating acute myocardial infarction (MI) predicts poor prognosis with papillary muscle infarction as an important mechanism. Hyperenhancement in cardiovascular magnetic resonance (CMR) images has a high spatial resolution to identify small areas of myocardial necrosis. The value of CMR to identify papillary muscle irreversible injury, however, is not well defined.

Purpose: We attempted to visualize papillary muscle hyperenhancement and to explore its association with mitral regurgitation in patients after acute MI.

Methods: We studied 29 patients with first reperfused acute MI (26 males) on a 1.5 T scanner applying an inversion recovery gradient echo pulse sequence (TR 5.5 ms, TE 1.4 ms, TI 200–250 ms) in 3 short and 3 long axis slices. Echocardiographic studies were performed on an Acuson Sequoia 512 system. The mean time delay between echocardiography and CMR was 3 ± 2 days. Two observers blinded to the echocardiographic data evaluated the CMR images visually for a consensus diagnosis of papillary muscle involvement as defined by the presence of a high signal intensity area in the papillary muscle. Results of this analysis were then correlated to echocardiographic identification of relevant mitral regurgitation.

Table 1.

	RVF group	NonRVF group	p-Value
RVEDV (ml)	287.9 ± 85.8	175.3 ± 55.8	p = 0.01
RVESV (ml)	220.9 ± 84.0	125.3 ± 58.2	p = 0.02
RV EF (%)	25.2 ± 11.6	31.1 ± 11.9	NS
RV SV (ml)	66.6 ± 16.8	49.7 ± 13.9	p = 0.055
RV CO (l/min)	5.6 ± 1.7	4.3 ± 1.8	NS
LVEDV (ml)	428 ± 191.3	256.9 ± 82.5	p = 0.04
LVESV (ml)	367.5 ± 196.5	213.7 ± 86.3	NS
LV EF (%)	15.5 ± 6.1	18.9 ± 8.7	NS

Table 1. Diagnostic performance of papillary muscle hyperenhancement to identify mitral regurge.

	Echo+	Echo–	Total
CMR+	20	2	22
CMR–	4	3	7
Total	24	5	29

Results: Using echocardiography, mitral valve regurgitation was identified in 83% of the patients. Table 1 summarizes the results. CMR-derived diagnosis of papillary muscle infarction had 83% sensitivity and 60% specificity to detect mitral regurgitation.

Conclusion: Contrast-enhanced CMR can be used to detect papillary muscle infarction in patients with mitral regurgitation after acute myocardial infarction. This may have an important impact on risk stratification of these patients.

255. Reproducibility of Dobutamine Stress MRI and Implications for Clinical Trials

Mushabbar A. Syed, MD, W. Patricia Ingkanisorn, MD, Kenneth L. Rhoads, MD, D. Ian Paterson, MD, Jonathan Hill, MD, Richard O. Cannon, III, MD, Andrew E. Arai, MD. *National Institutes of Health, Bethesda, MD, USA.*

Introduction: Reproducibility of serial stress testing remain unknown despite their widespread use in clinical trials. Dobutamine stress MRI has excellent diagnostic and prognostic value and is being used as an integral part of clinical trials.

Purpose: The purpose of this study was to test the reproducibility of dobutamine MRI.

Methods: A total of 28 patients with coronary artery disease (CAD) and CCS class III or IV angina, not amenable to revascularization underwent dobutamine MRI for eligibility to a phase I/II stem cell trial (15 patients, by protocol, had 2 dobutamine MRI studies prior to treatment; median 13 days apart). This provided a unique opportunity to study the reproducibility. Anti-anginal medications were withheld on the morning of the study. Cine MRI was performed at each stage; a perfusion scan was performed at peak stress. Significant CAD was defined as $\geq 70\%$ stenosis or a positive ancillary stress test. To analyze inter-observer variability, consensus MRI reading was compared with blinded reading by 3 cardiologists.

Results: Patients averaged 56 ± 11 years (19 males), 22 had prior myocardial infarction, 24 had prior revascularization. Overall, cine MRI was moderately sensitive (57%) but highly specific (100%), sensitivity was increased to 75% in patients who achieved $\geq 80\%$ predicted maximum heart rate (PMHR), while specificity remained unchanged at 100%. Abnormal perfusion had a sensitivity of 62% (68% if $\geq 80\%$ PMHR) and a specificity of 83%.

For reproducibility, there were no significant differences in dobutamine dose, atropine dose, hemodynamic response, or angina between stress tests. There was also no significant difference in the number of ischemic segments detected (3.1 ± 3.2 vs. 3.5 ± 3.5 , $p=0.8$). Standard deviation of absolute difference (SDdiff) in number of ischemic segments was 3.2. Thus, a sample size of 23 subjects could detect resolution of 2 ischemic segments. Reproducibility of perfusion scans suggests a sample size <10 could detect an improvement in two segments (SDdiff=1.7). Interobserver interpretations correlated well in terms of number of ischemic segments vs. a consensus reading ($r=0.86, 0.81, \text{ and } 0.86$ for each of 3 observers).

Conclusions: Dobutamine stress MRI appears to be a reproducible method that could be used as a highly specific endpoint in a relatively small clinical trial, with an endpoint defined by resolution of ischemia in two segments of the heart. The sample size estimates need to be adjusted for some nondiagnostic scans. The intermediate sensitivity may be related to medications or small ischemic zones.

256. Myocardial Perfusion Improvement Detected by MRI in Patients Undergoing Surgical Revascularization and Bone Marrow Cells Implant

Carlos E. Rochitte, MD,¹ Luis H. Gowdak, MD,² José E. Krieger, MD, PhD,³ Marcello Zapparoli, MD,¹ José R. Parga, MD,¹ Luiz F. R. Avila, MD,¹ José A. F. Ramires, MD, PhD,² Sérgio A. Oliveira, MD, PhD⁴. ¹*Cardiovascular Magnetic Resonance Laboratory, Heart Institute - InCor- University of Sao Paulo Medical School, São Paulo, Brazil,* ²*Clinical Cardiology Division, Heart Institute -InCor- University of Sao Paulo Medical School, São Paulo, Brazil,* ³*Molecular Biology Laboratory, Heart Institute -InCor- University of Sao Paulo Medical School, São Paulo, Brazil,* ⁴*Cardiovascular Surgery Division, Heart Institute -InCor- University of Sao Paulo Medical School, São Paulo, Brazil.*



Introduction: Adult bone marrow cells (BMC) are involved in tissue repair and vascular growth, and might be used therapeutically in ischemic tissues. We hypothesize that intramyocardial injection of autologous BMC is safe and well-tolerated, and may help increase perfusion and the number of viable cells in patients (pt) undergoing incomplete surgical revascularization for diffuse coronary artery disease (CAD). Myocardial stress perfusion imaging with dipyridamole by MRI (MPI) has been shown to detect myocardial ischemia.

Purpose: Our objectives were: to investigate whether intramyocardial injection of autologous BMC is safe and well-tolerated; to evaluate myocardial perfusion by MPI in the entire left ventricle in patients undergoing incomplete surgical revascularization and receiving BMC for diffuse coronary artery disease (CAD).

Methods: 10 pt (8 men), age=59±1 years-old, with 3-vessel disease, limiting angina (class III–IV CCS), and who were not optimal candidates for “complete” surgical revascularization due to the extension of the disease were enrolled. BMC were obtained immediately prior to surgery, and the lymphomonocytic fraction separated by density gradient centrifugation. During surgery, injections of BMC were performed in the non-grafted areas of ischemic myocardium. Pt underwent MPI during stress with dipyridamole (0.56 mg/kg/4 min) in a 1.5T CV/i GE scanner, using an hybrid gradient-echo with multiple read-out. MR studies were performed before and 30 days after surgery. MPI was analyzed by 2 observers and classified using a 17-segment model and a perfusion defect score (0 for no perfusion defect, 1 for mild defect and 2 for moderate/severe defect). A total ischemic score was calculated as the mean score (sum/17 segments). An injected area score was calculated as the sum of the score within the injected area divided by the number of injected segments).

Results: In non-grafted areas, we injected 32 × 106 cels/mL or 130 × 106 cels/pt (CD34+=1.30±0.40%). Injected segments included the inferior wall in 7 pts and the anterior wall in 3. There were no major complications (including malignant arrhythmias) or deaths. MPI improved in both grafted and non-grafted, injected territories (Figure 1).

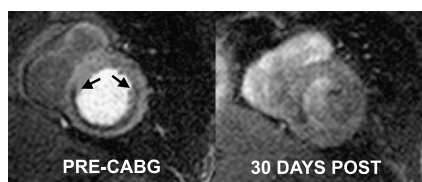


Figure 1.

Table 1.

	Baseline	30 Days	p
Total score	0.65±0.14	0.21±0.07	p=0.01
Injected score	1.21±0.13	0.43±0.21	p=0.02

All patients remained free of angina in the follow-up.

Thirty-days vs. baseline MRI showed reduction in the total ischemic score (0.65±0.14 vs. 0.21±0.07; P=0.01). Moreover, the ischemic score of the injected area was reduced significantly (1.21±0.13 vs. 0.43±0.21; P=0.002) (Table 1).

Conclusions: In the short-term, intramyocardial injection of autologous BMC is safe and well-tolerated, and may have contributed to increase myocardial perfusion in non-grafted areas. This strategy could lead to a new therapeutic option for the treatment of patients suffering from a more advanced (diffuse) CAD not suitable for complete myocardial revascularization provided these findings are confirmed in a larger series of pt with longer follow-up.

257. In Women with Symptoms of Ischemic Heart Disease, Combining Global and Regional Myocardial Perfusion Status Determined Using MRI Better Assigns Risk: Results from the NHLBI-Sponsored Women’s Ischemia Syndrome Evaluation (WISE)

Mark Doyle, PhD,¹ Gerald M. Pohost, MD,² Eduardo Kortright, PhD,³ Leslee J. Shaw, PhD,⁴ Delia B. Johnson, PhD,⁵ William J. Rogers, MD,⁶ Anthon Fuisz, MD,⁷ Steven E. Reis, MD,⁸ Barry L. Sharaf, MD,⁹ Carl J. Pepine, MD,¹⁰ Noel Bairey-Merz MD,¹¹ Sunil Mankad, MD,¹ Diane A. Vido, MS,¹ Sheryl F. Kelsey, PhD,⁵ Marian B. Olson, MS,⁸ Robert W. W. Biederman, MD.¹ ¹Allegheny General Hospital, Pittsburgh, PA, USA, ²University of Southern California, Los Angeles, CA, USA, ³University of New Orleans, New Orleans, LA, USA, ⁴ACRI, Atlanta, GA, USA, ⁵Epidemiology Data Center, Graduate School of Public Health, Pittsburgh, PA, USA, ⁶University of Alabama at Birmingham, Birmingham, AL, USA, ⁷Washington Hospital Center, Washington, DC, USA, ⁸University of Pittsburgh Medical Center, Pittsburgh, PA, USA, ⁹Rhode Island Hospital, Providence, RI, USA, ¹⁰University of Florida, Gainesville, FL, USA, ¹¹Cedars-Sinai Research Institute, Los Angeles, CA, USA.

Introduction: The WISE study was organized to improve diagnostic tests for assigning risk in women with symptoms of ischemic heart disease (IHD). Magnetic resonance (MR) myocardial perfusion imaging (MPI) can be quantitatively analyzed to calculate perfusion indices. The perfusion indices can be used to assess the presence of regional ischemia or scar (RIS) or averaged to generate a global myocardial perfusion index (GMPI).

Hypothesis: We hypothesize that global assessment of myocardial perfusion better assigns risk than assessment of regions of relative hypoperfusion.

Methods: Women (n=133), mean age 56±11 (31–85) years, 32% minorities with symptoms of IHD underwent MR and single photon positron emission computed tomography (SPECT) MPI evaluation. Follow-up was conducted over 38±14 months to monitor the occurrence of myocardial infarction (MI) or all-cause death. Quantitative myocardial perfusion analysis was performed on MR data by registering first pass perfusion images, extracting time intensity curves for the myocardium and normalizing using the left ventricular blood pool signal. Integrating the normalized time intensity curve formed the GMPI. Comparison of the normalized slopes and intensities between regions was used to detect RIS. In a blinded manner, the MR and SPECT MPI data were used to categorize patients as having a RIS; or by MR as having a GMPI in the lower 25th percentile.

Results: At follow-up, 10 pts (7%) experienced an MI or death. Kaplan Meier event-free survival analysis was performed and the log rank statistic calculated between low and high risk groups for: SPECT RIS 1.99 (p=0.16), MR RIS, 1.03 (p=0.31); low MR GMPI, 6.78 (p<0.01). Using the MR data, patients categorized as having either a low GMPI or a RIS had a log rank statistic of 8.49 (p<0.005).

Conclusions: Kaplan Meier event-free survival analysis was used to assess time to cardiac death or MI (n=10, 7%) and compared using a log rank statistic. A low MR GMPI was associated with a 6.8-fold increased risk of death or MI (82% event-free survival as compared with 96% event-free survival for those with a high MR GMPI, p<0.0001). When combined with RIS data, the presence of a low GMPI or RIS were significant estimators of hard cardiac events (p<0.005). Moreover, in women with symptoms of IHD, complete reliance on identification of regional hypoperfusion underestimated the risk of experiencing a serious adverse event irrespective of modality, i.e. SPECT or MR.

258. Prediction of Left Ventricular Remodeling by Infarct Size Obtained by Contrast-Enhanced MRI in Patients with Reperfused Acute Myocardial Infarction

Gunnar K. Lund,¹ Achim Barmeyer,¹ Alexander Stork,² Meike Knfel,¹ Ulrike Schlichting,¹ Maythem Saeed,³ Gerhard Adam,² Thomas Meinertz.¹ ¹Cardiology, Herz-zentrum, Hamburg, Germany, ²Radiology, Hamburg, Germany, ³Radiology, San Francisco, CA, USA.

Introduction: After acute myocardial infarction (AMI), several parameters have been proposed for early identification of patients at risk for left ventricular (LV) remodeling, including ejection fraction, LV volumes, infarct size and release of cardiac enzymes. Contrast-enhanced (CE) and cine magnetic resonance imaging (MRI) represent accurate methods to estimate infarct size and to quantify LV function and volumes.

Purpose: The purpose of the current study was to analyze which clinical or MRI parameter predicts best the occurrence of LV remodeling in patients after reperfused AMI.

Methods: CE-and Cine-MRI were performed in 36 patients (age: 54±12 years) with first reperfused AMI (CK max: 1064±830 U/L) at baseline (5.6±3.9 days after AMI) and at follow-up (7.6±2.8 months after AMI) using a 1.5 T scanner. Infarct size was measured 10 min after injection of 0.1 mmol/kg Gd-DTPA using a T1-weighted TurboFLASH inversion recovery sequence. Infarct size was calculated as % of LV area using a threshold method including only that enhanced myocardium with a signal intensity>+2.0 SD of remote normal myocardium. LV ejection fraction, mass and volumes were quantified at baseline and follow-up using Cine-MRI. LV remodeling was defined as an increase in end-diastolic volume (EDV) by >20% compared to baseline.

Results: LV ejection fraction improved from baseline to follow-up from 51±11% to 55±10% (P<0.01). LV mass decreased from 207±42 g to 179±43 g (P<0.0001) and EDV increased from 149±37 ml to 159±52 ml (P<0.05). LV remodeling occurred in 9 out of 36 patients (25%). The increase in EDV at follow-up correlated with the following parameters at baseline: ejection fraction (r=0.65, P<0.0001); infarct size by CE-MRI (r=0.54, P<0.001); end-systolic volume (r=0.40, P<0.05) and CKMB (r=0.35, P<0.05). Stepwise multiple regression analysis identified infarct size by CE-MRI as the most powerful predictor of LV remodeling. An infarct size >22% of LV area at baseline predicted LV remodeling with high sensitivity (78%), specificity (96%) and diagnostic accuracy (92%).

Conclusion: After reperfused AMI, the degree of LV remodeling is directly related to the infarct size at baseline. An infarct size >22% of LV area discriminates patients who are at high risk for LV remodeling from those who maintain normal LV dimensions.

259. Evaluation of Myocardial Infarction by 2D, 3D Single Breath-Hold and 3D-Navigator Myocardial Delayed Enhancement MRI

Marcello Zapparoli, MD,¹ Manojkumar Saranathan, PhD,² Fábio B. Rocha, MD,¹ Márcia L. O. Mugnaini, MD,¹ Marly Uellendahl, MD,¹ Jose R. Parga, MD,¹ Luiz F. R. Avila, MD,¹ Jose A. F. Ramires, MD, PhD,³ Thomas Foo, PhD,² Carlos E. Rochitte, MD.¹ ¹Cardiovascular Magnetic Resonance Laboratory, Heart Institute-InCor-University of São Paulo Medical School, São Paulo, Brazil, ²Applied Science Laboratory, GE Medical Systems, Baltimore, MD, USA, ³Cardiology Clinical Division, Heart Institute-InCor-University of São Paulo Medical School, São Paulo, Brazil.

Introduction: Two-dimensional myocardial delayed enhancement (2D MDE) MRI has been shown to detect

myocardial infarction (MI). This technique is able to predict the recovery of left ventricular (LV) function after revascularization and has similar results to those of positron emission tomography. The 2D MDE sequence requires repeated breath-holds for covering the entire LV, which takes several minutes, generates slice misalignment and needs frequent changes on the inversion time (TI). Moreover, it provides inadequate imaging quality in patients that cannot hold their breath appropriately. Two new techniques, based on three-dimensional (3D) acquisition of the entire LV during a single breath-hold (3DBH) or using navigator-echo gating (3DNAV) were developed to not only overcome those limitations but also speed up image acquisition with little or no loss of image quality.

Purpose: Our objectives were to compare measurements of infarct size and transmuralty obtained by 2D, 3DBH and 3DNAV MDE sequence.

Methods: We studied 10 patients with MI in a 1.5T SIGNA CV/i GE scanner. All patients received 0.2 mmol/kg of gadolinium-based contrast 10-20 minutes prior to image acquisition. The 2D MDE was a inversion recovery (IR) prepared fast gradient-echo (FGRE) sequence. The 3D techniques were IR prepared FGRE sequences and used Variable Sampling in Time (VAST) segmentation to reduce the acquisition time. For each slice partition, k-space data was acquired over 2 R-R intervals, resulting in a scan time of 2N

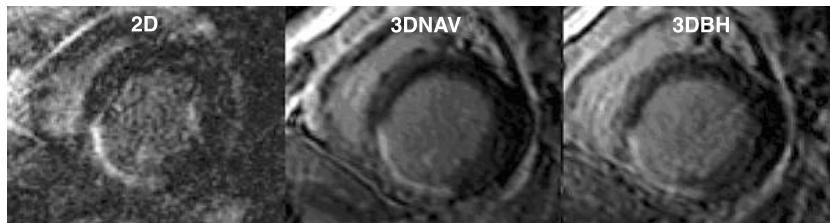


Figure 1.

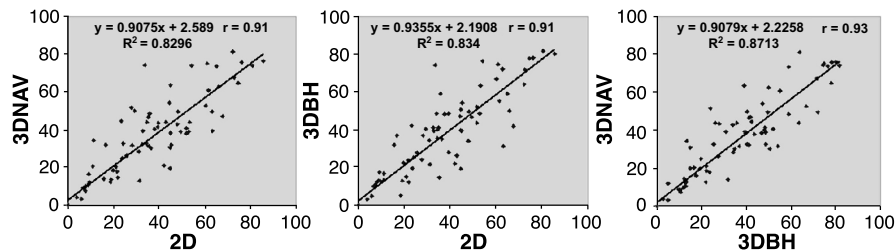


Figure 2. (View this art in color at www.dekker.com.)

Table 1. Infarct size.

	Mean difference	95% CI
3DNAV vs. 2D	-1.32	-7.78/5.15
3DBH vs. 2D	-0.22	-4.56/4.14

heartbeats for N slice partitions. Measurements of infarct size (%LV mass) and transmuralities were done by planimetry in short-axis images. Infarct transmuralities were measured in 3 short-axis slices per LV (apical, medial and basal), segmented in 6 radial segments and calculated as percent of enhanced area of each segment. We performed simple linear regression and Bland-Altman analysis for comparison of the 3 methods.

Results: Infarct size and transmuralities were similar among the three methods (Figure 1).

The infarct size, measured by 2D, 3DNAV and 3DBH methods were $9.6 \pm 2.0\%$, $9.8 \pm 1.9\%$ and $10.9 \pm 2.2\%$, respectively (p NS). There was a strong linear correlation between 2D vs. 3DNAV and 3DBH ($r=0.94$, $r=0.88$, $p<0.001$ for both) as well as between both 3D techniques ($r=0.93$, $p<0.001$, Figure 2).

The Bland-Altman comparisons showed good agreement among the methods. The mean difference and the 95% confidence interval are shown on Table 1.

For infarct transmuralities, a total of 96 segments were analyzed by all 3 methods. There was a good correlation among the methods. Correlation coefficient of 2D vs. 3DNAV and 3DBH were $r=0.91$ and $r=0.91$, respectively, with $p<0.001$ for both. The linear regression between both 3D techniques showed a good correlation ($r=0.93$, $p<0.001$). Bland-Altman plots showed a good agreement with mean differences close to zero (Table 2).

Conclusions: Infarct size and transmuralities can be accurately detected by single breath-hold and navigator three-dimensional myocardial delayed enhanced MRI. These techniques can be an adequate alternative for faster (3DBH) and more reliable MR exam in patients that cannot hold their breath (3DNAV).

Table 2. Infarct transmuralities.

	Mean difference	95% CI
3DNAV vs. 2D	-0.04	-20.59/20.58
3DBH vs. 2D	-0.39	-21.00/20.23

260. Prediction of Reversible Left Ventricular Dysfunction in Chronic Ischemic Heart Disease: Head-to-Head Comparison of Contrast-Enhanced Magnetic Resonance Imaging and Thallium-201 Single-Photon Emission Computed Tomography

Matthias Regenfus,¹ Christian Schlundt,¹ Johannes von Erffa,¹ Robert Krähner,¹ Michaela Schmidt,² Niels Oesingmann,² Torsten Kuwert,³ Werner Daniel.¹ ¹Medical Clinic II, FAU Erlangen-Nürnberg, Erlangen, Germany, ²Siemens Medical Solutions, Erlangen, Germany, ³Nuclear Medicine, FAU Erlangen-Nürnberg, Erlangen, Germany.

Objectives: Contrast-enhanced (ce) magnetic resonance imaging (MRI) has been shown to accurately assess myocardial viability. Comparative data to nuclear cardiology techniques as 201-Thallium (TI) single photon emission computed tomography (SPECT) is scarce. We compared ce MRI and TI SPECT to predict reversibility of left ventricular (LV) dysfunction in patients with chronic ischemic heart disease.

Methods: 25 patients (pts) with LV dysfunction (EF $33 \pm 12\%$) were examined on a 1.5T scanner. Functional cine studies (TrueFISP) and ce images (inversion recovery Turbo FLASH) 5 min after injection of 0.1 mmol/kg Gd-DTPA were acquired. Rest-redistribution SPECT was performed according to standard protocols. 9 months after revascularization (bypass surgery: n=15; percutaneous intervention: n=10) pts were repeatedly examined with cine MRI. A 17-segment model of corresponding basal, midventricular and apical slices was analysed independently for ce MRI and SPECT. Segmental hyperenhancement (HE) for MRI and tracer uptake for SPECT were quantified. For MRI segments were considered to be viable if showing less than 25% segmental HE, for SPECT, if more than 60% TI-201 uptake. Functional recovery in the follow-up MRI was correlated with prediction of viability by both imaging modalities. Moreover, LV ejection fraction (EF) for both MRI scans was determined by planimetry.

Findings: 79 of 161 (49%) dysfunctional segments, which had been revascularized, showed improved wall motion with follow-up MRI. Ce MRI showed a sensitivity of 94%, a specificity of 94%, and an accuracy of 94% to detect viable myocardium, whereas SPECT a sensitivity of 86% ($p=0.7$), a specificity of 56% ($p=0.002$), and an accuracy of 68% ($p=0.006$). On a patient basis, increase of LVEF >5% was shown in 10 (40%) pts. Multivariate regression analysis identified the dysfunctional-but-viable myocardial ratio by MRI as

the only predictor of increase in LVEF > 5% (p=0.03), whereas the equivalent by SPECT was not predictive. Receiver operator characteristics established a dysfunctional-but-viable myocardial ratio of 0.46 (sensitivity 91%, specificity 91%) by MRI, and 0.86 (sensitivity 56%, specificity 93%) by SPECT as the best discriminators. Hereby, the area under the curve was significantly larger for MRI (p<0.05).

Conclusions: Ce MRI, especially by virtue of its superior specificity, compares favorably to TI-201 SPECT for prediction of regional and global functional recovery in the setting of chronic myocardial ischemia.

261. Prevalence of Unrecognized Myocardial Infarction in Asymptomatic Type II Diabetes Mellitus

John Heitner, MD, Igor Klem, MD, Michael Elliott, MD, Diana McNeill, MD, Scott Joy, MD, Larry Wu, MD, Dipan J. Shah, MD, Manesh Patel, MD, Jonathan

Weinsaft, MD, Anna Lisa Crowley, MD, Peter Cawley, MD, Robert M. Judd, PhD, Raymond J. Kim, MD. *Duke University, Durham, NC, USA.*

Introduction: Prognosis of patients with ECG evidence of silent myocardial infarction (MI) is poor, with long-term mortality rates similar to patients with clinically recognized MI. Coronary artery disease (CAD) in patients with diabetes mellitus (DM) is notoriously asymptomatic and frequently in an advanced stage at the onset of clinical manifestations. Contrast-enhanced MRI can detect small MI (<1 g), long past the time window for detection by cardiac enzymes and with higher sensitivity than electrocardiography.

Purpose: 1) Evaluate the prevalence of silent MI in asymptomatic patients with type 2 DM. 2) Evaluate the relationship between traditional cardiac risk factors, serologic markers of inflammation, lipids, and renal function and the presence of asymptomatic MI on cardiac MRI.

Methods: We evaluated 41 consecutive, asymptomatic patients with type 2 DM and at least one additional cardiac risk factor for CAD. None of the

Table 1.

	HE –	HE +	Statistic	P value
Age	60.0	61.9	t=0.52	0.06048
Years of DM	8.6	12.7	t=1.42	0.1631
BMI	31.9	27.3	t=1.61	0.1162
HTN	23 (66%)	4 (67%)	Fisher's	1.0000
Hyperlipidemia	26 (74%)	3 (50%)	Fisher's	0.3344
FH of CAD	12 (34%)	2 (33%)	Fisher's	1.0000
Smoking	4 (11%)	0 (0%)	Fisher's	0.6122
PVD	2 (6%)	2 (33%)	Fisher's	0.0952
Insulin	10 (29%)	3 (50%)	Fisher's	0.3607
Metformin	22 (63%)	1 (17%)	Fisher's	0.3860
Sulfonurea	11 (31%)	2 (33%)	Fisher's	1.0000
Glitizone	5 (14%)	0 (0%)	Fisher's	0.5808
ASA	17 (49%)	2 (33%)	Fisher's	0.6681
ACE-inhibitor	20 (57%)	3 (50%)	Fisher's	1.0000
ARB	7 (20%)	0 (0%)	Fisher's	0.3502
B-blocker	9 (26%)	4 (67%)	Fisher's	0.0685
Statin	21 (60%)	0 (0%)	Fisher's	0.0086*
HgbA1-c	7.62	7.30	t=0.85	0.4031
Urine MA	5.1	8.6	Wilcoxon	0.9662
CRP	0.37	0.42	Wilcoxon	0.9780
Homocysteine	7.49	8.36	t=0.60	0.5543
Creatinine	1.08	1.05	t=0.08	0.9387
Wall motion	3	4	Fisher's	0.0045*
AoW thickness	2.56 mm	2.37 mm	t=0.48	0.6350
AoW area	1.52 mm ²	1.47 mm ²	t=0.20	0.8467
EF	59.9%	52.5%	t=2.32	0.0258*

Copyright © Marcel Dekker, Inc. All rights reserved.

patients had a known history of CAD. DM patients (age 45–75) were recruited from an outpatient family medicine and endocrinology clinic. All patient underwent cine (True FISP) and contrast-enhanced (segmented, inversion-recovery pulse sequence, 0.1 mmol/kg gadolinium) cardiac MRI using a 1.5 T Siemens Sonata scanner. Regional wall motion and the presence and transmural extent of MI were analyzed employing a 17-segment model by 3 readers (consensus) blinded to patient data. Wall thickness of the descending thoracic aorta was determined using a T2 weighted turbo spin echo sequence. Lipid panel, hs-CRP, homocysteine, creatinine, urine microalbumin, HgbA1C and an ECG were obtained. ECG's were analyzed for pathologic Q-waves by Minnesota criteria.

Results: The average age was 60 yo with a history of DM for 9.2yrs (mean HgbA1-c 7.6) and a BMI of 31. Six of the 41 patients (15%) had evidence of left ventricular hyperenhancement (myocardial infarction). The relationship between baseline clinical characteristics, left ventricular wall motion, and aortic wall measurements with the presence of hyperenhancement (HE) are shown in Table 1. There was no significant relationship between clinical risk factors, serologic markers, aortic wall measurements, or diabetic medications with the presence of HE. None of the 21 patients on a statin had evidence of myocardial hyperenhancement $p < 0.01$. Although the presence of wall motion abnormalities was related to the presence of HE, $p < 0.005$, there was only a moderate correlation. None of the patients with HE had pathologic Q waves on ECG by Minnesota criteria.

Conclusion: Silent myocardial infarction occurs in a significant minority of type II diabetic patients who are asymptomatic and have normal electrocardiograms.

262. Ventricular Remodeling Following Acute ST-Segment Elevation Myocardial Infarction in Patients Undergoing Primary Angioplasty

Edwin Wu, MD,¹ Daniel C. Lee, MD,¹ Thomas A. Holly, MD,¹ Lubna Choudhury, MD,¹ Sheridan N. Meyers,¹ F Scott Pereles, MD,² Francis J. Klocke, MD,¹ Robert O. Bonow, MD.¹ ¹Department of Medicine, Division of Cardiology, Northwestern University, Chicago, IL, USA, ²Department of Radiology, Northwestern University, Chicago, IL, USA.

Introduction: Delayed contrast-enhanced images (ceMRI) following an acute MI can detect salvageable,

viable myocardium. There have been previous reports of poor contrast penetration into the center of infarcted myocardium that may be indicative of a “no-reflow” phenomenon, and this may be an additional indicator for negative ventricular remodeling. Therefore, the transmural extent of hyperenhancement may not completely account for changes in ventricular remodeling.

Purpose: A combination of delayed ceMRI and cine imaging can define parameters predictive of ventricular remodeling and long-term systolic function in patients who had undergone an emergent revascularization.

Methods: Eighteen subjects underwent cine and ceMRI within 7 days of an acute ST-segment MI and again after a minimum follow-up time of 3 months. All had undergone successful emergent angioplasty and reperfusion within 24-hours of presentation for chest pain. Left ventricular (LV) end-diastolic volume (EDV), left ventricular end-systolic volume (ESV) and ejection fraction (EF) were measured by planimetry from multiple short-axis trueFISP cine slices encompassing the entire left ventricle. Additionally, a delayed, inversion-recovery turboFLASH pulse sequence 5 to 10 minutes following IV gadolinium administration was used to determine the area and location of hyperenhancement (HE), the transmural extent of HE, and the presence of hypo-enhancement or “no-reflow.” In addition, the HE arc length was measured on one representative short-axis slice to assess for circumferential expansion. Subjects were divided into two groups based on the absence (Group A, n=7) or presence of transmural HE with “no-reflow” (Group B, n=8). Three subjects were excluded from the final analysis due to small infarction sizes (<10 gm of total infarction) (Figure 1).

Results: The difference between baseline EF, EDV and ESV between the two groups were not statistically significant (EF $38 \pm 10\%$ vs. 32 ± 9 ; EDV 191 ± 119 cc vs. 167 ± 32 cc; ESV 119 ± 70 cc vs. 115 ± 35 cc). Additionally, the initial infarct size on ceMRI was 43 ± 23 gm in Group A and 50 ± 18 gm in Group B ($p = 0.5$). Subjects in Group A manifested an increase in mean EF ($38 \pm 10\%$ to $47 \pm 6\%$, $p < 0.01$) with a subsequent decrease of HE of $41 \pm 22\%$ ($p < 0.01$) and circumferential length of $12 \pm 11\%$ ($p < 0.03$) of their original sizes. However, subjects in Group B, despite a decrease of $24 \pm 28\%$ of original HE infarct size, showed no change in circumferential length ($28 \pm 14\%$ to 29 ± 16 mm, $p = \text{NS}$) or EF ($32 \pm 9\%$ to $33 \pm 9\%$, $p = \text{NS}$).

Conclusions: Given similar degrees of infarcted myocardium and EF, the presence of “no-reflow” may represent microvascular obstruction and more profound LV damage which may adversely effect subsequent LV volumes and EF. These data support the concept that patients with “no-reflow” have more negative



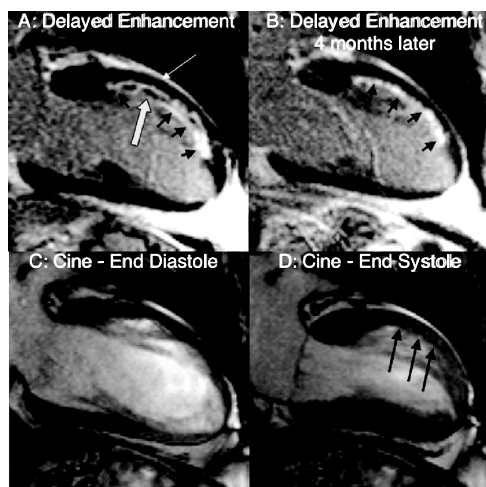


Figure 1. Image (A) shows a delayed contrast-enhanced image with an area of increased HE to the anterior wall (small black arrows). The large white arrow indicates an area of “no-reflow.” Note the presence of an epicardial rim of viable myocardium (small white arrow). Image (B) reveals persistent HE 4 months after an acute MI (black arrows). Image (C) and (D) are end-diastolic and end-systolic cine still-frames obtained 4 months following the acute MI in the same patient. The black arrows in image (D) reveal persistent akinesis to the anterior wall of infarction despite successful angioplasty reperfusion. The EF went from 35% post MI to 36% four months later with an associated increase in EDV and ESV. (View this art in color at www.dekker.com.)

remodeling and infarct expansion independent of the transmural extent of hyperenhancement.

263. Left Ventricular Structure and Function in the Madit-II Population

Sunil T. Mathew, MD, Andressa Borges, MD, Joseph Levine, MD, Yi Wang, ScD, Jeannette McLaughlin, RN, William Schapiro, RT, Nathaniel Reichek, MD
Department of Research and Education, St. Francis Hospital, State University of New York at Stony Brook, Roslyn, Stony Brook, NY, USA.

Introduction: The Multicenter Automatic Defibrillator Implantation Trial (MADIT II) established new, simplified selection criteria for prophylactic implantation of defibrillators in patients with prior myocardial infarction, which have been widely endorsed and adopted. Case selection is based on a left ventricular ejection fraction (LVEF) of 30% or less by any clinical

technique. Single plane ventriculography, 2D-echocardiography, gated SPECT wall motion, and MUGA are all used, but each has major limitations in this population. Though the trial demonstrated a substantial survival benefit for defibrillator therapy, event rates in non-ICD patients were relatively low (20 month all-cause mortality 19.8%), arrhythmia recurrence rates in ICD patients are relatively low (10%/yr at our center) and the population identified as at-risk, is extremely large. Therefore, improved risk stratification from imaging data in this population may be of great value. In addition, other structural markers of arrhythmic risk besides EF may be important. In particular, since surviving myocardium adjacent to the infarct region is thought to be the locus of reentrant circuits for ventricular tachycardia in such patients, infarct size and morphology may be important. In addition, true 3D-volumetric assessment the left ventricle may be more valuable than clinical EF. Therefore we examined CMR LVEF volumes, and myocardial infarct (MI) size using CMR cine and delayed hyperenhancement (DE) imaging in patients fulfilling MADIT II inclusion criteria.

Methods: CMR was performed on 13 patients (age 66.6 ± 11.0 yrs, 12 men) fulfilling MADIT II criteria, with a history of myocardial infarction (MI) more than 3 months previously and LVEF on a clinical test of 30% or less. CMR was performed using a 1.5T scanner (Siemens Sonata). LV volumes and EF were determined using breath-hold TrueFISP cine in contiguous short axis slices from the LV apex through the mitral annular plane, quantitated using MASS (Medis). LV long axis cines in 3 planes were also obtained. To determine infarct size, 10 minutes after injection of 0.2 mmol/kg Omniscan, we began acquisition of TrueFISP (TFi) and TurboFLASH (TFL) delayed hyperenhancement (DE) images of the same contiguous short axis slices and the long axis slices, immediately after

Table 1. Volumetric data and infarct quantitation by CMR.

	Range	Mean	StdDev	Median
3D-LVEF	15–38	23	7	22
Infarct size (% LV Mass)	0–62	27	15	23
EDVol (ml)	174–405	300	69	279
EDVol/BSA (ml/m ²)	109–253	157	38	154
ESVol (ml)	108–335	230	66	227
ESVol/BSA (ml/m ²)	68–210	120	38	113
LVMass ED/BSA (g/m ²)	62–138	104	25	108

Copyright © Marcel Dekker, Inc. All rights reserved.

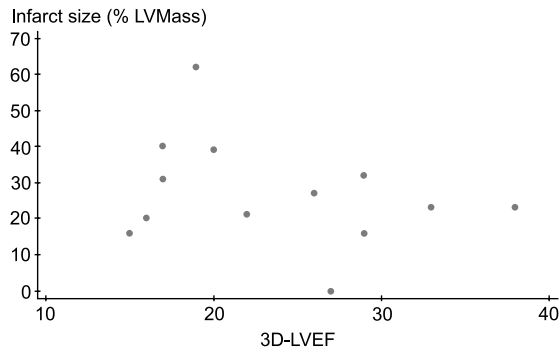


Figure 1. (View this art in color at www.dekker.com.)

determining optimal inversion time with TI scouts. If TFL data were incomplete or of limited quality due to patient fatigue (n=1), TF_i images were used for quantitation, with correction by a validated regression correction approach. DE regions were planimetered in Siemens Argus software. Infarct area, LV myocardial area, and MI size as % LV mass were calculated.

Results: Descriptive statistics of measured variables are summarized in Table 1. MI size as %LV mass is plotted versus CMR LV ejection fraction in Figure 1. CMR ejection fraction ranged from 15 to 38%, while end-diastolic and end-systolic volume indices ranged widely. Infarct size as % LV mass ranged from 0 to 62%. Spearman rank correlation testing revealed no significant correlation between infarct size as % LV mass and ejection fraction ($R = -0.092$).

Conclusions: Our results demonstrate wide heterogeneity of LV volume indices, ejection fraction, and infarct size in the population satisfying criteria for MADIT II, which may explain the relatively low event rates in this population and suggest wide variation in arrhythmic risk. CMR data may provide improved risk stratification for potentially lethal arrhythmias in post-infarct patients.

264. Multi-slice Delayed Hyperenhancement Imaging of Myocardial Infarction Using SENSE Accelerated Phase Sensitive Inversion Recovery True-Fisp

Peter Kellman, PhD,¹ Andrew C. Larson, MS,¹ Yiu-Cho Chung, PhD,² Orlando P. Simonetti, PhD,² Elliot R. McVeigh, PhD,¹ Andrew E. Arai, MD.¹ ¹NIH, Bethesda, MD, USA, ²Siemens Medical Solutions USA, Inc., Chicago, IL, USA.

Introduction: Following administration of Gd-DTPA, infarcted myocardium exhibits delayed hyperenhancement and can be imaged using an inversion-recovery sequence (Simonetti et al., 2001). Using a conventional segmented acquisition requires a number of breath-holds to image the heart. Single-shot phase-sensitive inversion-recovery (PSIR) true-FISP may be combined with parallel imaging using SENSE to achieve multi-slice full heart coverage with high spatial resolution (Chung et al., 2003; Pruessmann et al., 1999). PSIR techniques have demonstrated a number of benefits (Kellman et al., 2002) including consistent contrast and appearance over a relatively wide range of inversion recovery times (TI), improved contrast-to-noise ratio, and consistent size of the hyperenhanced region.

Purpose: To demonstrate imaging myocardial infarction with multi-slice coverage of the entire heart in a single breath-hold.

Methods: Infarct imaging was compared using 1) segmented IR-turboFLASH, and 2) multi-slice IR-true-FISP implemented on a Siemens Sonata 1.5T scanner. For both methods, the same spatial resolution ($1.4 \times 2.3 \text{ mm}^2$), FOV ($370 \times 300 \text{ mm}^2$), and TI (280 ms) were used. A stack of 8 short-axis slices was acquired with 6mm slice thickness and 3.6 mm gap. The IR-turboFLASH required 16 heart-beat breath-hold per slice, whereas the IR-true-FISP required a single 16 HB acquisition. Imaging was performed in diastasis with approximately the same acquisition window for both methods. Typical parameters for the IR-true-FISP sequence were: BW 977 Hz/pixel, TE/TR 1.2/2.7 ms, 50° readout flip angle (5° reference), 256×128 image matrix. Rate=2 SENSE acceleration was used to obtain the full 128 line resolution using 64 phase encodes acquired in a single heartbeat (172 ms window) with 2 R-R intervals between inversions. Typical parameters for the IR-turboFLASH sequence were: BW 140 Hz/pixel, TE/TR 3.9/8.5 ms, 30° readout flip angle (5° reference), 256×136 image matrix. The phase-encode dimension was slightly oversampled, yielding an effective resolution of 128 lines in this specific example. The 136 phase encodes were acquired in 16 heartbeats collecting 17 lines per heartbeat with 2 R-R intervals between inversions. The segment duration was 145 ms per R-R interval, acquired during diastasis. A custom 8-element cardiac phased-array (Nova Medical, Inc.) was used. A B₁-weighted phased-array combined phase-sensitive reconstruction method was used (Kellman et al., 2002) for all sequences. This previously described approach acquires a reference image at the same cardiac phase, during the same breath-hold during alternate heart beats to estimate both the background phase and surface coil B₁-maps.

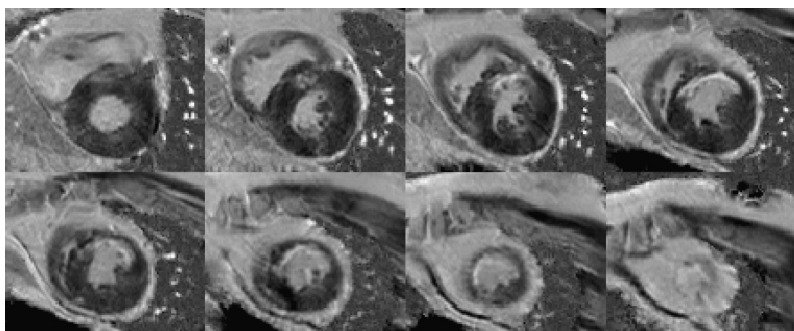


Figure 1. Short-axis stack acquired in 8 separate breath-holds using segmented IR-turboFLASH with single-slice-per-breath-hold.

Images were acquired approximately 20 minutes after administering a double dose (0.2 mmol/kg) of contrast agent (Gd-DTPA, Berlex Magnevist). CNR between MI and normal myocardium was calculated using measured signal intensities and pre-scan noise measurement. Measured CNR was compared with values predicted based on simulation of the magnetization during inversion-recovery for both methods.

Results: A stack of short-axis images of the heart for a patient with anterior MI is shown in Figures 1 and 2 acquired using both methods, respectively. The measured CNR for the segmented turbo-FLASH method was approximately 2.2 times that of the true-FISP with SENSE which was close to predicted.

Conclusions: Multi-slice coverage of the entire heart in a single breath-hold acquisition is possible using SENSE accelerated phase-sensitive inversion-recovery true-FISP. Using SENSE acceleration, it is possible to use single-shot true-FISP without compromising spatial resolution. Since the single-shot method is insensitive to breathing, the multi-slice acquisition, achieved by catenating several single-shot acquisitions, may be either breath-held for better slice registration, or free-breathing in cases where patients have difficulty holding their breath.

REFERENCES

- Chung, Y. C., et al. (2003). *JCMR* 5(1):40–41.
 Kellman, P., et al. (2002). *MRM* 47:372–383.
 Pruessmann, K. P., et al. (1999). *MRM* 42:952–962.
 Simonetti, O. P., et al. (2001). *Radiology* 218:215–223.

265. Normal Age- and Sex-Related Values of Left Ventricular Volumes, Myocardial Mass and Ejection Fraction Obtained with Cardiac Magnetic Resonance Using Fiesta Imaging

Nikolay P. Nikitin, MD, PhD,¹ Ramesh de Silva, MRCP,¹ Klaus K. A. Witte, MRCP,¹ Angela Lowe,² Elena I. Lukaschuk, MSc,¹ Andrew L. Clark, MD,¹ John G. F. Cleland, MD, FRCP, FACC.¹ ¹Academic Unit of Cardiology, University of Hull, Hull, United Kingdom, ²Lister Healthcare, Leeds, United Kingdom.

Introduction: Cardiovascular magnetic resonance (CMR) is increasingly used for the evaluation of

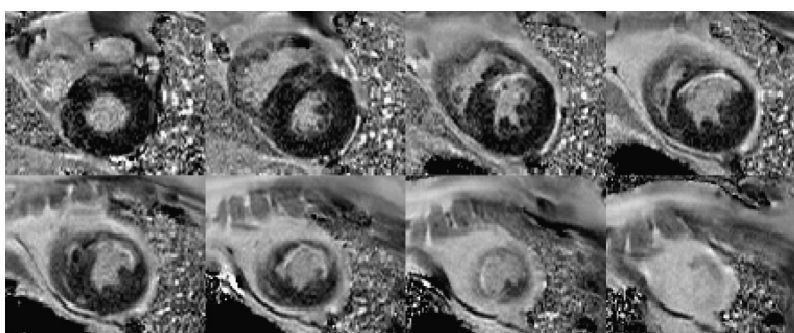


Figure 2. Short-axis stack acquired in a single breath-hold using multi-slice IR-true-FISP.

patients with cardiac disease. In order to correctly assess left ventricular (LV) anatomy and function in cardiac patients, it is essential to establish the normal ranges of LV volumes, myocardial mass and ejection fraction in healthy subjects of different ages and both sexes.

Methods: 102 healthy subjects (range 22 to 91 years) underwent CMR on a 1.5 Tesla scanner (Signa CV/i, GE Medical Systems) using ECG-triggered breath-hold FIESTA imaging. The multi-slice cine data sets covering the left ventricle from apex to base were analysed to calculate LV end-diastolic volume (EDV), end-systolic volume (ESV), end-diastolic myocardial mass (EDMM) and ejection fraction (EF) with the use of MRI-MASS software system (MEDIS, Leiden, NL). The indices of EDV, ESV and EDMM were obtained by correcting for body surface area (BSA).

Results: EDV was 101 ± 25 ml (95% C.I., 96–106 ml), EDV index was 56 ± 12 ml/sq.m. (95% C.I., 54–58 ml/sq.m.), ESV was 36 ± 13 ml (95% C.I., 34–39 ml), ESV index was 20 ± 7 ml/sq.m. (95% C.I., 19–21 ml/sq.m.), EDMM was 97 ± 22 g (95% C.I., 93–102 g), EDMM index was 53 ± 9 g/sq.m. (95% C.I., 52–55 g/sq.m.), and EF was $65 \pm 7\%$ (95% C.I., 63–66%). BSA tended to decrease with age principally because younger volunteers were taller than their older counterparts. However, despite these demographic distinctions, no age-related differences in LV volumes, EDMM and EF were found. Women had lower BSA than men (1.65 ± 0.11 vs. 1.96 ± 0.14 sq.m., $p < 0.001$) due to both shorter heights and lower body weights. EF was not affected by sex ($64 \pm 6\%$ in men vs. $65 \pm 7\%$ in women, NS). EDV and ESV were higher in men than in women (109 ± 26 vs. 93 ± 20 ml, $p = 0.001$ and 39 ± 13 vs. 33 ± 12 ml, $p = 0.01$ correspondingly). However, there were no significant differences between the sexes in EDV and ESV indices (56 ± 13 vs. 56 ± 11 ml/sq.m., $p = 0.76$ and 20 ± 7 vs. 20 ± 7 ml/sq.m., $p = 0.80$, respectively). Men had higher EDMM and EDMM index than women (112 ± 19 vs. 80 ± 12 g, $p < 0.001$ and 57 ± 8 vs. 49 ± 7 g/sq.m., $p < 0.001$, respectively).

Conclusions: Age- and sex-related reference values of LV volumes, myocardial mass and ejection fraction measured with cardiac magnetic resonance using FIESTA imaging are presented. LV ejection fraction is not dependent on age or sex. There are no significant changes in LV volumes and myocardial mass with age. LV volumes are higher in men than in women but there are no sex-associated differences in LV volume indices corrected for BSA. Men have higher LV mass and mass index.

266. Accuracy and Reproducibility of Acute Myocardial Infarct Size Measurements by Contrast Enhanced CMR

Anja Wagner, MD,¹ Heiko Mahrholdt, MD,² Louise Thomson, MD,¹ Claudio Kupfahl, MD,² Gabriel Meinhardt, MD,² Wolfgang Rehwald, PhD,¹ Igor Klem, MD,¹ Udo Sechtem, MD,² Raymond J. Kim, MD,¹ Robert M. Judd, PhD.¹ ¹Duke Cardiovascular Magnetic Resonance Center, Duke University, Durham, NC, USA, ²Robert Bosch Medical Center, Stuttgart, Germany.

Introduction: There has been a growing interest in myocardial infarct (MI) size measurements as a surrogate end point for clinical trials. Currently, ^{99m}Tc-sestamibi single photon emission computed tomographic (SPECT) imaging is thought to be the best available measurement tool for infarct size determination (Gibbons et al., 2000).

We hypothesized that contrast enhanced CMR (ceCMR) may serve as an advantageous imaging technique for infarct size determination. To date, the reproducibility and accuracy of acute myocardial infarct measurement using the delayed enhancement technique of CMR has not been established.

Purpose: To determine the accuracy and reproducibility for acute MI size measurements by ceCMR to establish the foundation for the use of this technique as an end point in clinical trials.

Methods: Fourteen dogs and 30 patients with first acute MI were studied. Accuracy was studied in dogs two days after reperfused MI and by comparing in vivo CMR images to infarct size determined histologically (TTC). Images were acquired every 5 min (5–45 min post contrast agent (ca)) with 1) fixed inversion time (TI) (250 msec for 0.1 mmol/kg, 300 msec for 0.2 mmol/kg Gd-DTPA) 2) variable TI set by the scanner operator to null signal from normal myocardium. Reproducibility was studied in patients with acute MI (infarct age 4.4 ± 2.3 d, peak CK 1375 ± 902) scanned with a variable TI at 5 and 30 min post-ca (0.15 mmol/kg Gd-DTPA).

Results: In dogs, compared to TTC CMR infarct size using a fixed TI was 102% (± 11) and 103% (± 7 SD) for 0.1 and 0.2 mmol Gd-DTPA, resp. at 5 min post-ca, and decreased to 59% (± 24 SD) and 62% (± 17 SD) of TTC infarct size by 45 min post-ca ($p < 0.001$). For variable TI, conversely, CMR infarct size remained constant from 5 to 45 min post-ca ($p = \text{NS}$, 95% limits of agreement: -3.29 and 5.2% and 2.93 and 4.7% 5 and 45 min after post-ca, resp. Figure 1).

In patients, we observed a large range of infarct sizes (1.1%–46% of LV) and infarct size determined



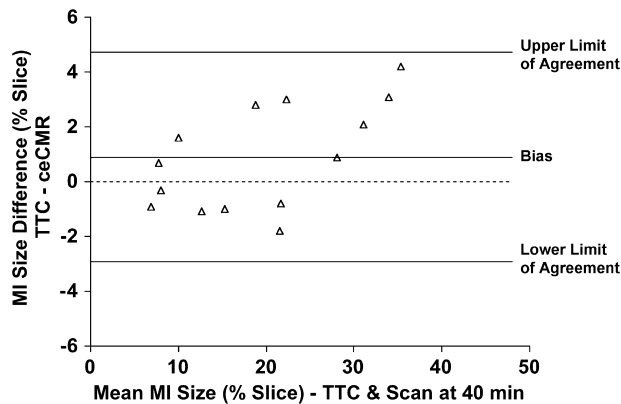


Figure 1. Accuracy.

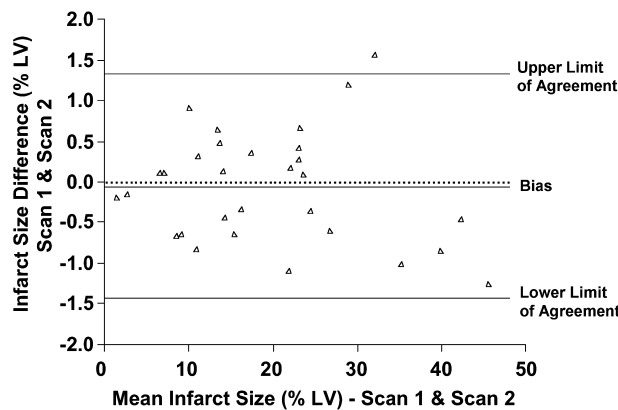


Figure 2. Reproducibility.

by ceCMR (using a variable TI) remained constant between 5 and 30 min post-ca (95% limits of agreement: -1.4 and 1.3% of LV Figure 2).

Conclusions: The animal data indicate that ceCMR measures acute MI size with an accuracy of $\pm 3.8\%$ of infarct size. The single-site patient data indicate a reproducibility of $\pm 1.4\%$ of LV mass, provided that pulse sequence parameters (TI) account for clearance of the contrast agent. Based on these results, a clinical trial designed to evaluate a candidate therapeutic intervention would require approximately four times fewer patients if ceCMR rather than ^{99m}Tc -sestamibi SPECT was used to define the infarct size end-point (Gibbons et al., 1994).

REFERENCES

- Gibbons, R. J., et al. (1994). *J. Am. Coll. Cardiol.*
 Gibbons, R. J., et al. (2000). *Circulation.*

267. A Study of Heart Muscle Injury in Complex/Multi Vessel Percutaneous Coronary Intervention as Assessed by Delayed Enhancement MRI

Joseph B. Selvanayagam,¹ Italo Porto,² Steffen E. Petersen,¹ Jane M. Francis,¹ Keith M. Channon,³ Adrian Banning,² Stefan Neubauer.¹ ¹Department of Cardiovascular Medicine, University of Oxford Centre for Clinical Magnetic Resonance Research, John Radcliffe Hospital, Oxford, United Kingdom, ²Department of Cardiology, John Radcliffe Hospital, Oxford, United Kingdom, ³Department of Cardiovascular Medicine, John Radcliffe Hospital, Oxford, United Kingdom.

Introduction and Purpose: In recent years, stenting and the use of new and potent anti-platelet agents have broadened the use of Percutaneous Coronary Intervention (PCI) by improving the safety and durability of the procedures. Nevertheless, there are a subset of patients with complex coronary lesions (including those with active thrombus) in whom the use of standard balloon dilatation and stenting can result in significant distal embolization, platelet activation, and microinfarction. Delayed enhancement MRI (DE-MRI) of the heart has been shown to reliably identify areas of irreversible myocardial damage with high spatial resolution. We sought to study the rate and magnitude of new irreversible injury associated with complex/multi vessel PCI in the current era, and correlated this with the change in post procedure cardiac Troponin I.

Methods: 17 patients undergoing complex (bifurcation lesions, lesions with thrombus) and/or multi-vessel PCI were studied at 1.5T. All patients received best standard care including clopidogrel and abciximab. Patients underwent pre-procedure and post-procedure (24 hours) cine MRI for global left ventricular function (True FISP sequence) and delayed enhancement MRI (DE-MRI; segmented inversion recovery Turbo FLASH sequence) for irreversible myocardial injury. Cardiac troponin I measurements were obtained pre PCI and 24 hours post PCI.

Results: Mean age of patients studied was 62 ± 11 years. Seven out of 17 (29%) had presentation with acute coronary syndrome. Mean number of vessels treated were 1.6 ± 0.6 . Eight out of 17 patients (47%) had evidence of delayed hyperenhancement in their initial scan, with a mean mass of 9.2 ± 5.4 g. Post procedure, 4/17 (24%) had evidence of new myocardial necrosis as measured by DE-MRI. The mean mass of new hyperenhancement (assuming a myocardial specific gravity of 1.05 g/cm^3) was 4.8 ± 2.5 g. All four of these patients had evidence of post-procedural troponin rise

(range 1.1–9.4 ug/L). There was an excellent linear correlation between the mass of new myocardial hyperenhancement and the change in post PCI troponin I (Spearman Rank Correlation $r^2=0.78$; $p=0.006$). The mean pre-procedure and post procedure left ventricular ejection fraction was $64\% \pm 10\%$ and $62\% \pm 12$ respectively ($p>0.05$).

Conclusion: In patients undergoing complex PCI, the rate of new myocardial necrosis as measured by DE-MRI is relatively low. There was an excellent agreement between MRI markers of post PCI necrosis and peri-procedure cardiac Troponin I elevation. The prognostic significance of post PCI hyperenhancement remains to be determined.

268. High Sensitivity but Low Specificity of Qualitative MRI Stress Perfusion in Low Risk Patients

Ralf Wassmuth, MD, Nidal Al-Saadi, MD, Rainer Dietz, MD, Matthias G. Friedrich, MD. *Franz-Volhard-Clinic, Humboldt-University Berlin, Berlin, Germany.*

Introduction: In clinical routine MRI perfusion studies are often evaluated qualitatively. We tested in how far adenosine stress perfusion defects match significant coronary artery stenoses in a low risk outpatient population.

Methods: Out of 221 consecutive MRI stress perfusion studies 44 patients (20%, 44 to 77 years, median 62 years, 36 men) were referred to coronary angiography based on the decision of the referring physician. Symptoms were graded as typical ($n=16$) or atypical ($n=28$) by clinicians independent from MRI. Perfusion studies were done at rest and after adenosine stress (140 mcg/kg/min over 4 minutes) in a 1.5 T scanner using a hybrid EPI/GRE sequence. Three short axis slices were acquired at every heartbeat after infusion of 0.1 mmol/kg Gd-DTPA. Typical in-plane resolution

was $2.7 \times 2.0 \text{ mm}^2$. MRI studies were classified as typical CAD-related stress-induced focal defect or no such defect in a 12-segment-model. Angiograms were evaluated independently and blinded to the MRI. Stenoses of at least 50% were considered significant.

Results: Pretest probability was 50%. MRI yielded in a sensitivity of 95% and a specificity of 32% to predict significant coronary stenosis in a segment-based analysis. The negative predictive value was 88%.

Conclusion: In a population with a low pretest probability, qualitative MRI stress perfusion offers high sensitivity but low specificity to predict significant coronary artery stenoses. A negative MRI stress perfusion has a high negative predictive value to rule out significant coronary disease.

269. Comparison of Individually Adapted Breath-Hold and Free-Breathing Coronary MRA using Steady State Free Precession

Cosima Jahnke, MD, Ingo Paetsch, MD, Rolf Gebker, MD, Bernhard Schnackenburg, PhD, Axel Bornstedt, PhD, Eckart Fleck, MD, Eike Nagel, MD. *Cardiology, German Heart Institute Berlin, Berlin, Germany.*

Background: With flow independent steady state free precession (SSFP) sequences an improved coronary artery visualization in comparison to previous techniques can be achieved. We assessed the influence of free-breathing, navigator-gating (NAV) versus breath-holding (BH) on image quality of SSFP coronary MRA using an identical spatial resolution.

Methods: 40 consecutive patients with suspected coronary artery disease underwent MR imaging of the left or right coronary artery using SSFP (TR/TE/flip: 4.5 ms/2.3 ms/90°; Philips Intera CV 1.5T) twice. Correction of breathing motion was done once with real time prospective navigator and again with BH. Maximal BH duration was individually determined and

Table 1.

	Visual score (low=1, high=4)	Vessel sharpness (%)	Visible vessel length (mm)	Visible side branches
BH-LAD	2.7±0.7	45±4	71±24	3.9±1.6
NAV-LAD	3.4±0.4*	45±6	86±33*	4.9±2.3*
BH-RCA	2.8±0.6	50±4	115±23	2.4±0.8
NAV-RCA	3.5±0.5*	47±6	121±25	2.8±10.8*

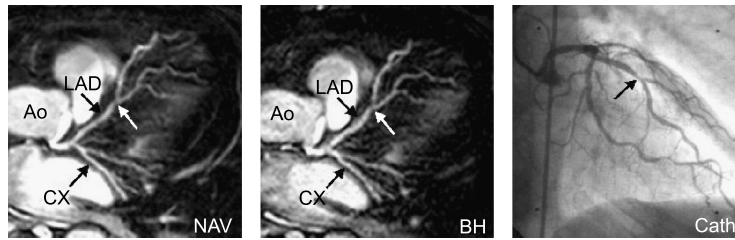


Figure 1.

the duration of data acquisition was adapted using different SENSE-factors. The following quantitative parameters were determined: visual score, vessel sharpness, visible vessel length, number of visible side branches. Diagnostic accuracy was calculated in comparison to invasive x-ray angiography.

Results: With NAV more coronary artery segments yielded interpretable results (84% vs. 62%*) and 13% more coronary segments were correctly diagnosed resulting in a significantly higher diagnostic accuracy (79.7% vs. 89.0%*). In addition, the quantitative parameters for image quality showed a significant superiority of the NAV approach (see Table 1, Fig. 1).

Conclusions: Free-breathing, navigator corrected coronary MRA is superior to breath-holding regarding image quality and diagnostic accuracy of stenosis detection.

Methods: Dynamic first pass MR perfusion imaging (Philips Intera CV; Turbo-Gradient-Echo techniques; spatial resolution $2.7 \times 2.7 \times 8$ mm) was performed in 32 patients after peripheral i.v. administration of Gd-BOPTA during adenosine stress (140 $\mu\text{g}/\text{min}/\text{kgBw}$). Two doses (0.05 and 0.025 mmol/kgBw) and four different injection speeds (8, 4, 3, 2 ml/s) were used. Signal intensity time curves were determined in the LV bloodpool and myocardial segments supplied by normal coronary arteries and upslope as well as peak enhancement were noted using commercially available software (MASS[®], Medis).

Results: A significant correlation was found between the upslopes in the LV bloodpool and the myocardium (r square=0.89, $p < 0.001$) (Figure 1, up). However, LV bloodpool and myocardial upslopes were independent of the dosage and the injection speed.

270. Determinants of Myocardial Response in MR Perfusion Measurements

Rolf Gebker, MD,¹ Ingo Paetsch, MD,¹ Cosima Jahnke, MD,¹ Bernhard Schnackenburg, PhD,² Axel Bornstedt, PhD,¹ Eckart Fleck, MD,¹ Eike Nagel, MD.¹
¹Internal Medicine-Cardiology, German Heart Institute Berlin, Berlin, Germany, ²Philips Medical Systems, Hamburg, Germany.

Introduction: The most important choices for imaging during the first pass of an injected contrast agent relate to the pulse sequence protocol, the type and dosage of the contrast agent that is being used, the mode of injection and the application of postprocessing algorithms. So far a systematic evaluation of the contrast agent application scheme has not been reported.

Purpose: To evaluate the role of different dosages and injection speeds of contrast media for MR-perfusion assessment.

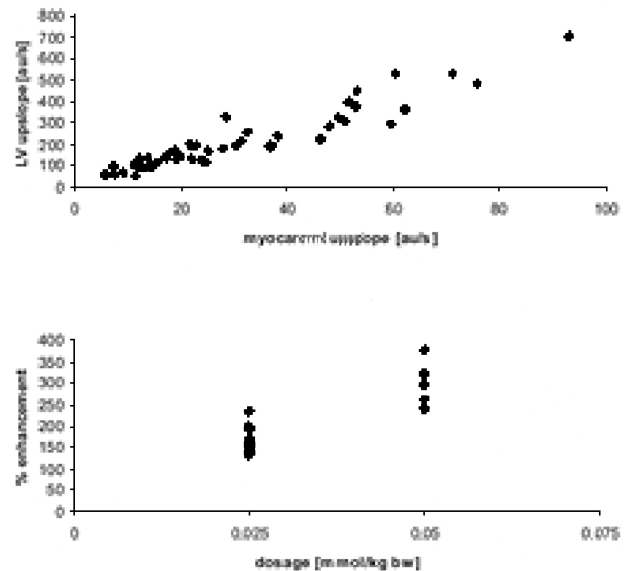


Figure 1. (Top) myocardial vs. LV upslopes. (Bottom) myocardial enhancement vs. dosage.

Higher Gd-doses led to significantly higher enhancement ($p < 0.001$) (Figure 1, bottom).

Conclusion: In healthy myocardial segments, the myocardial upslope is mainly determined from the LV bloodpool upslope, which—in contrast—is independent from contrast agent dosage or injection speed. Myocardial enhancement, however, is dose dependent. Thus, a simple correction for the LV bloodpool upslope allows to normalize a wide variety of input parameters. Differences of myocardial upslope or peak signal intensity after correction should be mainly dependent on blood flow.

271. Coronary Artery Motion Tracking in Swines Using MR Tracking Catheters

Ehud J. Schmidt,¹ Ryuichi Yoneyama,² Charles L. Dumoulin,³ Motoyase Hayase,² Eric N. Klein³. ¹GE Medical Systems ASL, Boston, MA, USA, ²Cardiology, Massachusetts General Hospital, Boston, MA, USA, ³GE Global Research Center, Niskayuna, NY, USA.

Introduction: Coronary artery motion varies at phases in the cardiac cycle, and along the length of the vessels. Understanding this translational and rotational motion is key to high-resolution MR imaging of the vessel lumen and walls, as this motion produces image blurring and artifacts (Schar et al., 2003). An MR Tracking method is shown to accurately measure this motion. Precise motion understanding may be used in combined imaging&tracking catheters to prospectively or retrospectively correct images for intra-imaging motion.

Purpose: Utilize Magnetic Resonance (MR) Tracking catheters to provide high-temporal resolution, three dimensional spatial information, on coronary motion

Methods: MR Tracking (Dumoulin et al., 1993) utilizes MRI gradients applied along the X (Left–Right), Y (Anterior–Posterior) and Z (Superior–Inferior) directions. When small-FOV radio-frequency (MR Tracking) coils are used for reception, the received signal in each provides its spatial position in these 3 directions. MR Tracking catheters (135 cm length, 1.5–2.3 mm diameter), consisting of three tracking coils spaced 25 mm apart, provided 15–20 frames-per-sec, X, Y and Z spatial positions with an accuracy of ± 0.4 –0.5 mm. The catheters were placed under X-ray Fluoro guidance into the LAD, RCA and LCX of 5 swines. The animals were scanned in a 1.5 Tesla GE CV/i MRI scanner. ECG-gated 3D motional data was



Figure 1. (View this art in color at www.dekker.com.)

acquired at 3 levels in the arteries (Distal, Mid, Proximal), during multiple 20–30 second breath-holds. Data-processing involved averaging positional information from the same cardiac phase amongst R–R cycles sharing a common heart-rate, in order to display mean motional characteristics.

Results: Figure 1 is a gradient-echo coronal heart image with Green square, Yellow circle and Blue triangle overlays denoting tracking coils positioned in the RCA at 7.5 cm, 5.0 cm, and 2.5 cm, distances, respectively, from the aortic root, in a pig with 85 BPM heart-rate.

Figure 2 shows the 3D motion, as a function of cardiac phase, at the three tracking coils (color coded as in Figure 1). Red dots indicate the first cardiac phase after QRS and motion is clockwise, ending at the green dot (last cardiac phase). Artificial lines connect the same cardiac phase at the three coronary levels to illustrate changes in vessel orientation. Upper-right inset shows mid-tracking-coil S–I (red), A–P (pink) and L–R (blue) motion over 3 cycles.

Conclusions: At a rapid heart rate there are practically no regions where the RCA is stationary. Motion in the proximal RCA is largest and drops off more distally, reflecting a vessel which is both displacing and rotating during the cardiac cycle. Motion patterns of the LCX and LAD were also studied. The observed coronary motions are similar to human coronary motion, as inferred from EBCT (He et al., 2001; Lu et al., 2001) and Cine-MRI (Foo et al., 2000; Saranathan et al., 2001) images. It is important to note that the spatial precision of the inferred information is: a. generally 2D in nature, providing only in-plane motion, b. obtained only at one point in the vessels, so rotational information is absent, and c., is of inferior spatial resolution to that shown here. Correcting MRI images utilizing the precise nature of the motion may be important for obtaining sub-millimeter resolution images of the vessels (Botnar et al., 2003).



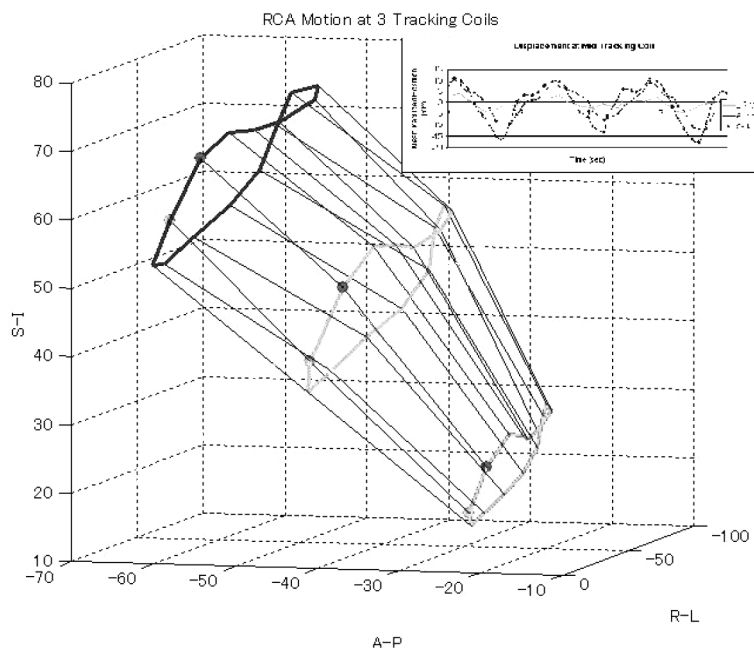


Figure 2. RCA motion at 3 tracking coils. (View this art in color at www.dekker.com.)

REFERENCES

Botnar, R. M., Buckner, A., Kim, W. Y., et al. (2003). *JMRI* 17(5):169–615.
 Dumoulin, C. L., Souza, S. P., Darrow, R. D. (1993). *MRM* 29:411–416.
 Foo, T. K., Ho, V. B., Hood, B. S. (2000). *Radiology* 214:283–289.
 He, S., Dai, R., Chen, Y., et al. (2001). *Acad. Radiol.* 8:48–56.
 Lu, B., Mao, S.-S., Zhuang, N., et al. (2001). *Invest. Radiol.* 36(5):250–256.
 Saranathan, M., Ho, V. B., Hood, M. N., et al. (2001). *JMRI* 14:368–373.
 Schar, M., Kim, W. Y., Stuber, M., et al. (2003). *JMRI* 17(5):538–544.

272. Accurate Measures of Cardiac Output and Stroke Volume by Phase Contrast MRI in Patients with Ischemic Heart Disease: Validation by Right Heart Catheterization

Christopher J. McGann,¹ Michael D. Puchalski,² Henry Buswell,³ Edward V.R. DiBella.³ ¹Cardiology, University of Utah, Salt Lake City, UT, USA, ²Pediatric Cardiology, University of Utah, Salt Lake City, UT,

USA, ³Radiology, University of Utah, Salt Lake City, UT, USA.

Introduction: Phase contrast cine MR imaging (PC-MRI) is evolving as a tool to make fast, accurate measurements of cardiac function with a single breath hold. Early studies demonstrated close correlations between PC-MRI and cine MR volumetric measurements of left and right ventricular stroke volumes in normal patients (Kondo et al., 1991). More recently, PC-MRI has been shown to correlate well with invasive oximetry and indicator dilution techniques in patients with left-to-right intracardiac shunts (Hundley et al., 1995; Beerbaum et al., 2001). Published data is not available that validates PC-MRI flow analysis in patients with ischemic heart disease (IHD) and wide ranging ejection fractions.

Purpose: The purpose of this study was to determine whether measurements of cardiac output (CO) and stroke volume (SV) by PC-MRI closely correlate with the gold standard of right heart catheterization (RHC) in patients with IHD.

Methods: Seventeen patients with IHD (EF range 15.5 to 61.0%) and a prior RHC (within three weeks) subsequently underwent PC-MRI with measurements obtained from the ascending aorta (AA) and main pulmonary artery (MPA), 2 cm above the coronary arteries and valve respectively. MR images were acquired with a 1.5-T GE Signa cv/nv using a four

Copyright © Marcel Dekker, Inc. All rights reserved.

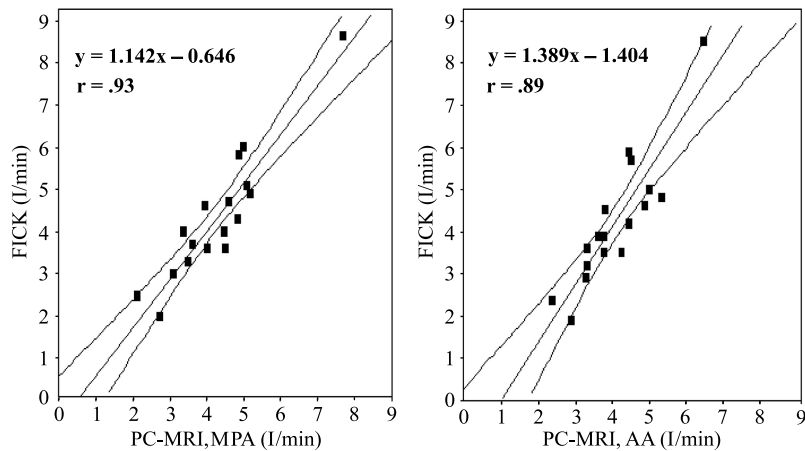


Figure 1. Graphs show correlation between CO by Fick vs. PC MRI in the main pulmonary artery (left) and Fick vs. PC-MRI in the ascending aorta (right).

coil cardiac array. PC-MRI volume analyses were performed using commercially available software (MEDIS FLOW). Two blinded operators analyzed PC-MRI data. RHC was performed with a Swan Ganz Catheter and CO was calculated using the Fick Equation with assumed values for oxygen consumption. Flow measurements were performed perpendicular to the axis of flow using a flip angle of 15°, a TE/TR=3/7.6 msec, bandwidth±31.2 kHz, FOV 40 cm, slice thickness of 5 mm, and acquisition matrix 256×128. PC data was obtained from planes over 20 phases of the cardiac cycle during a single breath hold with peak velocity set 200–300 cm/sec.

Results: Mean hemodynamic parameters were not significantly different between the three methods. Mean values determined by indirect Fick, PC-MRI in

MPA, and PC-MRI in AA were as follows: 1) CO 4.24±0.78 (SE 0.37), 4.27±0.64 (SE 0.30), 4.06±0.50 (SE 0.24) liters/min 2) SV 61±10 (SE 4.8), 62±10 (SE 4.1), 58±8 (SE 3.8) milliliters. Figure 1 shows the close linear relationship between CO measured by indirect Fick vs. PC-MRI in the MPA and AA (r=0.928 and 0.885 respectively). The slopes of the regression equations were not significantly different from 1 with 95% CI (0.889–1.396 and 0.987–1.790). Similar close correlations were found for SV measures by indirect Fick and PC-MRI in the MPA and AA (r=0.900 and 0.815 respectively). The slopes of the regression equations were not significantly different from 1 with 95% CI (0.779–1.345 and 0.629–1.436). Figure 2 shows mean differences for CO measurements by PC-MRI MPA and AA vs. Fick (MPA

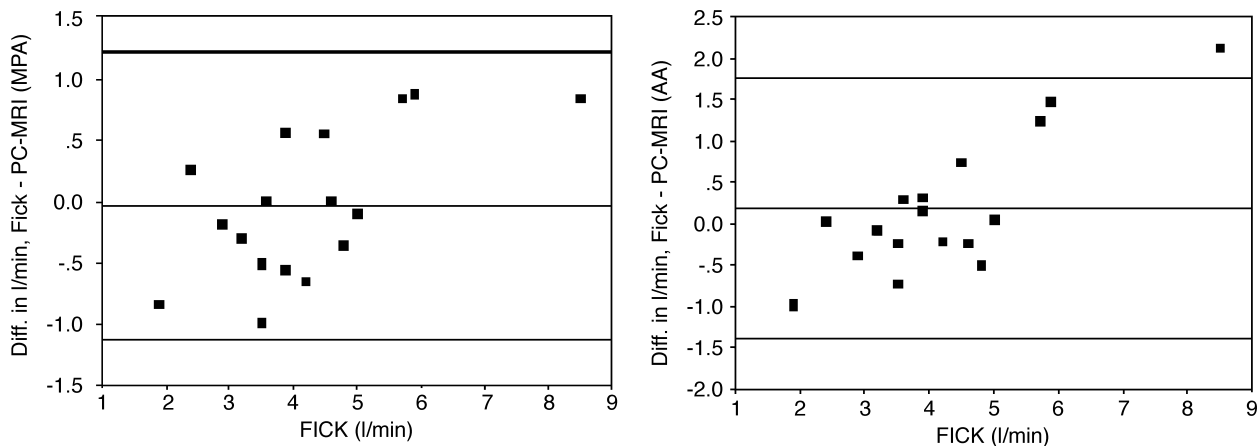


Figure 2. Bland–Altman plots for CO between Fick and PC-MRI in the main pulmonary artery (left) and ascending aorta (right). Upper and lower limits: mean±SD.

–0.038±0.59 l/min, AA 0.17±0.81 l/min). Mean difference for SV measurements by PC-MRI vs. Fick (MPA –0.59±8.70 ml, AA 3.12±11.49 ml) also showed good agreement.

Conclusions: In patients with IHD and a wide range of ejection fractions, PC-MRI measures of CO and SV correlated closely with those values obtained by RHC. As these measurements can be obtained more quickly and easily than volumetrics by cine MRI, imaging time can be significantly reduced in cases where more detailed LV function is not needed. In addition, MRI flow measurements in the MPA appear more accurate than those obtained in the AA. This may be due to the more complex anatomy and flow dynamics in the AA.

REFERENCES

- Beerbaum, P., et al. (2001). *Circulation* 103:2476–2482.
 Hundley, W. G., et al. (1995). *Circulation* 91:2955–2960.
 Kondo, C., et al. (1991). *AJR* 157:9–16.

273. Application of T2-Weighted TRIM-, Truefisp Cine-Sequences and Detection of Signal Late Enhancement Allows Prospective Estimation of Infarct Size and Functional Recovery in Patients with Acute Myocardial Infarction and a Differentiation Between Hibernating and Stunned Myocardium

Udo Sprengel,¹ Thomas Wetzel,¹ Thorsten Nitschke,¹ Verena Lubinski,¹ Martin Klocke,¹ Olivia Braun,¹ Norbert Schulze-Waltrup,¹ Niels Oesingmann,² Michaela Schmidt,² Thomas Scheffold,³ Hubertus Heuer.¹ ¹Cardiology, St. Johannes Hospital, Dortmund, Germany, ²Siemens, Erlangen, Germany, ³Cardiology, Institut für molekulare und klinischen Herz-Kreislaufforschung der Universität Witten/Herdecke, Dortmund, Germany.

Introduction: Non viable myocardium can be detected via MRI after injection of Gd-DTPA. Using T1-TFL-scans non viable myocardium shows a signal late enhancement (LE).

Purpose: The aim was to investigate whether patients (p) with acute angina and increase of troponin (T), CK, CKMB) indicating an acute myocardial infarction show a different signal behaviour of the myocardium in the MRI than p with stabile angina indicating chronically coronary heart disease.

Methods: We investigated 69 p mean age 56 (34–79) y. (41 m; 28 f) (49 p with acute myocardial infarction and 20 p with stabile angina) after coronarangiography, PTCA and stent implantation in a MR-scanner. The MR scans were performed on 1.5T Siemens system immediately after the intervention 14 days, 6 weeks and 3 month later. We used TrueFISP-Cine in 4-, 2-chamber and short axis view to determine left ventricular function and wall motion. For tissue characterisation T2-TIRM (TI 170 ms) and T1-2D-and 3D-TFL-images were added after injection of Gd-DTPA.

Results: All 69 p had regional contractile dysfunction in the first investigation. 29/49 p with an increase of T, CK and CKMB showed a LE in the myocardium. All 29 p had a hyperenhancement in the corresponding area in T2-TIRM images indicating myocardial edema. In 17/29 p no recovery of contractility could be observed after 3 month. In 12/29 p a partial recovery of the contractility could be seen after 3 month. 11/49 p with an increase of T, CK and normal CKMB showed no LE in the first scan and a complete recovery of function after 3 month. In 9/49 p with increased T, normal CK and CKMB no LE could be detected during the first scan. 7/20 p without LE showed also a hyperenhancement in the T2-TIRM scans in the dyskinetic area. After 6 weeks and 3 month a normal contractility and a loss of hyperenhancement in TIRM-image could be seen. All 20 p with stabile angina had no signal enhancement in the T2-TIRM images and no LE in the T1-TFL-images in the first and following scans. After 14 days myocardial function was normal.

Conclusions: The detection of LE is a useful diagnostic tool in p with acute angina. In combination with T2-TIRM and cine-sequences it allows an early determination of infarct region and prospective estimation of functional recovery of the myocardium and the differentiation between hibernating and stunned myocardium.

274. MRI Detection of Thrombus in Left Ventricular Aneurysms

Naeem Merchant, MD, Yves Provost, MD, Eli Konen, MD, Yuesong Yang, Tracey Elliot, MD, Jagdish Butany, MD, Narinder Paul, MD. *Medical imaging, Toronto General Hospital, Toronto, ON, Canada.*

Introduction: Left ventricular aneurysms (LVA), which occur in approximately 2–4% of post MI patients, are



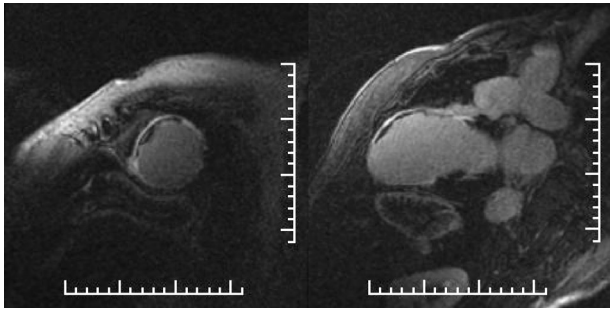


Figure 1.

a late complication of myocardial infarctions. They most commonly result from a large anteroseptal, transmural infarct which heals to form thin scar tissue. This scar tissue paradoxically bulges during systole forming the ventricular aneurysm. The lack of systolic contraction leads to stasis of blood within the aneurysm and clot formation. Identifying the presence of clot can decrease morbidity from embolic episodes by initiating anti-coagulant therapy, and is vital information to surgeon if revascularization and LVA resection is considered. In most clinical practices, echocardiography is considered the modality of choice for identification of LV clot.

Purpose: The purpose of the study is to evaluate the ability of MRI in identifying LV clot in LVA patients.

Methods: Cardiac MRI studies were performed in 23 patients with suspected LVA. All patients underwent LVA resection with pathology review of the resected aneurysm. The MRI study was performed on 1.5T GE CVi scanner and consisted of trans-axial and short-axis Fiesta images, Gadolinium enhanced first pass perfusion, and delayed enhanced images at 10 and 15 minutes in the short axis and two chamber projections. Two blinded reviewers evaluated the MRI studies for the presence of clot.

Results: MRI identified LVA clot in 9/23 patients (39%). Pathology review of the resected aneurysm confirmed LV clot in all nine patients. No false negatives or false positives occurred (Fig. 1).

Conclusions: MRI is an excellent modality to identify the presence of LV clot in the setting of LVA.

275. Comparison of Rest and Dobutamine Tagged MRI with Infarct Transmurality Defined by Myocardial Delayed Enhancement

Marly M. Uellendahl, MD,¹ Sérgio D. Florenzano, MD,¹ Marcello Zapparoli, MD,¹ Fábio Berezowsky Rocha, MD,¹ Marcia Lima de Oliveira Mugnaini, MD,¹ José Rodrigues Parga, MD, PhD,¹ Luiz Francisco Rodrigues de Ávila,¹ Nael F. Osman, PhD,² Carlos Eduardo Rochitte, MD, PhD.¹ ¹Cardiovascular Magnetic Resonance Laboratory, Heart Institute-InCor-University of São Paulo Medical School, São Paulo, Brazil, ²Radiology, Johns Hopkins University, Baltimore, MD, USA.

Introduction: Recently myocardial delayed enhanced MRI (MDE) has been recognized as best method in distinguishing reversible from irreversible myocardial injury. It is of critical importance in the clinical management of patients with acute and chronic coronary artery disease (CAD). Usually, infarct transmural (IT) by visual score has been used to predict the potential for regional contractility recovery. An objective measurement of regional contractility in comparison to infarct transmural is still missing. Moreover, based on the available data, infarct transmural from 25–75% has yet an uncertain potential for recovery.

Purpose: Our objective were to compare infarct transmural to rest and low-dose dobutamine tagged MRI and to evaluate objectively the potential for myocardial contractile improvement.

Methods: We studied 5 patients (80 segments) with prior myocardial infarction (MI) that underwent cardiac MRI in a 1.5T CVI GE scanner. We acquired myocardial tagging short-axis images at rest and during 10 mcg/kg/min of dobutamine and delayed

Table 1.

%	IT 0	IT 1	IT 2	IT 3	p (ANOVA)
REST ECC	13.6±0.9	8.0±1.8	4.1±2.2	3.5±1.7	<0.01
DOB ECC	13.0±1.3	8.9±1.7	6.5±2.0	4.5±1.9	<0.01
p (test t)	NS	NS	NS	NS	

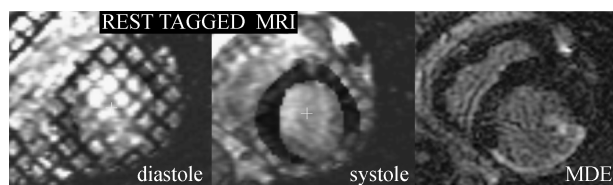


Figure 1.

enhanced MRI on the same locations 10–20 minutes after 0.2 mmol/kg of gadolinium-based contrast. We analyzed 3 short-axis slices of each left ventricle (LV), one apical, one medial and one basal slice. Infarct transmuralities were classified visually as: 0 (no enhancement), 1 ($\leq 25\%$ of transmuralities), 2 (25–75% of transmuralities) or 3 ($>75\%$ of transmuralities) for each segment of a 16-segment model. Tagged-MRI was analyzed using the HARP software tool (Diagnosoft, Inc.) and mid-wall circumferential shortening (Ecc) was defined for each segment as the contractility index. Comparison between rest and dobutamine Ecc were done by Student t test and among the degrees of transmuralities by ANOVA.

Results : Mean maximum systolic Ecc for all segments with no enhancement was $13.6 \pm 0.9\%$ at rest and $13.0 \pm 1.3\%$ during dobutamine, p NS. For subendocardial infarcts (transmuralities score 1) rest and dobutamine Ecc were $8.0 \pm 1.8\%$ and $8.9 \pm 1.7\%$, respectively, p NS. For transmuralities score 2 (25–75%), rest and dobutamine Ecc were $4.1 \pm 2.2\%$ and $6.5 \pm 2.0\%$, respectively, p NS. For score 3 rest and dobutamine Ecc were $3.5 \pm 1.7\%$ and $4.5 \pm 1.9\%$, respectively, P NS. Although changes from rest to dobutamine were not significant, even for segments without enhancement, when we selected those with no enhancement and not adjacent to infarcted segments (remote segments) the rest and dobutamine Ecc were $13.7 \pm 1.1\%$ and $16.1 \pm 1.4\%$, respectively p=0.03. The transmuralities scores showed significant differences on rest and dobutamine Ecc (p<0.01 for both, Table 1).

Infarct transmuralities correlated significantly with Ecc measured by tagged MRI, so that the higher the infarct transmuralities the lower the Ecc (Fig. 1).

Conclusion: Rest circumferential shortening measured by tagged-MRI can objectively evaluate the potential for myocardial contractile improvement and was strongly correlated to infarct transmuralities by myocardial-delayed enhancement. Low-dose dobutamine circumferential shortening increased significantly only on remote segments. On adjacent and infarcted segments, including those with transmuralities score 2, dobutamine tagged MR was unable, on this

initial data, to further stratify the potential for contractility recovery.

276. Coronary Vessel Wall Thickness and Area in Patients with Non-ST Coronary Syndromes: Acute versus Late Follow-up Comparison Using Black-Blood Magnetic Resonance Imaging

Juliano L. Fernandes,¹ Carlos V. Serrano, Jr,¹ Otavio R. Coelho,² Carlos E. Rochitte,¹ Luiz F. Avila,¹ Jose P. Filho.¹ ¹Heart Institute (InCor)—University of Sao Paulo Medical School, Sao Paulo, Brazil, ²University of Campinas (UNICAMP), Campinas, Brazil.

Introduction: In vivo noninvasive imaging of the coronary artery wall can detect the effects of vascular remodeling in humans. Increased inflammatory activity may influence atherosclerotic lesions and affect arterial remodeling.

Purpose: Since patients with acute coronary syndromes are characterized by elevated markers of inflammatory disease we sought to investigate using in vivo black-blood magnetic resonance imaging (MRI) whether visualization of the coronary vessel wall could discriminate differences in vascular remodeling in patients with coronary atherosclerosis during an acute and chronic stage of the disease.

Methods and Results: Six patients with non-ST acute coronary syndromes were selected and followed for six months. A total of eleven proximal coronary segments from the left anterior descending artery and right coronary artery were analyzed after a maximum of 5 days from the acute event and again after a 6 month event free period of follow-up. Patients were studied in a commercial 1.5 Tesla cardiovascular magnetic resonance scanner using a black-blood MRI sequence. Coronary artery lumen and vessel wall were analyzed. Mean coronary wall thickness was 3.85 ± 0.69 mm (range, 2.6 to 5.0 mm) during the acute phase versus 2.94 ± 0.66 mm (range, 1.8 to 3.8 mm) in the chronic phase. The wall area was also increased during the acute phase with 59.64 ± 10.22 mm² (range, 45 to 79 mm²) versus 44.55 ± 12.34 mm² (range, 31 to 73 mm²). The differences for wall thickness and wall area were both statistically significant (P=0.01 and P=0.02, respectively). No significant changes in luminal area were found along the follow-up (20.0 ± 4.36 mm² vs. 18.64 ± 6.14 mm²).

Conclusions: Patients with coronary artery disease had increased coronary wall thickness and area during acute coronary syndromes compared to the chronic



stage of the disease. This may help our understanding of the plaque lesion regression process and provide new data for future associations with clinical events.

277. Microvascular Obstruction Related to Primary Angioplasty by Magnetic Resonance Imaging with Acute Myocardial Infarction

Kyu Ok Choe, MD,¹ Byoung Wook Choi, MD,¹ Young-Jin Kim, MD,¹ Namsik Chung, MD,² Se-Joong Rim, MD². ¹*Diagnostic Radiology, Yonsei University College of Medicine, Seoul, Republic of Korea,* ²*Cardiology, Yonsei University College of Medicine, Seoul, Republic of Korea.*

Introduction: Microvascular obstruction in acute myocardial infarction can be caused by various mechanisms including microembolization during the revascularization procedure such as angioplasty or stenting. With increasing primary intervention in acute myocardial infarction and emergence of contrast-enhanced magnetic resonance imaging (MRI), microvascular obstruction related with angioplasty can be easily detected as hypoenhanced region within hyperenhanced lesion with contrast-enhanced MRI.

Purpose: To investigate the microvascular obstruction related to primary angioplasty with stenting in acute myocardial infarction by using contrast-enhanced magnetic resonance imaging.

Methods: Consecutive 32 patients with acute myocardial infarction determined by CK-MB profile were enrolled and divided into two groups a group treated by primary angioplasty and stenting without using protecting device for microembolization on admission (PA group, n=20, aged 61.8±9.5) and the other group initially treated by thrombolytic therapy (TT group, n=12, aged 55.9±10.9). MRI was performed from 0 to 20 days (mean 4.4 days) after primary angioplasty and from 0 to 27 days (mean 6.1 days) after onset of symptom in TT group. Perfusion MRI was performed with TFE-EPI single shot pulse sequence in 3–4 short-axis slices for 50–60 s with contrast-enhancement. Delayed-enhanced MRI encompassing the entire left ventricle was performed with a multi-shot, TFE, inversion prepulse 10 minutes after contrast administration (TR=5.4 ms, TE=1.6 ms, FA=15, voxel size=1.37 × 1.37 × 10 mm). Presence of both hypoenhancement in perfusion MRI and hypoenhancement within hyperenhancement on the same location in delayed-enhanced MRI was determined as microvascular obstruction and the prevalence of microvascular obstruction in each group was compared.

Infarct-size, level of CK-MB and troponin-T, and degree of stenosis of infarct-related artery were compared between the PA and TT groups and between the group with microvascular obstruction and the rest.

Results: Nine patients (45%) in the PA group showed hypoenhancement within hyperenhanced region in delayed-enhancement studies, which showed early hypoenhancement in perfusion study too. No patients in the TT group showed hypoenhancement in delayed-enhancement imaging even in the case of hypoenhanced region in perfusion study. The microvascular obstruction was observed on the exactly same territory of primary angioplasty and stenting. Peak value of CK-MB and Troponin-T were significantly higher in the PA group than in the TT group ($330.8 \pm 270.0 > 100.46 \pm 122.60$ p=0.009), ($5.72 \pm 7.97 > 0.60 \pm 0.70$, p=0.021). However, the level of the enzymes was not significantly different between in patients with microvascular obstruction and in patients without in the PA group. Therefore CK-MB and Troponin-T did not predict the presence of microvascular obstruction. Totally-transmural infarction determined by MRI (n=5) was observed only in patients revealing microvascular obstruction. Transmural extent of infarct-size measured in delayed images in patients with microvascular obstruction was larger than that in the TT group and that in patients without microvascular obstruction in the PA group ($84 \pm 19\% > 55 \pm 31\%$, $62 \pm 13\%$ respectively, p<0.05). The degree of stenosis of infarct-related artery was not different between the TT and the PA group.

Conclusions: Microvascular obstruction is frequent with the primary angioplasty and it can be detected with delayed imaging with contrast-enhanced MRI. The microvascular obstruction occurring in primary angioplasty may undermine the benefit of primary angioplasty in acute myocardial infarction.

278. Cardiac MRI Stress Perfusion and Delayed Enhancement Imaging in the Evaluation of Patients with Known or Suspected Coronary Artery Disease

Ricardo C. Cury, MD,¹ Cesar A. M. Cattani, MD,² Luiz A. G. Gabure, MD,³ Douglas J. Racy, MD,³ Jose L. Gois, MD,² Thomas J. Brady, MD,¹ Sergio S. Lima, MD³. ¹*Radiology, Massachusetts General Hospital, Boston, MA, USA,* ²*Cardiology, Beneficencia Portuguesa Hospital, Sao Paulo, Brazil,* ³*Radiology, Beneficencia Portuguesa Hospital, Sao Paulo, Brazil.*



Introduction: Most clinical studies that used First-pass perfusion Magnetic Resonance Imaging (FPMRI) assessed inducible ischemia through rest and stress perfusion images. However, a considerable portion of such patients may be expected to have had previous myocardial infarction, either silent or clinically apparent. Contrast-enhanced MRI has also the potential to characterize tissue injury after myocardial infarction (MI).

Purpose: To demonstrate the ability of detecting and characterizing myocardial perfusion deficits using a combined MR approach with stress FPMRI followed by delayed enhancement imaging in patients clinically known or suspected of CAD, using X-ray coronary angiography as a gold standard.

Methods: 47 patients (38 men, mean age of 63 ± 5.3 years) were prospectively enrolled between June 2001 and January 2003. 14 patients (30%) had a prior history of myocardial infarction with recurrent angina including 8 patients with prior CABG surgery. Patients were selected if they had recently undergone or were waiting to undergo coronary angiography from one day to three weeks of the MR study. All subjects underwent cardiac MRI using a 1.5 Tesla MR system (CV/i, General Electric Medical Systems). After the assessment of cardiac morphology and function, Gadopentetate Dimeglumine (Gd DTPA) was injected in bolus and a first-pass perfusion protocol in hyperemia induced by dipyridamole (0.56 mg/Kg) was acquired, which yielded 4 to 6 slices in short-axis view covering the entire left ventricle every other heartbeat. A second bolus of Gd-DTPA was injected (0.1 mmol/Kg IV at 2 ml/s) and 10 minutes later delayed enhancement images were acquired. The myocardial segments were divided according to the three main coronary artery territories. A 70% or larger diameter stenosis was considered to be severe in coronary angiography. Two observers interpreted qualitatively the combined evaluation of the gadolinium first-pass stress perfusion and delayed enhancement images by consensus, which were blinded to the results of X-ray coronary angiography.

Results: X-ray coronary angiography showed severe stenosis in 31 patients (67%). Perfusion deficits were observed in 32 patients (51 coronary artery territories). The FPMRI yielded an overall sensitivity of 77%, specificity of 88%, and accuracy of 83% comparing to coronary angiography. Delayed enhancement imaging was positive in 15 patients including the fourteen with previous clinical history of myocardial infarction or CABG surgery. By correlating stress FPMRI with delayed enhancement images, we could differentiate perfusion deficits in viable myocardium (inducible ischemia—20 coronary artery territories) from perfusion deficits in non-viable myocardium (myocardial infarction—31 coronary artery territories).

Conclusions: The current results showed the ability of this combined MR approach in the detection and further characterization of myocardial perfusion deficits in a population with known or suspected CAD. We advocate that this MR approach may be more reliable to detect inducible ischemia and myocardial infarction than rest and stress perfusion MR imaging.

279. Elevated Coronary Calcium Score is Associated with Left Ventricular Dysfunction in Asymptomatic MESA Participants

Thor Edvardsen, MD, PhD,¹ Robert Detrano, MD, PhD,² Boaz D. Rosen, MD,¹ Li Pan, MS,³ Jeffrey J. Carr, MD,⁴ Shenghan Lai, MD, PhD,¹ David A. Bluemke, MD, PhD,³ João A. C. Lima, MD.¹ ¹Cardiology, Johns Hopkins University, Baltimore, MD, USA, ²Cardiology, UCLA School of Medicine, Torrance, CA, USA, ³Radiology, Johns Hopkins University, Baltimore, MD, USA, ⁴Radiology, Wake Forest University, Winston-Salem, NC, USA.

Introduction: Coronary artery disease is the leading cause of left ventricular dysfunction and heart failure in the US and Europe. Coronary artery calcium score (CAC) by CT is a specific, quantifiable marker of coronary atherosclerosis. Regional myocardial function can be accurately determined by measuring myocardial strain and strain rate by MRI tagging.

Purpose: We investigated whether local atherosclerosis alters regional LV systolic function measured by MRI tagging in participants of the Multi-Ethnic Study of Atherosclerosis (MESA).

Methods: MESA is an observational prospective study of men and women from 4 ethnic groups with no history of symptomatic cardiovascular disease. They were studied by CT and in addition 217 had LV strain and strain rate measured by MRI. We focused the analysis to the LAD territory to enhance confidence of regional correspondence between local CAC and function.

Results: Regional measures from the LAD territory demonstrated a correlation between peak systolic strain rate and positive CAC, ($r=0.42$ $p<0.001$). Strain measures from the anterior and septal wall were also associated with CAC ($r=0.27$, $p<0.01$ and $r=0.26$, $p<0.01$, respectively). Further analyses to determine the threshold for dysfunction showed that participants with LAD CAC>200 (highest quartile) had decreased function compared to those with zero score and those with positive CAC<200 (lower quartiles, see Figure 1).

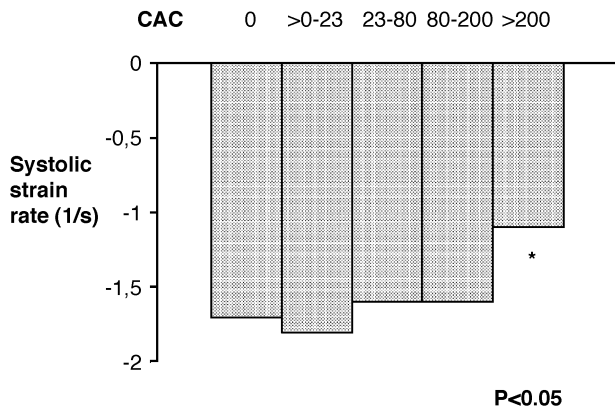


Figure 1.

Conclusions: LAD CAC score is directly related to decreased LV function in the LAD territory of asymptomatic adults without history of previous infarction or angina. These results indicate a potential link between sub-clinical atherosclerosis and LV dysfunction in asymptomatic individuals.

280. Myocardial Delayed Enhancement MRI Detects Silent Myocardial Infarction in Renal Transplant Candidate

Joalbo M. Andrade, MD,¹ Luiz H. Gowdak, MD,¹ Flávio J. Paula, MD,² José R. Parga, MD,¹ Luiz F. Ávila, MD,¹ José A. F. Ramires, MD,¹ José J. G. Lima, MD,¹ Carlos E. Rochitte, MD.¹ ¹Heart Institute-InCor-University of São Paulo Medical School, São Paulo, Brazil, ²Nephrology, University of São Paulo Medical School, São Paulo, Brazil.

Introduction: Myocardial delayed enhancement magnetic resonance imaging (MDE) has been able to detect areas of myocardial necrosis or fibrosis in post-infarction myocardium. This technique has not only a good correlation with electrocardiography signs of infarction, elevated myocardial enzymes, and with radionuclide nuclear imaging techniques, but also the ability to detect small or micro infarcts, which has been a difficult task for other imaging modalities. Therefore, MDE technique would have the potential to investigate silent myocardial infarction in high-risk population. This use has not been explored extensively and has not been studied in subgroups of patients with high risk to

develop silent myocardial infarction, specifically in renal transplant candidates.

Purpose: The aim of this study was to evaluate the ability of delayed enhancement cardiac magnetic resonance imaging (MDE) to detect silent myocardial infarction in patients with renal failure and renal transplant candidates with or without diabetes mellitus.

Methods: Forty-nine high-risk renal transplant-candidate patients without clinical history of acute myocardial infarction, 37 males (75.5%), mean age of 59.3 years, 22 patients (44.9%) with diabetes mellitus, were referred to cardiac magnetic resonance imaging. High-risk patients for CAD was defined by the presence of one of the following criteria: 1) insulin-dependent diabetes mellitus, 2) age more than; 50 years, 3) a history of angina, 4) history of congestive heart failure, and 5) an abnormal electrocardiogram (excluding left ventricular hypertrophy). MDE was performed in all patients in a 1.5 T scanner CV/i GE Medical System, as part of the pre-evaluation for renal transplant and used the following parameters: TR 7.3 ms, TE 3.2 ms, TI 150–250 ms, matrix 256x192, FOV 34–38 ms, slice thickness 8.0 mm, and slice gap 2.0 mm. The gadolinium dose was 0.2 mmol/kg body weight injected intravenously. MDE were interpreted by 2 observers and classified the myocardial involvement as subendocardial or focal/multi-focal pattern. Left ventricular mass and infarct size were measured by planimetry.

Results: The prevalence of MDE in renal transplant candidate patient group was 28.6% (14 patients), 44.9% (8 patients) in the subgroup of patient with diabetes mellitus and 22.2% (6 patients) in the subgroup without (Table 1, p NS between subgroups). The prevalence of silent myocardial infarction in renal candidate patients is considerably high, even in those without diabetes mellitus, a well-know risk for silent myocardial infarction, showing similar rates as in diabetic patients. The mean infarct size as percent of LV was 5.5±4.4%. Fifty percent (7 patients) of the

Table 1. MDE in renal transplant candidate with and without diabetes mellitus.

	MDE positive	MDE negative	Total
Diabetes mellitus	8	14	22
Non diabetes mellitus	6	21	27
Total	14	35	49

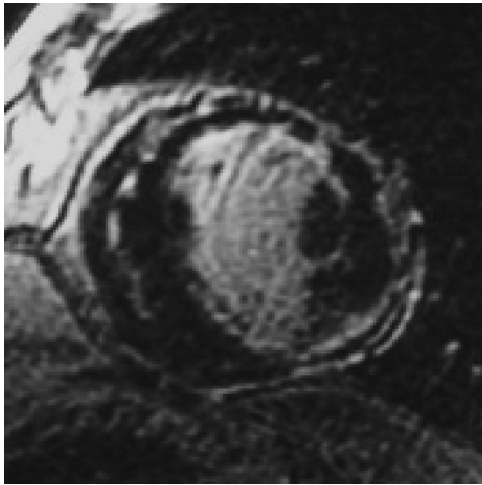


Figure 1.



Figure 2.

patients with positive MDE have a subendocardial myocardial enhancement (Figure 1).

The remaining 7 patients have a focal/multi-focal pattern of myocardial delayed enhancement (Figure 2).

It is important to note that these group infarct sizes are small and maybe below the limit for detection by radionuclide studies (due to spatial resolution limitation).

Conclusions: Myocardial delayed enhancement magnetic resonance imaging is a useful tool to detect small areas of silent myocardial infarction in high-risk renal transplant candidate patients. Due to the small size and focal pattern myocardial infarction, this is one group of patients that should be investigated preferably by myocardial delayed enhanced MRI rather than radionuclide studies.

281. Diagnostic Values of Delayed Contrast-Enhanced MRI and First-Pass Dynamic MRI in Predicting Myocardial Viability in Patients After Acute Myocardial Infarction

Kakuya Kitagawa, MD,¹ Hajime Sakuma, MD,¹ Yasutaka Ichikawa, MD,² Tadanori Hirano, MD,² Katsutoshi Makino, MD,³ Kan Takeda, MD.¹ ¹Radiology, Mie University Hospital, Tsu, Japan, ²Radiology, Matsusaka Central Hospital, Matsusaka, Japan, ³Cardiology, Matsusaka Central Hospital, Matsusaka, Japan.

Introduction: Previous studies demonstrated that first-pass dynamic magnetic resonance (MR) imaging provides information regarding microvascular integrity, and hyperenhancement on delayed contrast enhanced MR imaging indicates the presence of myocardial necrosis. However, the clinical diagnostic value of first-pass MR imaging in patients with acute myocardial infarction (MI) has not been well established.

Purpose: To compare the diagnostic values of first-pass MR imaging and delayed-enhanced MR imaging in predicting functional recovery of regional myocardial contraction in patients after acute myocardial infarction (MI), and to determine whether first-pass MR imaging should be routinely employed in addition to delayed-enhanced MR imaging.

Methods: Eighteen patients (mean age 60 ± 13 years) with first acute MI were scanned in a 1.5 T clinical scanner (Magnetom Vision; Siemens). First-pass and delayed contrast-enhanced MR images were obtained 5.5 ± 2.5 days after the onset of acute MI. The presence and extent of first-pass hypoenhancement and delayed hyperenhancement were analyzed by using a 12-segment model. Regional systolic wall thickening (SWT) was measured on cine MR images obtained 273 ± 130 days after contrast enhanced MR study with use of commercial software (MASSPlus; MEDIS medical imaging systems). First-pass dynamic MR images were acquired on short-axis planes with a saturation recovery turbo fast low-angle shot (FLASH) sequence (TR, 1.6 ms; TE, 1.2 ms; TI, 10 ms; flip-angle, 8 degree) after intravenous bolus injection of gadolinium contrast medium (Gd-DTPA, 0.05 mmol/kg). Delayed contrast-enhanced MR images were obtained with an inversion-recovery prepared segmented turboFLASH sequence (TR, 6 ms; TE, 3.4 ms; flip-angle, 15 degree) 20 minutes after administration of Gd-DTPA (total dose of 0.15 mmol/kg). Inversion time was adjusted in each patient to minimize the signal intensity of normal myocardium.

Table 1. Prediction of preserved SWT in chronic phase by first-pass MRI and delayed-enhanced MRI.

Extent of delayed hyperenhancement	Extent of first-pass hypoenhancement	
	51–100% of tissue	0–50% of tissue
51–100% of tissue	9.1% (2/22)	45.5% (15/33)
0–50% of tissue	–	89.4% (144/161)

Follow-up cine images were obtained with a segmented turboFLASH sequence (TR, 50 ms; TE, 4.8 ms).

Results: Infarct related vessels included 10 left anterior descending arteries and 8 right coronary arteries. Delayed enhanced MR imaging revealed hyperenhancement in all patients, while hypoenhancement on first-pass MR imaging was observed in 67% (12/18) of the patients. The sensitivity, specificity, and accuracy of first-pass MR imaging and delayed enhanced MR imaging in predicting impaired SWT (<20%) on follow-up cine MR images were 36.4% vs. 69.1%, $p < 0.0001$; 98.8% vs. 89.4%, $p < 0.002$; and 82.9% vs. 84.3%, n.s. respectively. First-pass MR imaging was useful for predicting functional recovery of the segments with delayed hyperenhancement of 51–100% of tissue. In these segments, preserved SWT was observed in 15/33 segments (45.5%) when extent of first-pass hypoenhancement was 1–50% of tissue, but in only 2 of 22 segments (9.1%) when first-pass hypoenhancement was 51–100% of tissue (Table 1).

Conclusions: While the sensitivity of first-pass MR imaging is limited, complementary use of first-pass MR imaging can enhance the diagnostic performance of delayed-enhanced MR imaging because hypoenhancement during first-pass is highly specific to determine non-viable myocardium.

282. Artifact Suppression in Delayed Hyperenhancement Imaging of Myocardial Infarction using B₁-Weighted Phased Array Combined Phase Sensitive Inversion Recovery

Peter Kellman, PhD, Christopher K. Dyke, MD, Anthony H. Aletras, PhD, Elliot R. McVeigh, PhD, Andrew E. Arai, MD. *NIH, Bethesda, MD, USA.*

Introduction: Myocardial viability assessment using Gd-DTPA hyperenhancement MRI is gaining clinical acceptance (Kim et al., 1999, 2000). Using recent MRI methods (Simonetti et al., 2001) myocardial

infarction may be imaged with high spatial resolution and good contrast. Following administration of Gd-DTPA, infarcted myocardium exhibits delayed hyperenhancement and can be imaged using an inversion recovery sequence.

Oscillations in the transient approach to steady state for regions such as CSF with long T₁ may cause artifacts in breath-held, segmented imaging. B₁-weighted phased-array combining (Roemer et al., 1990) provides an inherent suppression ghost artifacts. Image reconstruction uses phase sensitive detection with B₁-weighted phased-array combining to optimize SNR. Phase sensitive inversion recovery (PSIR) techniques have demonstrated a number of benefits (Kellman et al., 2002) including consistent contrast and appearance over a relatively wide range of inversion recovery times (TI), improved contrast-to-noise ratio, and consistent size of the hyperenhanced region.

Purpose: To demonstrate suppression of CSF artifact using B₁-weighted phased-array combining method for imaging myocardial infarction.

Methods: A B₁-weighted phased array combined phase sensitive reconstruction method was used (Kellman et al., 2002). This previously described approach acquires a reference image at the same cardiac phase, during the same breath-hold during alternate heart beats to estimate both the background phase and surface coil field maps.

The sequence was implemented on a GE Signa 1.5T scanner using the following typical parameters: BW ±31.25 kHz, TE/TR 3.4/7.8 ms, 20° readout flip angle (5° reference), FOV 360 × 270 mm², 256 × 96 image matrix. The 96 phase encodes were acquired in 12 heartbeats collecting 16 lines per heartbeat with 2 R–R intervals between inversions. The segment duration was 125 ms per R–R interval, acquired during diastasis. A standard 4-element cardiac phased-array was used. Images are usually acquired between 10 and 30 minutes after administering a double dose (0.2 mmol/kg) of contrast agent (Gd-DTPA, Berlex Magnevist).

Results: Long axis images of the heart are shown to illustrate the artifact suppression using B₁-weighted phased-array combining. There is a greater prevalence for this artifact with the 4-chamber view. Root-sum-of-squares magnitude combined and B₁-weighted phased-array combined phase sensitive reconstructions are shown in Figure 1(a) and (b), respectively. Both magnitude and phase sensitive images were acquired using the same breath-hold data. An artifact may be observed in the magnitude image that is not present in the B₁-weighted phased-array combined phase sensitive image which is reconstructed using the same data. The magnitude images for the individual coils are shown in

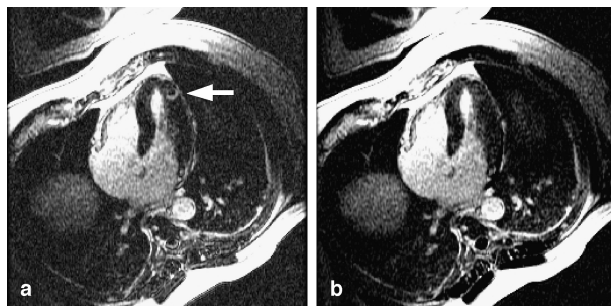


Figure 1. Images illustrating (a) artifact in root-sum-of-squares magnitude combined image, and (b) suppressed artifact in B_1 -weighted phased-array combined PSIR image.

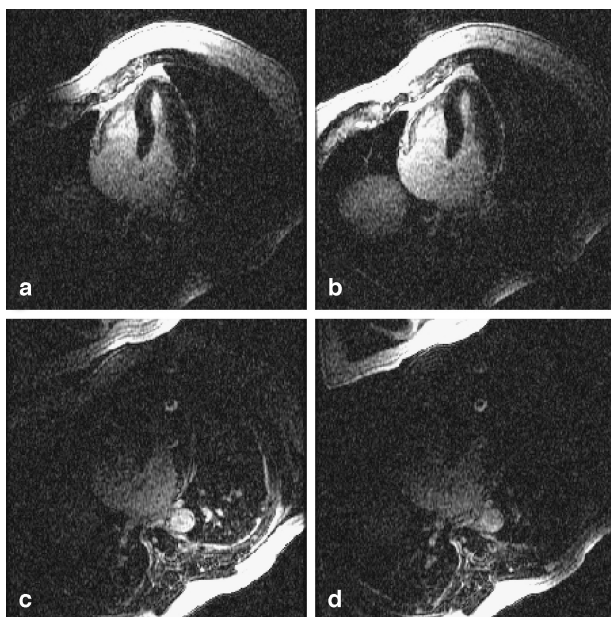


Figure 2. Individual coil images illustrating B_1 -weighting of ghost artifacts. The CSF artifact from spinal cord is evident in back coil images (c),(d), and suppressed in chest coil images (a),(b).

Figure 2. The artifact is clearly caused by ghosting of the CSF in the spinal cord, and is only evident in the back coils, Figure 2(c) and (d). The CSF artifact is suppressed by the B_1 -weighting. The suppression was calculated to be 4:1.

Conclusions: Hyperenhancement imaging of myocardial infarction using inversion recovery sequences with breath-held, segmented acquisition may lead to an artifact in regions with long T_1 such as CSF. The CSF artifact is rather small, unlike larger breathing or motion related artifacts, and is less well recognized as

an artifact. B_1 -weighted phased-array combined phase sensitive reconstruction provides an inherent degree of artifact suppression that is shown to effectively mitigate this artifact.

REFERENCES

- Kellman, P., et al. (2002). *MRM* 47:372–383.
 Kim, R. J., et al. (1999). *Circulation* 100:1992–2002.
 Kim, R. J., et al. (2000). *N. Engl. J. Med.* 343:1445–1453.
 Roemer, P. B., et al. (1990). *MRM* 16:192–225.
 Simonetti, O. P., et al. (2001). *Radiology* 218:215–223.

283. SPECT and CMR for the Hemodynamic Assessment of Intermediate Stenoses in Coronary Artery Bypass Grafts

Liesbeth P. Salm,¹ Jeroen J. Bax,¹ Hubert W. Vliegen,¹ Susan E. Langerak,¹ Wouter Jukema,¹ Hildo J. Lamb,² Ernest K. J. Pauwels,³ Albert De Roos,² Ernst E. Van der Wall.¹ ¹Cardiology, Leiden University Medical Center, Leiden, Netherlands, ²Radiology, Leiden University Medical Center, Leiden, Netherlands, ³Nuclear Medicine, Leiden University Medical Center, Leiden, Netherlands.

Introduction: In the evaluation of intermediate stenoses (40–70% narrowing) in coronary artery bypass grafts, coronary angiography has been considered the gold standard. However, assessing the hemodynamic significance of intermediate stenoses remains difficult.

Purpose: To determine whether intermediate stenoses in coronary artery bypass grafts are hemodynamically significant, as explored by single photon emission computed tomography (SPECT) and cardiovascular magnetic resonance (CMR).

Methods: 25 patients underwent angiography for recurrent chest pain, late after bypass surgery. Ischemia was determined from stress-rest perfusion SPECT. Baseline and adenosine stress average peak velocity were obtained at CMR, and coronary flow velocity reserve (CFVR) was calculated. Stenoses were considered hemodynamically significant on CMR when CFVR was reduced (<2.0), and/or stress-rest SPECT imaging demonstrated abnormal perfusion.

Results: CFVR could not be obtained in 11 of 57 grafts. For the remaining 46 grafts, the agreement



between SPECT and CFVR was good (83%; $\kappa=0.61$). Grafts were divided into mild stenosis (<40%; n=17), intermediate stenosis (40–70%; n=23), and severe stenosis ($\geq 70\%$; n=17). The majority of mild stenoses had normal perfusion on SPECT (88%) and/or normal CFVR (85%), as compared with 94% of severe stenoses having abnormal perfusion and 69% reduced CFVR. In intermediate stenoses, 61% had abnormal SPECT results and 50% reduced CFVR, but also 39% had normal SPECT results and 50% intact CFVR.

Conclusion: Approximately half of the (angiographically) intermediate stenoses had abnormal SPECT and/or CMR results, demonstrating the need for hemodynamic assessment of these stenoses. Both SPECT and CMR can provide this functional information.

284. First-Pass Perfusion of Papillary Muscles Assessed by Cardiac MRI Predicts Ischemic Mitral Regurgitation in Patients with Coronary Artery Disease

Philipp Boyé, Hassan Abdel-Aty, Nidal Al-Saadi, Rainer Dietz, Matthias G. Friedrich. *Working Group Cardiovascular Magnetic Resonance, Klinik fuer molekulare und klinische Kardiologie, Berlin, Germany.*

Introduction: Ischemic mitral regurgitation (MR) predicts poor prognosis in patients with coronary artery disease. In these patients, papillary muscle dysfunction may be caused by hypoperfusion. Cardiovascular Magnetic Resonance (CMR) first-pass perfusion sensitively detects small myocardial perfusion defects.

Purpose: We investigated the correlation between first-pass perfusion of the papillary muscles and mitral regurgitation as assessed by standard techniques.

Methods: We studied 43 patients (34 males) with clinical evidence for myocardial ischemia on a 1.5T CMR system, acquiring 3 short axis views with a GRE-EPI hybrid sequence (TE 1.3 to 1.7; flip angle 25°; slice thickness 10 mm). Echocardiography or cardiac catheterization was performed within 12±11 days and evaluated for the presence of mitral regurgitation. CMR images were visually assessed for papillary muscle perfusion, classified as “normal” or “hypoperfused.” All observers were blinded to the results of the other techniques.

Results: Relevant mitral regurgitation was detected in 19 patients. Papillary muscle hypoperfusion was detected in 25 of 43 patients. A perfusion defect in the papillary muscle was detected in 18/19 patients with mitral regurgitation (sensitivity 94%), but only in 7/24 patients without mitral regurgitation (specificity 71%).

Conclusions: Perfusion deficits of the papillary muscles are frequently associated with mitral regurgitation in patients with coronary artery disease. CMR may serve as a valuable tool to detect an ischemic origin of mitral regurgitation in coronary heart disease.

285. Reproducibility of Infarct Size Quantification: Comparison of Three Imaging Sequences Using Contrast Enhanced MRI

Karin Schreiber,¹ Stephan Nekolla,¹ Hubertus Buelow,¹ Tareq Ibrahim,² Markus Schwaiger.¹ ¹Nuklearmedizinische Klinik des Klinikums Rechts der Isar der TU Muenchen, Muenchen, Germany, ²Deutsches Herzzentrum und 1. Medizinische Klinik des Klinikums Rechts der Isar der TU Muenchen, Muenchen, Germany.

Introduction: Infarct size measurement is an important clinical issue in management of patients with chronic myocardial infarction. Contrast enhanced MRI has shown the potential to identify scar tissue and therefore can be used for infarct size quantification.

Purpose: The purpose of this study is to compare various imaging sequences in the same patient population regarding quantitative defect size assessment.

Methods: In 25 patients (65±15 y, 20 M) with chronic myocardial infarction, contrast enhanced (ceMRI) was performed on a 1.5 T system (Sonata, Siemens). Data were acquired using three inversion recovery sequences (FLASH 3D, TrueFISP 2D, phase-sensitive TrueFISP 2D) between 20 and 40 min. p.i. of Gd-DTPA providing complete coverage of the left ventricle. With exception of the phase sensitive sequence which does not rely on an explicit inversion delay, this parameter was individually adjusted using a T1 scout scan. The visual image quality was rated on a four scale rate (excellent, good, fair, unreadable). LV contours were drawn manually, the regional signal intensity (SI) was automatically quantified in four layers from endo- to epicardium. For defect quantification, regional data was transferred into “polar maps.” Defect extent was determined using thresholds in every layer and accumulated for total defect size. Ratios between endo- and epicardial signal intensity were calculated in order to differentiate between transmural (T) and non-transmural (NT) defects. The defect sizes were compared to coregistered SPECT/PET studies with previously established thresholds for Tc-99m MIBI or N-13-PET.

Results: Image quality appeared best with FLASH 3D. There was no significant difference between the



Table 1.

	FLASH 3D	TrueFISP 2D	PSIR TrueFISP
Image quality	1.5	2.1	1.9
Breath holds required	4	5	3
R (T and NT) Slope	0.69	0.63	0.71
(T and NT) Slope	0.42	0.58	0.62
R (T only) Slope	0.95	0.82	0.87
(T only) Slope	0.78	0.85	0.86
Mean defect size (%LV)	17±11	20±14	21±16
Mean difference (%LV)	0.5±5	-1.6±7	2.6±8

sequences for mean defect size and mean difference. Non-transmural infarct size was significantly larger with ceMRI as compared to scintigraphic data as shown by correlation coefficient (R) and slope when separating transmural from non-transmural defects (Table 1).

Conclusion: The delineation of irreversible tissue injury by ceMRI is reproducible despite variation in imaging sequences. However, each measurement requires standardization and optimization of threshold criteria in comparison to reference method.

286. Myocardial Characterization by Dobutamine Stress MR Cine, Perfusion, and Infarct Imaging Accurately Predicts Adverse Clinical Outcomes

Anna K. Y. Chan, MD,¹ Rajiv A. Patel, MD, PhD,¹ Marcus A. Averbach, MD,¹ Nagesh Anavekar, MD,¹ Ronald Skorstad,² E. Kent Yucel, MD,² Raymond Y. Kwong, MD.¹ ¹Cardiology, Brigham and Women's Hospital, Boston, MA, USA, ²Radiology, Brigham and Women's Hospital, Boston, MA, USA.

Introduction: Cardiac MRI with dobutamine stress provides information regarding contractile reserve, first pass myocardial perfusion (FPMP), and myocardial infarction in a single imaging session. The utility of this comprehensive approach of myocardial characterization in predicting cardiac events from coronary artery disease (CAD) is not known.

Purpose: To determine the utility of myocardial characterization and clinical endpoint prediction by dobutamine stress MRI.

Methods: 60 patients referred for dobutamine stress MRI for assessment of CAD were included in the study. Dobutamine was administered by standard infusion up to 40 mcg/kg/min with atropine for heart rate augmentation. Four patients did not achieve 80% of age maximal target heart rate and were excluded from further analysis. Steady state free precession cine imaging of 3 short-axis and 3 long-axis planes were acquired at each stage followed by FPMP at peak stress. FPMP was acquired with 6–7 short-axis locations across the LV at peak stress with 1 image acquired every 2–3 cardiac cycles. Infarct imaging by delayed hyperenhancement was performed with 0.15 mmol/kg gadolinium-DTPA. Dobutamine stress cine, FPMP, and delayed hyperenhancement were analyzed independently according to the 16-segment model. Regional wall motion was graded on a 4-point scale.

Myocardial ischemia during dobutamine stress cine imaging was defined either by 1) worsening of regional systolic wall thickening by ≥1 grade confirmed on both short and long-axis cine, or 2) presence of any segmental hypoenhancement on FPMP with a lack of matching segment of delayed hyperenhancement. Follow-up was successful in all patients at 6 months or longer after the MRI. Clinical endpoints included death, acute myocardial infarction, unstable angina, and decompensated heart failure.

Results: At follow up of 6 months, 6 (11%) patients reached clinical endpoints among which 4 deaths (3 cardiac and 1 non-cardiac), 1 acute myocardial infarction, and 1 hospitalization for decompensated heart failure. All 6 patients who reached clinical endpoints had evidence of ischemia by MRI. 13

Table 1. Detection of clinical endpoints by dobutamine stress MRI (cine, perfusion, and combined).

	Ischemia by dobutamine cine alone	Abnormal dobutamine FPMP alone	Ischemia by dobutamine FPMP	Ischemia by combined cine and FPMP
Diagnostic study	45/56 (80%)	36/56 (64%)		56/56 (100%)
Sensitivity	11/14 (79%)	13/14 (93%)	11/14 (79%)	18/21 (86%)
Specificity	28/31 (90%)	13/22 (59%)	23/27 (85%)	25/35 (71%)

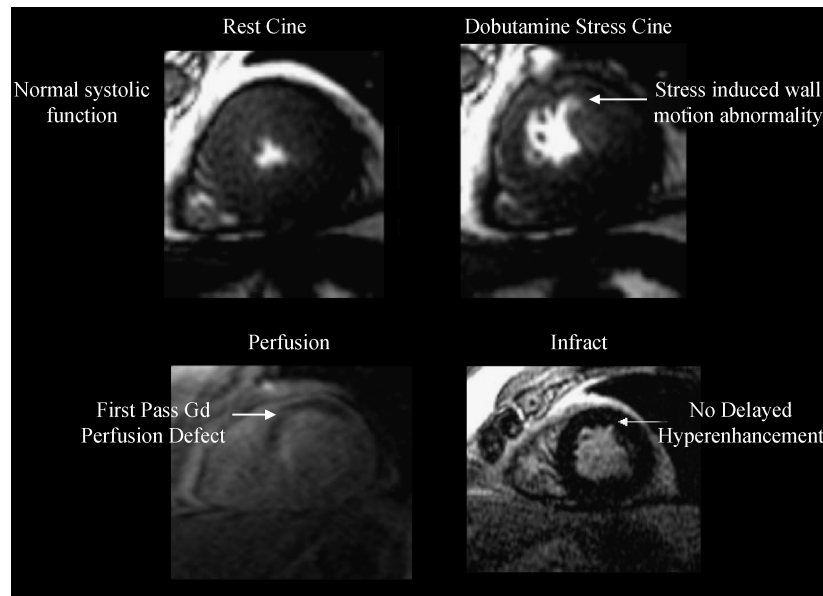


Figure 1.

(23%) patients had no ischemia on MRI and all were free of clinical events at 6 months.

11 (20%) dobutamine cine and 20 (36%) FPMP were non-diagnostic due to technical difficulty. In the detection of significant CAD, presence of ischemia on dobutamine cine when compared to FPMP, had a sensitivity of 79% vs. 93% ($p < 0.01$), and a specificity of 90 vs. 59% ($p < 0.01$). Characterizing myocardium by combining FPMP and delayed hyperenhancement improves the specificity compared to FPMP alone but at the cost of a lower sensitivity (Table 1, Fig. 1).

Conclusions:

1. Dobutamine stress MRI accurately predicts adverse clinical events in patients being referred to noninvasive assessment of CAD.
2. Dobutamine cine function imaging, FPMP, and delayed hyperenhancement imaging, provide complementary diagnostic utility in the characterization of myocardium in CAD.

287. Relationship Between Non-viable Myocardium and Regional Left Ventricular Function in Chronic Ischemic Heart Disease

Arunark Kolipaka,¹ George P. Chatzimavroudis,² Richard D. White,¹ Randolph M. Setser.¹ ¹Radiology,

Cleveland Clinic Foundation, Cleveland, OH, USA, ²Chemical and Biomedical Engineering Department, Cleveland State University, Cleveland, OH, USA.

Introduction: Delayed enhancement (DE) magnetic resonance imaging (MRI) has been shown to accurately depict the extent and distribution of myocardial infarction (Kim et al., 1999). Previously, a dog model of myocardial infarction demonstrated significantly diminished wall thickening in segments with >20% transmural extent of infarction (Lieberman et al., 1981).

Purpose: To study the relationship between the extent of left ventricular (LV) myocardial scarring and wall thickening in patients with chronic ischemic heart disease (CHID).

Methods: DE-MRI was performed in 23 patients using an inversion recovery TurboFLASH sequence (FOV 300–360 mm², TE 4 ms, TR 8 ms, α 30°, TI 190–470 ms) approximately 20 minutes after intravenous injection of 0.2 mmol/kg Gd-DTPA; with (n=9) or without (n=14) phase sensitive reconstruction (Kellman et al., 2002). TrueFISP cine imaging (TE 2 msec, TR 4.1 msec, flip angle 60°, slice thickness 8–10 mm, FOV 300–360 mm², RFOV 80–100%, initial matrix 256 (Lieberman et al., 1981)) was also performed for segmental wall motion analysis. For both types of imaging, 3 representative short-axis slices were acquired at the base, mid-ventricle and apex. In DE images, the endocardial and epicardial contours were manually delineated and images were manually



thresholded using an interactive region-filling tool (Modified Argus, Siemens Corporate Research, Princeton, NJ). Quantitative analysis of thresholded images was performed (Matlab v6.5): %SCAR was defined as the ratio of non-viable to total myocardial pixels; %TRANS was determined by evaluating 180 radial spokes at each level and computing the transmural extent of non-viable tissue along each spoke (only spokes with non-viable pixels originating at the subendocardium were included). In cine images the epicardium and endocardium were delineated at end-diastole and end-systole (using Argus) for calculation of systolic wall thickening (SWT).

All results were subdivided regionally using a 16-segment LV model. %SCAR and %TRANS results were grouped into 6 intervals based on the extent of scar (as shown in Figure 1). The significance of differences between scar extent intervals was assessed using one-way ANOVA with Tukey's pairwise comparison.

Results: All patients demonstrated increased LV dimensions (end-diastolic volume: 274 ± 76 ml) with impaired systolic function (ejection fraction: $28 \pm 11\%$). Figure 1 shows SWT as a function of %SCAR (left) and %TRANS (right) scar extent intervals.

On average, all LV scar extent intervals demonstrated impaired SWT (≤ 1 mm) due to resting myocar-

dial ischemia in some segments (with or without non-viable tissue). In general, SWT deteriorated further as %SCAR and %TRANS increased. A threshold was observed at 40% extent of scarring: intervals with >40 %SCAR (or >40 %TRANS) showed significantly reduced SWT compared to the "0" interval (i.e. segments without scar). Previously, a dog model of single vessel coronary artery disease demonstrated a similar threshold at 20 %TRANS (Lieberman et al., 1981). However, the current study has shown that both the amount of myocardial scar in a LV segment and the transmural extent of scar exhibit identical threshold phenomena, but that this threshold occurs at 40% extent of scarring in patients with CHID.

Conclusions: On average, LV function is impaired in patients with CHID, with diminished SWT in all segments. Furthermore, SWT is significantly reduced in segments with >40 %SCAR (or >40 %TRANS) relative to segments with lesser scarring.

REFERENCES

Kellman, P., et al. (2002). *Magn. Reson. Med.* 47:372–383.
 Kim, R. J., et al. (1999). *Circulation* 100:1992–2002.
 Lieberman, A. N., et al. (1981). *Circulation* 63:739–746.

288. Direct Comparison of Sensitivity Encoded (SENSE) Assisted Single Breath-Hold Volumetric Delayed Enhancement (DE) Imaging of the Left Ventricle (LV) and Navigator Guided Free Breathing 3D DE Imaging

Mercedes Pereyra, RT,¹ Roshan Ravindran, MB, ChB,¹ Eric Douglas, RT,¹ Veronica Lenge, MD,¹ Raja Muthupillai, PhD,² Scott D. Flamm, MD.³ ¹Department of Radiology, St. Luke's Episcopal Hospital, Texas Heart Institute, Houston, TX, USA, ²Department of Radiology, St. Luke's Episcopal Hospital, Texas Heart Institute, Philips Medical Systems, Cleveland, Ohio, Houston, TX, USA, ³Department of Radiology and Cardiology, St. Luke's Episcopal Hospital, Texas Heart Institute, Houston, TX, USA.

Introduction: Delayed enhancement (DE) imaging following Gd-DTPA administration has been shown to identify regions of irreversible myocardial injury

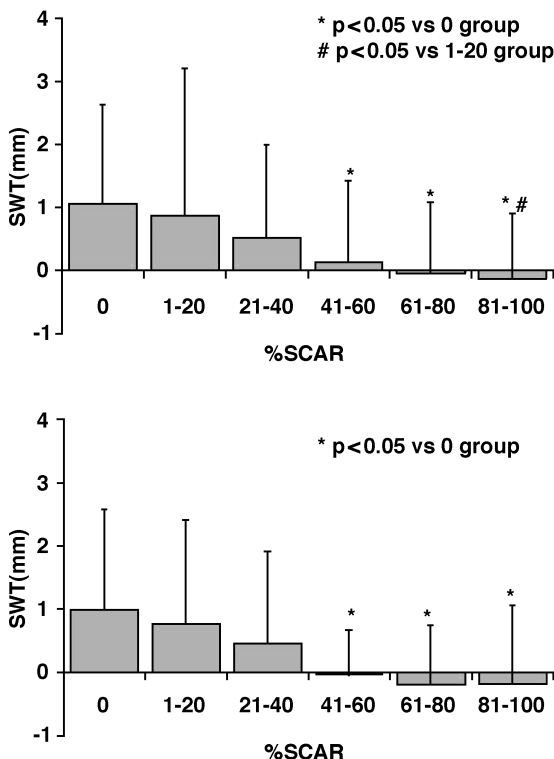


Figure 1. (View this art in color at www.dekker.com.)



Conventional 2D DE techniques acquire a single slice per breath-hold requiring several breath-holds to cover the entire left ventricle (LV). This is time consuming and often introduces misalignment of slices due to inconsistency in breathhold position through the examination. Volumetric techniques have been proposed in the literature to eliminate this problem, though with increase in the breath-hold duration. Sensitivity encoding (SENSE) has recently been described as a means for accelerating MR image acquisition in the context of DE imaging to reduce breath-hold duration. An alternative method to acquire high resolution volumetric DE data is a real-time navigator guided approach during free breathing.

Purpose: The purpose of this study was to directly compare the breath-held 3D DE imaging approach against 3D free breathing DE imaging using qualitative and quantitative metrics.

Methods: 13 patients (3/13 male, 59 ± 17 years), were imaged at 1.5 T (Philips Gyroscan NT-Intera) using a vectorcardiogram-gated, inversion-recovery TFE sequence, wherein, following a 180 pulse, a set of gradient echoes were collected in diastole using a 5 element cardiac surface coil. 10 contiguous short axis slices from the apex to base were acquired for both techniques. Specific acquisition parameters were: **BH 3D DE with SENSE**—TR/TE/flip/views per RR/scan duration=4.0/1.3/15/49/24 heart beats (hb) per volume; acquired voxel size: $1.6 \times 2.0 \times 10$ mm; reconstructed as: $1.5 \times 1.5 \times 10$ mm. **Nav 3D DE Technique**—TR/TE/flip/views per RR/scan duration=6.8/3.3/15/20/104 heart beats (hb) per volume; acquired voxel size: $1.1 \times 1.2 \times 10.0$; reconstructed as: $0.7 \times 0.7 \times 10$ mm. **Post processing**—The images were transferred to a post-processing workstation (EasyVision) and the following quantitative parameters were computed: Signal-to-Noise ratio (SNR) of blood, normal myocardium, and injured myocardium. Contrast-to-Noise ratio (CNR) between injured and normal myocardium, and between blood and normal myocardium were also computed. The two techniques were qualitatively

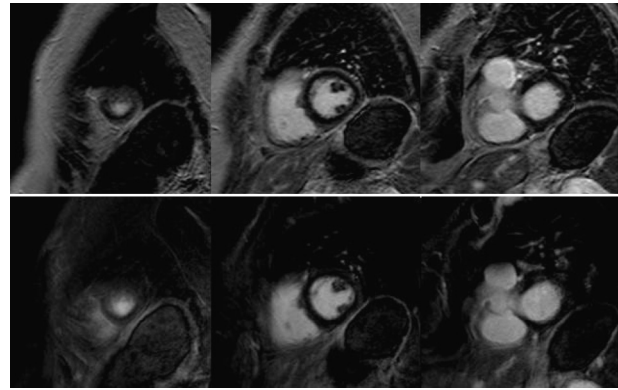


Figure 1. Representative images from the 3D-DE BH and 3D-DE Navigator techniques.

evaluated for overall image quality (IQ) on a scale of 1 through 4 (1: Excellent, 2: Good, 3: Moderate, 4: Poor, and respiratory artifacts on a scale of: 1: None or minimal; 2: Mild; 3: Moderate and 4: Severe).

Results: The navigator method, on average, required 200 heart beats to finish the acquisition with a 50% acquisition efficiency. Quantitative results showed that the myocardium was well suppressed in both methods ($SNR_{mus} = 2.5 \pm 1.6$ for BH-3D vs. 3.7 ± 1.3 for 3D-Nav), and there was little difference in SNR_{blood} between the two techniques. The CNR_{bl-my0} were also similar (20.1 ± 8.7 for BH-3D vs. 24.6 ± 9.5 for 3D-Nav) indicating preserved contrast between the two techniques. Although statistical significance could not be assessed due to the small number of cases, there was a trend toward higher $CNR_{injury-my0}$ for the 3D Nav approach 36.4 ± 22.4 vs. 27.2 ± 2.84 for the 3D-BH approach. Quantitative parameters evaluated are listed in Table 1, and some representative results are shown in Figure 1.

Conclusions: Our initial results show that it is clinically feasible to apply either SENSE assisted, single breath hold 3D-DE technique, or navigator guided free breathing 3D-DE technique. Based on the quantitative and qualitative parameters, both techniques yield comparable results. The quicker BH approach suffers from slightly lower spatial resolution, and T_1 blurring due to longer acquisition window. Effective myocardial signal nulling and higher spatial resolution are achievable in the 3D Navigator approach despite the prolonged acquisition time. The 3D Navigator approach may be suitable for pediatric patients, sedated patients, or when high spatial resolution is required, such as in serial quantitative determination of scar or fibrosis burden.

Table 1.

	3D-DE BH	3D-DE Nav
SNR_{myo}	2.5 ± 1.6	3.7 ± 1.3
SNR_{blood}	24.7 ± 11.2	26.6 ± 10.9
$CNR_{blood-my0}$	20.1 ± 8.7	24.6 ± 9.5
$CNR_{injury-my0}$	27.2 ± 2.8	36.4 ± 22.4
IQ	1.4 ± 0.8	1.2 ± 0.4
Resp. artifacts	1.5 ± 0.9	1.6 ± 0.7



289. Effect of Serum Cholesterol Levels on Coronary Vasoreactivity in Patients with Type II Diabetes Mellitus

Olakunle Akinboboye, MD, MPH, Yi Wang, DSc, Kathy McGrath, RN, Margurite Roth, RN, William Schapiro, RT (CMR), Khurram Moin, MD, Sunil Mathew, MD, Ralph DIM, MD, Dwaraka Pollepalle, RT, Nathaniel Reichel, MD. *Saint Francis Hospital, Roslyn, NY, USA.*

Introduction: Previous studies have shown that coronary endothelial function is often impaired in patients with diabetes mellitus (DM). Patients with DM, who have impaired endothelial function, were found to have higher cardiovascular morbidity and mortality than patients with normal endothelial function. However the determinants of endothelial function in patients with DM but without overt coronary disease have not been clearly defined. Endothelial function in the coronary vessels can be assessed by various techniques including cold pressor testing (CPT). Cold-pressor testing induces adrenergic receptor-mediated activation of the endothelium and smooth muscle cells of the vascular wall, leading to both vasoconstrictor and vasodilatory responses. The vasodilatory response is believed to be mediated through the beta-receptor with direct stimulation of nitric oxide synthesis and flow-dependent release of nitric oxide.

Purpose: The objectives of this study were to assess the magnitude and determinants of myocardial blood flow response to cold-pressor testing using first-pass contrast-enhanced MRI.

Methods: Eleven patients (5 females, mean age 59±9 with DM but without overt coronary artery disease, underwent MRI first-pass perfusion study at rest and following cold-water hand immersion for 120 seconds. A 1.5 T Siemens Sonata scanner (Siemens Medical Solutions, Malvern, PA) with a CP body array flex coil was used. Imaging was performed using TurboFLASH sequence with the following parameters TR/TE/FA=2.2 ms/1 ms/15°, data matrix 128×70, and usual voxel spatial resolution 3.6×2.7×8 mm³ based on the size of the patient. Contrast dose was 0.05 mmol/kg (Omniscan, Amersham). The

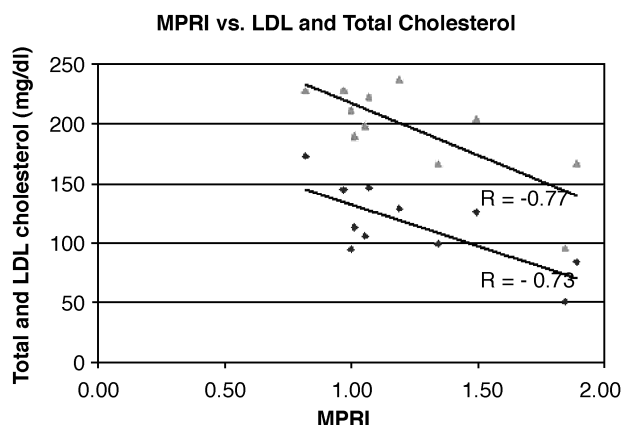


Figure 1. (View this art in color at www.dekker.com.)

steepness of the first pass signal intensity curve's upslope, determined by a linear fit, normalized to blood pool upslope (relative upslope) was determined at baseline and following CPT using MEDIS software (Medis Imaging Systems Inc., Leiden, The Netherlands). CPT myocardial perfusion reserve index (MPRI) was calculated by dividing CPT by baseline relative upslope. In addition the following serum assays were measured on the same day: total cholesterol (T chol), triglycerides (trig), HDL cholesterol (HDL), LDL cholesterol (LDL), Fasting blood glucose (FBS), C-reactive protein (CRP), insulin, hemoglobin A1c (H-A1c), and Von-Willebrand factor (VWF). Urinary microalbumin level (µalb), weight (Wt) and waist circumference (WC) were also measured.

Results: Mean weight 163±55 lbs, urinary microalbumin: 23±32 mg/dl, Waist Circumference: 106±9 cm.

Serum assays: (see Table 1 below).

Baseline relative upslope=9.6±3.4; CPT relative upslope=11.8±3.5 (p<0.01 for CPT vs. baseline relative upslope); MPRI=1.24±0.36; Of the variables tested, the significant correlates of MPRI were: Total cholesterol: r=-0.77 (p=0.005) and LDL r=-0.73, p=0.01) (Figure 1).

Conclusions: The magnitude of the vasodilatory response to cold-pressor stimulation in patients with diabetes mellitus is approximately 24% and it is

Table 1.

Tchol (mg/dl)	Trig (mg/dl)	HDL (mg/dl)	LDL (mg/dl)	FBS (mg/dl)	CRP (mg/dl)	Insulin (mg/dl)	HB A1c (%)	VWF (%)	µalb, mg/dl	1.24
192±41	177±107	42±11	114±32	148±43	4.7±3	12±5	7±1	109±57	23±32	0.36

inversely related to serum total cholesterol and LDL-cholesterol levels. Vasodilator reserve is abolished at minimally elevated levels of LDL and total cholesterol.

290. Optimized Suppression of Motion Artefacts for Coronary MRA: Evaluation of Breath-Hold Capability, Breath-Hold Patterns and Coronary Motion

Cosima Jahnke, MD, Ingo Paetsch, MD, Bernhard Schnackenburg, PhD, Axel Bornstedt, PhD, Rolf Gebker, MD, Eckart Fleck, MD, Eike Nagel, MD. *Cardiology, German Heart Institute Berlin, Berlin, Germany.*

Background: Understanding cardiac and respiratory motion is crucial for achieving an optimal suppression of motion artefacts for coronary MRA. Thus, the aim of this study was the evaluation of the patients individual breath-hold capability, the different breath-hold patterns and the rest periods of the left and right coronary artery.

Methods: 165 consecutive routine cardiac patients were examined (Philips Intera 1.5T system). Quantification of the maximal breath-hold capability was done in expiration using a dynamic navigator scan (temporal resolution 1 s). The same scan allowed the assessment of the individual breath-hold pattern. The rest periods of the left and right coronary artery were determined using a cine-bFFE scan with a transversal slice orientation (retrospective gating, 40 phases/cardiac cycle). The duration of the coronary artery moving less than 25% of its cross-sectional area was defined as rest period.

Results: Mean breath-hold capability was 29 ± 13 s (range 10 to 64 s). The different breath-hold patterns could be divided into 4 groups: In 56% of the patients the diaphragm exhibits a plateau during breath-holding; the second pattern was characterized by an initial drift followed by a plateau phase (13%). 18% of the patients showed a continuous drift of the diaphragm during the breath-hold and 13% of the patients had a completely irregular and unsteady behaviour of the diaphragm. Regarding the coronary motion we found in comparison to the RCA: 1) the rest period of the LCA was significantly longer (164 ± 77 vs. 125 ± 63 ms; $p < 0.01$); 2) however, in 14% of the patients the rest period of the LCA was shorter; 3) the LCA rest period started significantly earlier in the cardiac cycle (518 ± 150 vs. 539 ± 162 ms; $p < 0.01$); 4) however, in 22% of the patients the rest period of the LCA began later. There was no obvious correlation between the duration of the rest periods and the individual heart rate ($r = 0.4$) (Fig. 1).

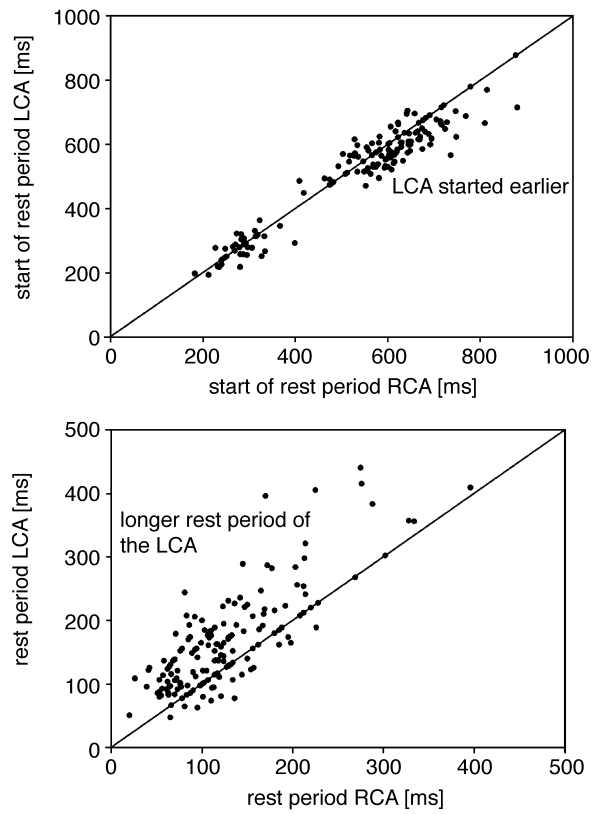


Figure 1.

Conclusions: One third of the patients showed a breath-hold pattern, which is unsuitable for sufficient breath-hold MR imaging. The rest periods of the LCA and RCA showed a large range of variability with no obvious correlation to heart rate. Thus, for each patient and each coronary artery, breath-hold duration and pattern as well as coronary artery rest period should be determined individually.

291. Magnetic Resonance First Pass Perfusion Reserve: Non-invasive Alternative to Determine Critical Coronary Stenoses in Guiding Revascularization Therapy

Prasad M. Panse,¹ Matthew Dickson,² Olaf Muhling,³ Neeta Panse,¹ Michael Jersoch-Herold,² Marco Costa,¹ Norbert Wilke.¹ ¹University of Florida, Jacksonville, FL, USA, ²University of Minnesota, Minneapolis, MN, USA, ³University of Munich, Munich, Germany.

Introduction: The arms of therapy for the treatment of coronary artery disease (CAD) are guided by the



presence of severity and grade of coronary artery stenoses (Critical vs. Non-critical). To date, there is no non-invasive test to assess the degree of Coronary artery stenoses. We utilized quantitative Myocardial First Pass Perfusion (MRFPP) reserve to assess graded coronary artery stenoses in patients.

Purpose: To support a non-invasive alternative to invasive diagnostic catheterization in grading severity of coronary artery disease.

To differentiate Critical from Non-critical stenosis.

Methods: 41 patients between ages of 34–78 with known CAD underwent coronary angiography and MRFPP. MRFPP was done at rest and maximal hyperemia in multi-slice T1 weighted imaging of the heart. Quantitative MR analysis was performed to obtain the absolute myocardial perfusion reserve in 8 sectors (Wilke et al., 1997). Coronary angiogram was analyzed independently by an experienced observer and each epicardial artery was categorized by the degree of stenosis. The perfusion reserve was then compared to the degree of stenosis in each sector. The sensitivity, specificity, positive predictive and negative predictive values in detecting critical coronary artery stenosis were calculated.

Results: The sensitivity, specificity, positive predictive value and negative predictive value for MRFPP imaging to detect severe stenosis defined as more than or equal to 75% area as determined visually from coronary angiograms are 67.6%, 90.1%, 56.5% and 94.5% for each sector (see Table 1).

The cutoff for severe coronary artery disease was 1.5 for the MRFPP reserve. On a per patient basis 30 patients were correctly diagnosed, 10 obtained false positive results and 1 had false negative results in comparison with graded stenosis by X ray angiography. Regions with 0–25 and 25–50% stenosis could be distinguished from each other and from all other levels of severity for coronary artery disease.

Conclusions: MRFPP can distinguish graded coronary artery stenoses with a high degree of specificity and negative predictive value.

This technique may be able to exclude further interventions in patients with known coronary artery

disease and absolute perfusion reserve greater than 1.5 in all sectors.

The low sensitivity in patients could be explained as a result of micro-vascular disease (Syndrome X), small vessel disease in diabetics or sub-endocardial ischemia. These pathological findings can be detected with MRFPP. Conventional X ray angiogram, though used as a gold standard, fails to detect these pathologies.

REFERENCE

Wilke, N., et al. (1997). Myocardial perfusion reserve: assessment with multislice quantitative first pass MR imaging. *Radiology* 204:373–384.

292. Feasibility of Combined Perfusion and Function Assessment Compared to Perfusion Alone By Dipyridamole Stress MRI

Mushabbar A. Syed, MD, D. Ian Paterson, MD, Kenneth L. Rhoads, MD, W. Patricia Ingkanisorn, MD, Christopher K. Dyke, MD, Andrew E. Arai, MD. *National Institutes of Health, Bethesda, MD, USA.*

Introduction: Studies of gated SPECT imaging have reported incremental diagnostic value of combining regional wall motion assessment with myocardial perfusion imaging (MPI) during exercise stress testing. Regional wall motion abnormalities (RWMA) consistent with inducible ischemia have also been described during vasodilator stress testing.

Purpose: We sought to investigate 1) the feasibility of acquiring cine images in addition to MPI at peak stress, 2) the incidence of wall motion abnormalities in dipyridamole stress testing.

Methods: We studied 26 consecutive patients with known or suspected coronary artery disease referred for dipyridamole stress MRI. All patients underwent baseline cine MRI by ECG-gated Steady State Free Precession technique (SSFP) using a GE excite 1.5T Signa scanner and a four element cardiac phased array coil. Dipyridamole was infused at a dose of 0.56 mg/kg over 4 minutes. MPI was obtained 3 minutes after completion of the infusion and was immediately followed by acquisition of 3 short axis cine slices (base, mid and apex) by cine MRI. Stress MRI results were compared with coronary angiographic stenosis (>50%).

Table 1. Critical coronary artery stenoses (75%).

		Positive predictive value	Negative predictive value
Sensitivity	Specificity	56.5	94.5
67.6	90.1		

Table 1. Test characteristics of MPI and RWMA.

	MPI	RWMA
Sensitivity	100%	73%
Specificity	87%	93%

Results: The mean age of the patients was 60 ± 12 years, 23 males and 3 females. Fourteen patients had known coronary artery disease (myocardial infarction=13, coronary angioplasty=9, coronary artery bypass surgery=5).

The hemodynamic response to dipyridamole infusion was characterized by a significant increase in heart rate from 67 ± 16 beats per minute to 92 ± 17 beats per minute ($p < 0.0001$) and increased rate-pressure product from 8668 ± 2558 to 11824 ± 3194 , ($p = 0.0002$): 11 patients reported chest pain during stress. Additional functional imaging (3 breath holds) at peak stress was well tolerated by all patients.

MPI was abnormal in 13 patients out of which 9 patients (69%) also had RWMA. Wall motion abnormalities were only seen in the presence of abnormal perfusion. Coronary angiography was performed in 17 patients, on average within 2 months of the stress MRI. Table 1 lists the sensitivity and specificity of MPI and RWMA.

Conclusion: A combined function and perfusion assessment is feasible, safe and well tolerated. A significant proportion of patients (69%) develop inducible RWMA during dipyridamole stress MRI in our study. This can improve diagnostic certainty for cases with equivocal perfusion abnormalities.

293. Prediction of Reversible Left Ventricular Dysfunction After Reperused Acute Myocardial Infarction: Head-to-Head Comparison of Contrast-Enhanced Magnetic Resonance Imaging and Thallium-201 Single-Photon Emission Computed Tomography

Christian Schlundt,¹ Johannes von Erffa,¹ Robert Krähner,¹ Michaela Schmidt,² Niels Oesingmann,² Torsten Kuwert,³ Werner Daniel,¹ Matthias Regenfus.¹
¹Medical Clinic II, FAU Erlangen-Nürnberg, Erlangen, Germany, ²Siemens Medical Solutions, Erlangen, Germany, ³Nuclear Medicine, FAU Erlangen-Nürnberg, Erlangen, Germany.

Objectives: Contrast-enhanced (ce) magnetic resonance imaging (MRI) has been shown to accurately assess myocardial viability. Comparative data to nuclear cardiology techniques as 201-Thallium (TI) single photon emission computed tomography (SPECT) is scarce. We compared ce MRI and TI SPECT to predict reversibility of left ventricular (LV) dysfunction in patients after reperused acute myocardial infarction.

Methods: 32 patients (pts) with LV dysfunction (EF $39 \pm 15\%$) were examined on a 1.5T scanner within 7.5 ± 4.3 (6–11) days of an reperused (stent placement: n=21; thrombolysis: n=11) acute myocardial infarction (MI). Functional cine studies (TrueFISP) and ce images (inversion recovery Turbo FLASH) 5 min after injection of 0.1 mmol/kg Gd-DTPA were acquired. Rest-redistribution SPECT was performed according to standard protocols. 7 months after the acute MI, pts were repeatedly examined with cine MRI. A 17-segment model of corresponding basal, midventricular and apical slices was analysed independently for ce MRI and SPECT. Segmental hyperenhancement (HE) for MRI and tracer uptake for SPECT were quantified. For MRI, segments were considered to be viable if showing less than 25% segmental HE, for SPECT, if more than 60% TI-201 uptake. Functional recovery in the follow-up MRI was correlated with prediction of viability by both imaging modalities. Moreover, LV ejection fraction (EF) for both MRI scans was determined by planimetry.

Findings: 151 of 255 (56%) dysfunctional segments showed improved wall motion with follow-up MRI. Ce MRI showed a sensitivity of 93%, a specificity of 91%, and an accuracy of 92% to detect viable myocardium, whereas SPECT a sensitivity of 87% ($p = 0.3$), a specificity of 58% ($p = 0.0008$), and an accuracy of 66% ($p = 0.003$). On a patient basis, increase of LVEF $> 5\%$ was shown in 13 (41%) pts. Multivariate regression analysis identified the baseline wall motion score and the dysfunctional-but-viable myocardial ratio by MRI as predictors of increase in LVEF $> 5\%$ ($p = 0.03$), whereas the dysfunctional-but-viable myocardial ratio by SPECT was not predictive. Receiver operator characteristics established a dysfunctional-but-viable myocardial ratio of 0.49 (sensitivity 100%, specificity 95%) by MRI, and 0.58 (sensitivity 86%, specificity 63%) by SPECT as the best discriminators. Hereby, the area under the curve was significantly larger for MRI ($p < 0.05$).

Conclusions: Ce MRI, especially by virtue of its superior specificity, compares favorably to TI-201



SPECT for prediction of regional and global functional recovery in the setting of acute myocardial ischemia.

294. First-Pass Cardiac MR Perfusion: Is Slower Better?

Marko K. Ivancevic, MSc,¹ Ivan Zimine, PhD,¹ Christophe Dornier, PhD,¹ David Foxall, PhD,² Dominique Didier, MD,¹ Aernout G. Somsen, MD, PhD,³ Alberto Righetti, MD,³ Jean-Paul Vallée, MD, PhD.¹
¹Radiology, Geneva University Hospital, Geneva, Switzerland, ²Engineering, Philips Medical Systems, Cleveland, OH, USA, ³Cardiology, Geneva University Hospital, Geneva, Switzerland.

Introduction/Purpose: In patients with coronary artery disease assessment of myocardial perfusion is of clinical and prognostic value. MR first pass perfusion imaging has become a widely used clinical tool for assessing myocardial perfusion. As a common belief, fast bolus injection and high image sampling rate are indispensable for accurate perfusion quantification. The high image acquisition rate limits spatial coverage. To allow for full heart coverage on a routine clinical MR system, we introduce a new acquisition strategy consisting of a slower injection of a higher contrast media (CM) dose and a slower sampling rate. The new protocol was assessed with a numerical simulation and a clinical study in patients with a history of myocardial infarction using 201-Tl SPECT as reference.

Methods: Simulations—Realistic pseudo-data were generated for both a narrow and a large aortic input, and myocardial response using the one-compartment-model. Gaussian noise (ranging between 0.5 and 8 times the noise level commonly observed in vivo) was added to the myocardial transit-time curves. Noise level was defined as the standard deviation of the baseline noise divided by the peak of the vascular input. Fully sampled (1 sample/sec), and undersampled (1 sample/2 sec, 1 sample/4 sec) myocardial transit-time curves were fitted to determine the perfusion first-order transfer parameters k_1 and k_2 (ml/g/min) of the one-compartment model for each noise level. Clinical—Twelve patients (all male, mean age 60 ± 11 years) with stable coronary artery disease and no acute symptoms underwent a rest/effort 201-Tl SPECT and a rest MR exam. MR imaging was performed on an Eclipse 1.5T MR system (Philips Medical Systems, Cleveland, OH)

with an RF-FAST sequence and following parameters: TI/TR/TE 28/3.74/1.5 ms, 50 kHz bandwidth, 40° FA, 90° – 180° preparation pulses, and a 112×128 matrix. A cardiac surface coil and ECG trigger were used. Eight slices were acquired during three to six heart beats, depending on patients heart rate. A bolus of 0.08 mmol/kg Gd-DTPA was injected in a brachial vein at 0.5 ml/s rate followed by 10 ml of isotonic saline with a Medrad Spectris MR injector. The myocardial response and the effect of the bolus on the perfusion values were evaluated in a simulation using the one-compartment model.

Results: Simulation—With the higher CM dose and slower injection rate the simulation showed an extended timing window in the myocardial transit-time curve allowing for lower temporal resolution without significant loss of accuracy in perfusion determination. Clinical—Regions were classified as normal, ischemic and infarcted according to the 201-Tl SPECT. In the corresponding regions no differences in average perfusion values were found by MRI between normal and ischemic tissue at rest (respectively 0.4 ± 0.21 and 0.4 ± 0.18 ml/g/min, $p > 0.9$). Significantly lower average perfusion value was found in the infarcted segments (0.27 ± 0.21 , $p < 0.0001$).

Conclusions: A decrease in perfusion at rest in infarcted regions, according to SPECT scintigraphy, was detected in patients. A slower injection of a higher contrast media dose allows to overcome the spatial limitation of cardiac MR perfusion assessment, and is therefore more advantageous than a short bolus. This protocol presents an important potential for clinical application in MRI evaluation of coronary heart disease.

295. Cardiac MRI in the Risk Stratification of Acute Chest Pain

George Javorsky, MBBS FRACP, Richard E. Slaughter, MBBS FRACR, Wendy E. Strugnell, BScApp. *Cardiovascular MRI Research Centre, The Prince Charles Hospital, Brisbane, Australia.*

Introduction: Acute chest pain is a major clinical presentation to hospital emergency departments. Cardiac MRI (CMRI) is a powerful tool in the assessment of known ischaemic myocardium. This study aims to investigate the use of CMRI in the acute chest pain diagnostic algorithm.

Purpose: To prove that a normal CMRI result (no perfusion defect at rest and no regional wall motion abnormality) in this patient group, would predict negative Troponin Is and no ischaemic ST changes on ECG in patients with no previous history of myocardial infarction.

Methods: Following initial assessment in the Emergency Department, patients with a diagnosis of suspected acute ischaemia but negative Troponin Is, no ECG changes and no other high risk features were asked to participate in the trial. Patients with a history of myocardial infarction were excluded. Following informed consent, a CMRI examination to assess regional wall motion abnormalities, myocardial perfusion at rest and delayed enhancement/viability was performed. This involved acquisition of LV short axis, long axis and four chamber SSFP cine acquisitions and first pass bolus imaging at rest, followed by delayed enhancement study for viability. The average examination time was 33 minutes. Irrespective of the results of the CMRI examination, the standard Prince Charles Hospital chest pain protocol was then continued. This includes repeat ECG and Troponin Is 6–8 hours post presentation in the Acute Chest Pain Assessment Unit plus an exercise stress test as indicated.

Results: Twenty five (25) patients were recruited between April and July 2003 (16 male and 9 female, age 35–73 years). Three withdrew due to claustrophobia or anxiety, and one was re diagnosed as unstable angina on repeat ECG prior to the CMRI.

Nineteen patients had a normal CMRI study and all had negative Troponin Is at 6–8 hours and no ischaemic ST changes on ECG. CMRI had 100% sensitivity in predicting this outcome.

Two patients had abnormal CMRIs. One had a rest perfusion defect with associated regional wall motion abnormality and without delayed enhancement. The repeat Troponin I was elevated with a maximum of 10.3 microunits/litre. Subsequent coronary angiography demonstrated an occluded first marginal branch and the patient went onto coronary angioplasty and stenting. The second abnormal MRI demonstrated an area of scar anteriorly with an associated regional wall motion abnormality. Coronary angiography demonstrated three vessel disease.

Conclusions: A normal CMRI study predicts negative troponins and no ischaemic ST changes on ECG at 6–8 hours post presentation. A normal CMRI study enables more expeditious assessment and procession of patients to functional stress testing, thereby reducing the time required to rule out acute cardiac ischaemia. CMRI is a valuable addition to the armamentarium available to the clinician, increasing confidence in making decisions in chest pain triage.

296. Cardiac MR Perfusion for Detection of Flow-Limiting Stenoses in an Out Patient Population with Chronic Stable Angina

Andrew M. Crean, MRCP FRCR, Richard Coulden, FRCP FRCR. *Radiology, Papworth Hospital, Cambridge, United Kingdom.*

Introduction: First-pass cardiac MR perfusion is a relatively recent method of imaging ischaemic myocardium which could have significant advantages over current techniques. Quantitative approaches have been described and validated in the literature but are reliant on accurate motion-correction software, as well as being extremely time-consuming to apply. A qualitative visual approach has the advantage of being intuitively simple to understand and could allow the technique to extend into clinical cardio-radiological practice.

Purpose: The aim of this study was to investigate the clinical utility of qualitative first-pass myocardial perfusion in an unselected patient population with chronic stable angina.

Methods: Patients with symptoms of chronic stable angina and a recent positive exercise test were invited to participate at out-patient clinics throughout the Cambridgeshire Health Authority region. Recruitment took place over an 18 month period from Sept. 01 to Feb. 03. All patients underwent both cardiac MR perfusion and conventional catheter angiography. Perfusion studies were performed on a 1.5T CV/i (GE Systems, Milwaukee) using a FGRET sequence. Studies were acquired under conditions of both rest and adenosine stress (140 mck/kg/min for 4 mins) and utilised a first-pass gadolinium bolus-tracking technique (0.1 mmol/kg at rest and stress). Conventional catheter angiography was undertaken with a minimum of 5 views and all stenoses assessed quantitatively. A cut off of 70% reduction in luminal diameter was used to define a significant stenosis. MR images were evaluated qualitatively for the presence or absence of a perfusion defect.

Results: 93 patients participated in the study. The prevalence of angiographically-significant disease was 66.7%. MR correctly identified the presence or absence of significant stenosis in 70 patients, although the two techniques were discordant in 23 patients. The sensitivity, specificity, positive predictive and negative predictive values for MR were 85.5%, 54.8%, 79.1% and 65.4% respectively. The likelihood ratio for a positive MR study was 1.9.

Conclusions: This study investigated the utility of cardiac MR first-pass perfusion in a “real world” clinical setting as opposed to a highly preselected patient group. The results—though promising—are perhaps not yet sufficiently discriminating to recommend the technique



as a gatekeeper for coronary angiography. However diagnostic performance is likely to improve with greater knowledge about the relationship between the persistence of a defect and the underlying degree of epicardial coronary stenosis. For now the technique remains promising but maybe not quite ready for prime-time.

297. Two Methods to Determine Hyperenhancement in Chronic Heart Failure Patients with Varying Aetiologies

Ramesh de Silva,¹ Klaus Witte,¹ Elena Lukaschuk,¹ Angela Lowe,² Andrew L. Clark,¹ Nikolay P. Nikitin,¹ John GF Cleland.¹ ¹Academic Cardiology, Hull CMR Research Group, Hull, United Kingdom, ²Lister InHealth, Leeds, United Kingdom.

Introduction: Revascularisation, whether pharmacological, percutaneous or surgical, and resynchronisation therapy are treatments used in chronic heart failure (CHF). Evidence show that a viable myocardial substrate confers a better outcome for both methods. Delayed enhanced cardiac magnetic resonance imaging (deCMR) identifies myocardial fibrosis as areas of hyperenhancement (HE) and is therefore a marker of non-viability. With increasingly widespread use of the above treatment options, reliable and time efficient methods are required to obtain information regarding the prevalence of HE in CHF patients.

Purpose: To compare two methods to determine the prevalence of HE in a cohort of CHF patients with varying aetiologies.

Methods: CMR images from 95 patients with symptoms and signs of heart failure referred to a tertiary centre heart failure unit were acquired using a clinical 1.5 Tesla scanner (Signa CVi, General Electric, USA). 8–10 short axis delayed enhancement images were acquired 15 minutes after automated injection of 0.15 mmol/kg gadodiamide (Nycomed Amersham, UK). Delayed enhancement images were obtained using a segmented inversion-recovery gradient-echo pulse sequence with an inversion delay adjusted to null the signal from the normal myocardium that ranged from 180–260 msec. The specific acquisition parameters were as follows: Field of View 340 × 250 mm, matrix 256 × 192, slice thickness/space 10 mm/4 mm, number of slices 8–10 depending on size of heart, TR 5.9 ms, TE 1.8 ms, flip angle 30°.

Two different methods were used to analyse late enhancement. The first was semiquantitative, incorporating a visual scoring system (visual method) based on the spatial extent of HE using a 17-segment model

proposed by the AHA. A four point scoring system was assigned based on the percentage of HE per segment (none=0, 1–25%=1, 26–75%=2, >76%=3). The total observed score was divided by the total possible score and expressed as a percentage of the left ventricle (LV) that had HE. The second quantitative method used planimetry (planimetry method) to obtain the mass of scar tissue (volume/ml × 1.05 g/cm³) which was expressed as the percentage of the LV mass that had HE. Data on LV mass, volumes and function were obtained by manual planimetry of the endo- and epicardial borders in systolic and diastolic phases in the short axis view. These cine images were acquired using ECG-triggered breath-hold FIESTA imaging.

Results: The mean age was 69 (±11) years, and 66 (70%) were male. The aetiology of CHF was as follows: ischaemic heart disease (IHD) 55 (58%), non-ischaemic cardiomyopathy (CM) 23 (24%), other 17 (18%). 40 (42%) of patients had hypertension. The mean ejection fraction was 40 (±16)% and 42 (44%) had some degree of HE. The two methods showed good correlation (r=0.93, p<0.0001). Good correlation was observed between EF and both the visual and the planimetry method (r=−0.42, p<0.0001 and r=−0.48, p<0.0001 respectively). Patients with IHD had a higher volume of scar tissue than patients without IHD (5.6 vs. 1.5 ml, p<0.0001), and patients with a non-ischaemic CM had a lower volume of scar tissue than in those without (1.1 vs. 4.9 ml, p<0.0001). Only 2 patients with non-ischaemic CM had evidence of HE.

Conclusions: It is unclear whether the diagnosis of a non-ischaemic CM needs to be revised in the presence of HE of the myocardium. Myocardial scarring is common in patients with CHF and can reliably be detected using less time consuming semi-quantitative visual methods. It will aid optimal patient selection for treatment options available in CHF.

298. Diagnostic Accuracy of 3D Navigator Gated Balanced FFE MRI for Detection of Coronary Artery Stenosis in Patients

Bernhard L. Gerber,¹ Emmanuel Coche,² Agnès Pasquet,¹ Joëlle Kefer,¹ Olivier Gurné,¹ Cécile Grandin,² Jean-Louis J. Vanoverschelde.¹ ¹Cardiology, Cliniques Universitaires St. Luc, Brussels, Belgium, ²Radiology, Cliniques Universitaires St. Luc, Brussels, Belgium.

Introduction: MRI is a promising technique for non-invasive coronary imaging. However, its use is still limited and data on its diagnostic accuracy for detecting coronary artery disease remains sparse.



Purpose: To evaluate the diagnostic accuracy of 3D navigator gated MRI to detect coronary artery disease in a large series of patients against quantitative coronary angiography.

Methods: Seventy consecutive patients (65±11 years, 56 men, 15 women) prospectively underwent coronary 3D coronary MRI prior to conventional diagnostic coronary angiography. MRI was performed on a 1.5 T (Integra CV, Philips) system using a EG gated, T2 prepped, 3D balanced field echo sequence with respiratory navigators. Four 3D stacks covering respectively the right coronary artery, the left main, left anterior descending coronary artery and the left circumflex coronary artery were acquired. MR images were reformatted using a soap-bubble tool and graded by 2 blinded readers for presence of >50% diameter stenosis in 15 coronary artery segments per patient. The diagnostic accuracy of both tests was compared against presence of >50% luminal diameter stenosis in vessels >1.5 mm size as detected by quantitative coronary angiography (QCA).

Results: The average duration of the MR coronary imaging study was 41±12 minutes. In four patients the exam could not be completed because of claustrophobia. According to invasive coronary angiography, 12 patients had single vessel, 12 patients had two-vessel, and 25 patients had three-vessel disease. Twenty one patients had no significant coronary artery disease. According to QCA, out of a total number of 807 coronary segments with >1.5 mm diameter, 145 (78%) presented more than >50% luminal stenosis. On a segmental basis, MRI had a relatively low sensitivity of 53% for identifying stenotic segments. However, specificity to exclude significant segmental stenosis was high (87%). Overall accuracy for detection of any segmental disease was 80%. Positive and negative predictive values in the population were 55% and 86% respectively.

Conclusions: In the present series, MRI had good accuracy to predict >50% luminal diameter stenosis on a segmental basis. In particular, the specificity and negative predictive value for excluding significant coronary artery stenosis were high. This suggests that coronary MRI might be an useful test to rule out significant coronary artery stenosis in humans.

299. Myocardial Salvage Detected by Delayed Enhanced MRI in Patients Treated by Primary Angioplasty

João F. P. Petriz, Sr., MD,¹ Marcelo Hadlich, MD,² Rodrigo Visconti, MD,² Luis Antônio Mendonça, PhD,² Clério Azevedo Filho, MD,² Adriano Mendes Caixeta,

MD,³ Cezar Medeiros,⁴ Miguel Rati,⁴ Jorge Moll Filho, MD,² Carlos E. Rochitte, MD.⁵ ¹Cardiovascular Magnetic Resonance, Rede D'Or & Labs and Rio de Janeiro State University, Rio de Janeiro, Brazil, ²Cardiovascular Magnetic Resonance, Rede D'Or & Labs, Rio de Janeiro, Brazil, ³Cath Lab, Rede D'Or & Labs and Rio de Janeiro State University, Rio de Janeiro, Brazil, ⁴Cath Lab, Rede D'Or & Labs, Rio de Janeiro, Brazil, ⁵Cardiovascular Magnetic Resonance, Rede D'Or & Labs and Heart Institute-InCor-University of São Paulo Medical School, Rio de Janeiro, Brazil.

Background: Percutaneous coronary interventions (PCI) in the treatment of acute myocardial infarction (MI) improve LV function preservation, survival and cardiovascular events rates. The time between the onset of symptoms and the coronary artery recanalization (symptoms-to-balloon time, SBT) has been considered a major clinical predictor. However, the time of the onset of symptoms can be inaccurate. The beginning of symptoms often does not coincide with the total coronary occlusion. Moreover, the possibility that reperfusion injury could limit myocardial salvage (MS) is usually not taken into account. Therefore, the clinical data may be imprecise to predict the MS. Myocardial delayed enhancement MRI (MDE) has been shown to detect and quantify precisely infarct size in humans.

Purposes: Our objectives were to detect MS by MDE and compare to clinical data and myocardial injury serum markers.

Methods: We studied 24 patients, mean age 61.3±11.6 years, 17 males, with MI treated with primary PCI. All patients underwent MR examination in a 1.5T magnet to investigate myocardial viability with MDE. Patients received 0.2 mmol/kg of gadolinium-based contrast 10-20 minutes prior to image acquisition. The MDE pulse sequence was a fast gradient-echo with an inversion-recovery preparation pulse using the following parameters: TR 3.6 ms, TE 1.8 ms, TI 230–280 ms, Flip Angle 25°, FOV 380–420, matrix 224×256, Slice Thickness/Gap 8.0/2.0, WFS 0.46 pixels.

A blind observer to the clinical and MR data analyzed the coronary angiography (CA) and measured the risk region as the number of segments (in a 48-segment model) that were considered dependent on the coronary bed distal to the occlusion level.

Infarct size by MDE was measured using the same segmental model. The score was defined so that 0 refers to no enhancement, 1 to 1–25% of transmural, 2 to 26–75% and 3 to 76–100%. The total score was divided by the maximum score. The MS was calculated as 100% minus the ratio of infarct size divided by risk region. We then compared the percent

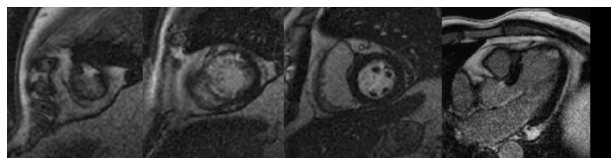


Figure 1.

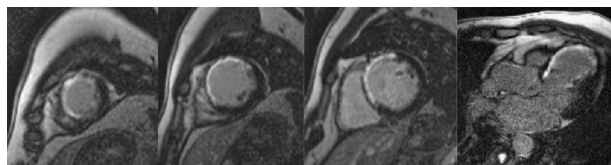


Figure 2.

salvaged myocardium with the clinical and serum markers data.

Results: The average MS was $42.4 \pm 7.3\%$, varying from 0 to 97%. The mean infarct size was $19.5 \pm 2.5\%$. Patients with SBT < 6 hours had significantly higher mean MS than patients with SBT > 6 hours ($57.0 \pm 7.9\%$ vs. $26.2 \pm 8.4\%$, $p=0.01$). However, there was a weak correlation between the SBT and MS defined by MRI ($r=0.45$, $p<0.03$). This was caused by several clinical cases where large MS was associated with long SBT (Figure 1), and small MS with short SBT (Figure 2).

Figure 1 shows an example of a small myocardial infarction with long SBT (16 h) and large MS. CA showed proximal LAD total occlusion (risk region 33% of LV mass). Infarct size was 10% of LV mass. Estimated MS was 70% of the risk region. The calculation is the following: $100\% - \{\text{MRI (infarct size}=10\%)\} / \{\text{CA (risk region}=33\%)\} = 70\%$ of MS.

Figure 2 shows an example of a large myocardial infarction with short SBT (2 hours) and small MS. CA showed proximal LAD total occlusion (risk region 33% of LV mass). Infarct size was 30% of LV mass. Estimated MS was 10% of the risk region. The calculation is the following: $100\% - \{\text{MRI (infarct size}=30\%)\} / \{\text{cate (risk region}=33\%)\} = 10\%$ of MS.

Conclusions: Myocardial salvage cannot be predicted with high accuracy and robustness only by clinical and serum markers in patients with acute myocardial infarction submitted to primary PCI. Infarct size by myocardial delayed enhanced MRI associated to coronary angiography data can estimate more accurately the myocardial salvage. Therefore, this technique is a useful tool and should be used routinely after acute myocardial infarction to estimate myocardial salvage.

300. End-Diastolic and End-Systolic Contrast-Enhanced Magnetic Resonance Imaging to Identify Transmural Extent of Myocardial Hyperenhancement and Contractility

Byoung Wook Choi,¹ Kyu Ok Choe, MD,¹ Young-Jin Kim, MD,¹ Namsik Chung, MD,² Donghoon Choi, MD.² ¹Diagnostic Radiology, Yonsei University College of Medicine, Seoul, Republic of Korea, ²Cardiology, Yonsei University College of Medicine, Seoul, Republic of Korea.

Introduction: To determine transmural extent of myocardial infarction with contrast-enhanced MRI (ce-MRI), imaging at end-diastole is necessary because the measured transmural extent can be affected by imaged cardiac phase, irreproducible cardiac phase other than end-diastole if nonenhanced viable myocardium has preserved or recovered contractility. However, ce-MRI at end-diastole (ED) or end-systole (ES) using segmented inversion-recovery pulse sequence has not been constantly possible due to limitation of imaging acquisition window by inversion recovery time and trigger window. Therefore we optimized ED and ES acquisition with ce-MRI.

Purpose: We studied the feasibility of imaging acquisition at ED and ES with segmented inversion-recovery fast gradient echo (IR-FGE) pulse sequence to simultaneously visualize and quantify the exact transmural extent of viability and contractility.

Methods: MRI was performed with a Gyroscan Intera (1.5 Tesla, Philips, Netherlands) in 18 patients with myocardial infarction (MI) (acute MI 7, recent MI 7, chronic MI 4). First, cine imaging in the short axis was performed using balanced FFE pulse sequence with 25 phases per cycle respectively. Secondly, contrast-enhanced MRI with the same registered slices as cine imaging was performed with a T1-TFE sequence (TR=5.4 ms, TE=1.6 ms, FA=15, voxel size= $0.68 \times 0.68 \times 10$ mm, 32 lines per a segment) and an inversion prepulse 10 minutes after the intravenous injection of Gd-DTPA at a dose of 0.2 mmol/kg body weight. To allow ED and ES imaging, ECG synchronization should use two RR-intervals for one acquisition of a segment of k-space by setting the heart rate to half that the half value of the true heart rate. Trigger delay time (TD) was adjusted to the sum of RR-interval plus the time between R-wave and the end-systole determined in cine images for ES imaging and to the RR-interval for ED imaging. The signal intensity of hyperenhanced region was measured at ED, ES ce-MRI. The wall thicknesses of ED and ES ce-MRI were compared with those of ED and ES cine images for validation of accurate imaging at end-diastole and



end-systole. With absence of thickening of nonenhanced epicardial region within infarcted segments at ES image compared to ED image and according to clinical status, stunned or hibernating myocardium was determined, which results were compared with the results by comparison of cine and ce-MRI.

Results: All the end-diastolic and end-systolic imaging could be acquired within 10 minutes. The signal intensity of hyperenhanced region was higher than normal myocardium in ED and ES images (652% & 678% higher respectively). Wall thicknesses of the ED and the ES images were greater than that of the ED and the ES cine images (7.5 ± 1.3 mm $>$ 6.2 ± 1.4 mm, 9.4 ± 1.8 mm $>$ 8.6 ± 1.8 mm respectively). Subendocardial, transmural, and no hyperenhancement was detected in 13 (acute 5, recent 5, chronic 2), 4 (acute 2, recent 1, chronic 1), and 1 (chronic) respectively. Systolic thickening could be measured exclusively at nonenhanced epicardial areas in subendocardial infarction with ED & ES ce-MRI, which was widely ranged 0–220%, therefore with these cases the transmural extent of hyperenhancement on ED decreased 0–30% on ES. According to absence of systolic wall thickening of the epicardially nonenhanced myocardium of subendocardial infarction, stunned myocardium was in 2 acute MI, no functional recovery in 1 recent MI, and hibernation in 2 chronic MI, which was same as the results by evaluation of combination of cine and ce-MRI.

Conclusions: ED and ES imaging is constantly feasible with segmented IR-FGE pulse sequence free from limitation of time for inversion-recovery and trigger window by using two RR-interval per acquisition of a segment of k-space and useful to simultaneously identify exact transmural extent of hyperenhancement and preserved or recovered contractility of nonenhanced region.

301. Reproducibility and Accuracy of Visual CMR Myocardial Perfusion Analysis

Patrick Sparrow, Sven Plein, John P. Ridgway, Mohan U. Sivananthan. *Cardiac MRI Unit, Leeds General Infirmary, Leeds, United Kingdom.*

Introduction: MR myocardial perfusion imaging potentially allows semiquantitative and even quantitative analysis, but these approaches remain time-consuming. In practice, visual analysis is therefore often carried out.

Purpose: To investigate the observer variability such a visual analysis and its accuracy to detect significant coronary artery lesions.

Methods: Thirty-two patients (29 male, 3 female) were included in this study. All patients underwent coronary x-ray angiography for clinical indications. MRI scanning was performed on a Philips 1.5T Intera CV system (Philips Medical Systems, Best, The Netherlands) with vectorcardiographic ECG-triggering and a 5 element cardiac synergy coil. Perfusion images were acquired with a T1 weighted saturation recovery dynamic fast segmented k-space pulse sequence (Turbo Field Echo=TFE, TR 3.1 ms, TE 1.6 ms, flip angle 15°, FOV as required to avoid image aliasing, matrix 160 × 112, reconstructed to 256 × 256, SENSE-factor 2, 4 short axis slices. Rest and Adenosine stress (140 mcg/kg/min for 5 minutes) studies were acquired separated by 30 minutes. A bolus of 0.05 mmol/kg Dimeglumin gadopentate (Magnevist, Schering AG, Berlin, Germany) was injected by a power injector by a flush of 10 ml Normal Saline.

Two separate observers analysed the data visually separately from each other and in a blinded fashion. Observer 1 was an experienced physician with over 250 stress CMR perfusion cases read prior to the study. Observer 2 had experience of less than 50 cases read. Each observer reported the presence of fixed and inducible perfusion defects for the three vascular territories following a standard AHA segmentation.

Agreement between the two observers was assessed and sensitivities and specificities of visual analysis to detect coronary stenoses of $>70\%$ in the proximal and mid coronary arteries on x-ray angiography were calculated.

Results: The two observers agreed in their assessment of 86 of 96 myocardial territories (89.6%). Sensitivities and specificities for detection of significant coronary stenoses were 70.2% and 98.2% for Observer 1 and 56.1% and 96.4% for Observer 2.

Conclusions: Myocardial perfusion CMR studies can be analysed visually with diagnostic accuracy similar to published semiquantitative methods, although in this study sensitivity was low compared with specificity. Inter-observer agreement was good, even between observers of different levels of expertise. However, the experienced observer in our study yielded higher sensitivity than the inexperienced observer. Training and experience are therefore important for accurate visual analysis of myocardial perfusion CMR data.



302. MR Myocardial Viability Imaging Technique Using Radial Sampling

Orhan Unal, PhD,¹ Tim Christian, MD,² WookJin Chun, MD,² Thomas M. Grist, MD.³ ¹Radiology/Medical Physics, University of Wisconsin, Madison, WI, USA, ²Cardiology, University of Wisconsin, Madison, WI, USA, ³Radiology, University of Wisconsin, Madison, WI, USA.

Introduction: The assessment of myocardial viability in patients with coronary artery disease and left ventricular dysfunction is important to predict which patients might benefit from revascularization. T1-weighted post-contrast MR imaging has shown promise in distinguishing infarcted from normal myocardium since infarcted myocardium regions exhibit higher signal than normal myocardium. Typically, the inversion time (TI) is set to null normal myocardium signal to increase the contrast between normal and infarcted myocardium. However, the TI to null normal myocardium signal varies from patient to patient and also depends on the contrast dosage. A technique that allows retrospective selection of TI to null normal myocardium would be advantageous.

A fast MR imaging technique that allows retrospective selection of TI to null normal myocardium would be advantageous. Due to the intrinsic oversampling of the center of the k-space in angularly undersampled projection reconstruction (PR) acquisition, retrospective selection of TI may be achieved by employing a sliding-window technique with a temporal aperture varying with radial distance.

Purpose: The purpose of this work is to demonstrate the feasibility of high temporal and spatial resolution imaging of myocardial viability in a single breath-hold with retrospective selection of TI following the administration of a contrast agent.

Methods: A fast 2D cardiac-gated segmented inversion-recovery gradient-recalled radial sampling technique with angular undersampling for T1-weighted post-contrast imaging of myocardial viability was developed. All experiments were performed on a 1.5 T Cardiovascular scanner (GE Medical Systems, Milwaukee, WI).

Projections were acquired as fractional echoes in the kx-ky plane through a range of angles spanning 180° in an interleaved fashion using typical scan parameters of TR/TE/Flip=5.4 ms/1.4 ms/20°, 64–128 projections, 4–8 projections per interleave, 16 interleaves, FOV=350 mm × 350 mm, slice thickness=5–10 mm, and receiver bandwidth of ±32 kHz.

During each heartbeat, interleaved sets of projections were repeatedly acquired at multiple time frames. At each time frame, one set of projections was

collected. Data were collected until an ECG trigger was detected, at which point the projection angle was incremented and the sequence started again and new sets of interleaved projections were acquired.

Results: When data from multiple frames are combined, streak artifacts were less visible and SNR was higher as expected. As currently implemented, our myocardial viability imaging technique produces moderate differences in signal intensity between enhanced regions and non-enhanced regions. Short scan times that were achieved with this imaging technique should make breathholding more tolerable to the elderly patients and those with respiratory problems. Note that this method also provides cine images of myocardial function as well as T1 maps to assess wall motion abnormalities or contractility. Further studies are already underway to optimize the current imaging technique to decrease streak artifacts and increase signal-to-noise ratio further. These advantages and our preliminary results suggest that a PR-based segmented inversion-recovery technique may be a viable alternative for the viability imaging of myocardium.

Conclusions: Our preliminary results suggest that a 2D cardiac-gated projection reconstruction-based inversion-recovery technique allows retrospective selection of inversion time (TI) for nulling myocardial signal. The method provides an attractive alternative for the imaging of the viability of myocardium as well as wall motion abnormalities. The imaging technique takes advantage of the oversampling of the center of the k-space in PR imaging technique as well as a sliding-window reconstruction technique with a temporal aperture varying with radial distance.

303. Measurement of Infarct Size by Contrast-Enhanced MRI Compared to 201Thallium-SPECT in Patients with Acute Myocardial Infarction

Gunnar K. Lund,¹ Alexander Stork,² Maythem Saeed,³ Martin P. Bansmann,² Jann H. Gerken,² Vika Müller,⁴ Janos Mester,⁴ Charles B. Higgins,³ Gerhard Adam,² Thomas Meinertz.¹ ¹Cardiology, Herzzentrum, Hamburg, Germany, ²Radiology, Hamburg, Germany, ³Radiology, San Francisco, CA, USA, ⁴Nuclear Medicine, Hamburg, Germany.

Introduction: Contrast-enhanced (CE) magnetic resonance imaging (MRI) represents a new method to



estimate infarct size in patients with acute myocardial infarction (AMI). Recent studies in animals have shown that CE-MRI may overestimate infarct size when validated by histology.

Purpose: The purpose of the current study was to compare measurement of infarct size by CE-MRI with 201Thallium (Tl) Single Photon Emission Computed Tomography (SPECT) in patients with first reperfused AMI.

Methods: CE-MRI was performed in 60 patients (age: 56 ± 13 years) at 6 ± 4 days after first reperfused AMI (CK max: 1038 ± 840 U/L) using a 1.5 T scanner (Siemens Vision). Infarct size was measured 10 min after injection of 0.1 mmol/kg Gd-DTPA using a T1-weighted TurboFLASH inversion recovery sequence with a time to inversion of 220–300 ms. Infarct size was calculated as % of left ventricular (LV) area by use of a threshold method including only that enhanced myocardium with a signal intensity $> +2.0$ SD of remote normal myocardium. SPECT imaging was performed 6 ± 4 days after AMI. Rest-Redistribution images were obtained at 4 hrs after injection of 75 MBq of 201Tl. Infarct size was quantified as % of LV area using a validated software (4D-MSPECT, University of Michigan).

Results: Infarct size was $20.7 \pm 11.5\%$ LV area by CE-MRI and $19.4 \pm 14.3\%$ LV area by 201Tl-SPECT ($P = ns$). Regression analysis revealed good correlation between measurement of infarct size by CE-MRI and by 201Tl-SPECT ($r = 0.73$, $P < 0.0001$). Bland–Altman analysis revealed a mean difference of $+1.3 \pm 9.8\%$ in infarct size between both modalities. A moderate correlation was found between infarct size by CE-MRI and maximal release of creatine kinase MB ($r = 0.46$, $P < 0.001$). In 6 of 30 (20%) patients with inferior AMI 201Tl-SPECT failed to detect the infarction, whereas CE-MRI visualized the infarction in all cases ($P < 0.01$).

Conclusion: The good correlation and agreement between 201Tl-SPECT and CE-MRI indicates that CE-MRI can be used to estimate infarct size 6 days after reperfused AMI. CE-MRI is more sensitive to detect inferior infarction compared to 201Tl-SPECT.

304. Determination of Myocardial Infarct Age by Contrast-Enhanced Cine Magnetic Resonance Imaging

Gilbert L. Raff, MD, Ralph E. Gentry, RT, James A. Goldstein, MD. *Cardiology, William Beaumont Hospital, Royal Oak, MI, USA.*

In patients with acute chest pain and resting wall motion abnormalities, differentiating acute myocardial infarction (AMI) and chronic myocardial infarction (CMI) can have therapeutic implications. Contrast-enhanced cine magnetic resonance imaging (CEC) has been shown to accurately diagnose microvascular obstruction (MO), a signature of AMI that is rarely seen in CMI.

Purpose: This study was designed to determine if CEC can distinguish between AMI and CMI.

Methods: In 43 patients with enzyme-documented AMI, we performed CEC within 36 hours of admission, and repeated this examination after 3 months. All patients were treated by reperfusion. Imaging was performed after administration of 0.20 mmol/kg of I.V. gadolinium-DTPA, using a Siemens Sonata 1.5T magnet. Nine 8 mm short-axis slices and two long-axis slices were acquired, using an-EKG gated, segmented k-space true-FISP pulse sequence. At 10 minutes post-injection, an inversion time was scanned for optimum myocardial nulling, then an inversion-recovery turbo-FLASH delayed hyperenhancement (IR-DE) study was done in identical slices. MO was defined as discrete endocardially-based hypoenhancing regions that became all or partially enhanced on IR-DE. MO was used as a criterion for AMI and wall thinning a criterion for CMI. All readings were blinded and read by two observers.

Results: In patients with AMI, MO was seen in 35/41 (81%) and abnormal wall motion without wall thinning in 37/41 (90%). The CMI pattern at 3 months was identified by abnormal wall motion with wall thinning in 10/43 (23%), and absence of MO in 41/43 (95%). Overall, sensitivity and specificity were 86% and 91% for the presence of AMI, compared with CMI.

Conclusions: Contrast-enhanced cine MRI can sensitively and specifically differentiate acute from chronic MI. This may have therapeutic implications in the management of patients with acute coronary syndromes.

305. Detection of Myocardial Viability in Ischemic Cardiomyopathy: Cardiac MRI versus SPECT

Begoña Igual, MD,¹ Alicia M. Maceira, MD,¹ Pilar Bello, MD,² Pilar López-Lereu, MD,¹ Jordi Estornell,¹ Joaquín Martín,¹ Miguel Palencia, MD.³ ¹Eresa, Hospital La Fe, Valencia, Spain, ²Department of Nuclear Medicine, Hospital La Fe, Valencia, Spain, ³Department of Cardiology, Hospital La Fe, Valencia, Spain.

Introduction: The presence, location and extension of viable myocardium in ischemic left ventricular



dysfunction determine the amount of functional improvement after revascularization. Gadolinium-enhanced cardiac magnetic resonance (CMR), due to its high spatial resolution and absence of attenuation artefacts, is a good non-invasive, radiation-free technique for diagnosis of viability.

Purpose: To assess and compare the utility of gadolinium-enhanced CMR and SPECT in the diagnosis of the presence, location, extension and transmurality of myocardial viability in patients with ischemic left ventricular dysfunction.

Methods: 15 patients (62±12 yrs, 2 females) with ischemic cardiomyopathy were included. Mean EF was 33±14%. In all cases both imaging techniques were used with a 16 segment model, and a total of 240 segments were analysed. Viability criteria: segments were considered not viable by CMR when gadolinium enhancement was present in >50% of segment thickness, and by SPECT when tracer uptake was <40%, persistent after sublingual nitroglycerine.

Results: 36 segments (15%) were considered not viable by CMR criteria (21 segments had transmural enhancement, 15 had enhancement >50% of wall thickness), 27 viable segments showed enhancement <50% of wall thickness. SPECT detected 53 non-viable segments (22%) (P=NS). There was a good concordance between both techniques (Kappa=0.713, p<0.001). The best agreement was found in those segments with transmural or nearly transmural gadolinium enhancement by CMR (94% agreement), and the worst in those segments with enhancement <50% (88% agreement), of which 3 were considered non-viable by SPECT and viable according to CMR criteria, due to the impact that CMR higher spatial resolution has on its diagnostic value.

Conclusions: CMR and SPECT identify a similar proportion of non-viable segments in patients with ischaemic cardiomyopathy and left ventricular dysfunction. Both techniques show a good concordance, but CMR is able to detect more viable segments due to its high spatial resolution.

306. Delayed Enhancement MRI and Rest/Stress SPECT Before and After CABG Show Early Recovery of Perfusion but Delayed Recovery of Function in Scarred and Dysfunctional Segments

Martin Ugander, MD,¹ Peter Cain, MD, PhD,¹ Per Johnsson, MD, PhD,² Hakan Arheden, MD, PhD.¹
¹Clinical Physiology, Lund University Hospital, Lund,

Sweden, ²Thoracic Surgery, Lund University Hospital, Lund, Sweden.

Introduction: Myocardial scarring assessed by delayed enhancement MRI (DE-MRI) may predict myocardial functional recovery after revascularization. The interaction between myocardial scarring and perfusion on quantitative functional improvement and its timecourse are not known.

Purpose: We hypothesized that the temporal coupling of perfusion and functional recovery would be affected by presence of scar.

Methods: 14 patients (mean age 67, range 53–83, 14 men) undergoing coronary artery bypass grafting (CABG) underwent GRE cine MRI, DE-MRI and stress/rest 99m-Tc-tetrofosmin SPECT imaging before and 1 and 6 months after CABG. Segmental perfusion (rest/stress SPECT), radial thickening (GRE cine MRI), and scar transmurality (DE-MRI) were all quantified in a blinded fashion using in-house developed software. A 12 segment short axis model was applied to 4 midventricular slices per patient at each timepoint (672 segments per timepoint). Segments with <30% thickening before CABG (290 segments) were analyzed for function, stress perfusion and stress induced ischemia over time according to presence of scar. Figures 1–3 show mean values±SEM. Stress induced ischemia was defined as the difference between rest and stress perfusion (%).

Results: Stress perfusion was lower in scarred compared to non-scarred segments at all time points (p<0.001). A significant increase in stress perfusion occurred at 1 month in both scarred and non-scarred segments (p<0.001 vs. before) with no further improvement at 6 months (p=NS) (Figure 1). Scarred segments displayed lesser thickening at all time points compared to non-scarred segments (p<0.01). However,

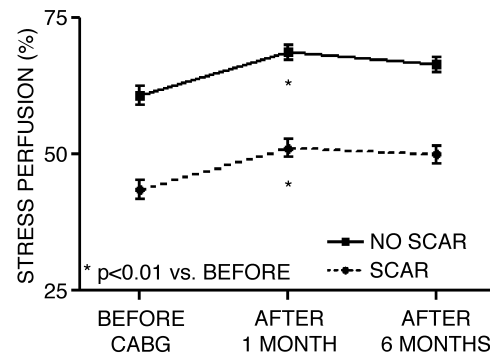


Figure 1. Stress perfusion in segments with dysfunction before CABG.

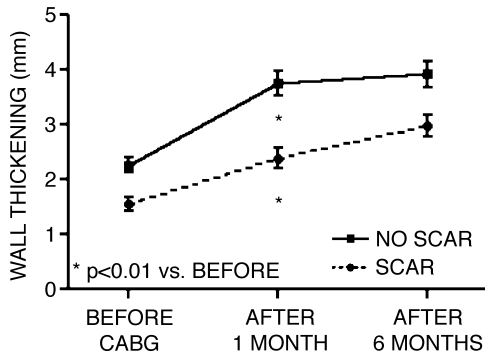


Figure 2. Wall thickening in segments with dysfunction before CABG.

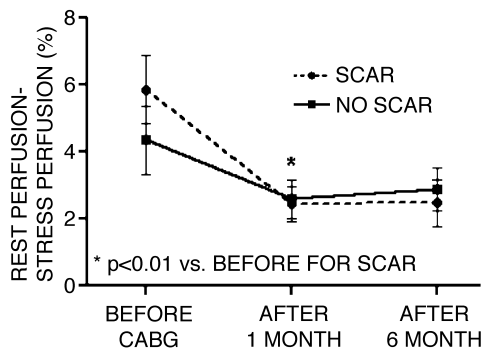


Figure 3. Stress ischemia in segments with dysfunction before CABG.

non-scarred segments improved most function at 1 month while scarred segments displayed a more delayed time course of functional recovery (Figure 2). Resting perfusion increased in both scarred and non-scarred segments between baseline and 1 month ($p < 0.01$), while no further improvement was seen between 1 and 6 months. In addition, the severity of stress induced ischemia decreased significantly between baseline and 1 month only in segments with scar ($p < 0.001$). Stress induced ischemia was effectively absent in both groups at 1 month, and unchanged between 1 and 6 months post-CABG (Figure 3).

Conclusions: Stress perfusion predominantly improves within 1 month in all segments after CABG. Function also improves within 1 month in non-scarred segments, while scarred segments had a more drawn out timecourse of functional recovery. This may reflect a more severe ischemic burden in segments with scar, such as that which may occur during repetitive stunning or hibernation.

307. Myocardial SPECT Perfusion Imaging versus Delayed Contrast Enhanced Magnetic Resonance Imaging for Infarct Sizing in Patients with Acute or Chronic Infarct

Erik Hedström,¹ John Palmer, PhD,² Martin Ugander, MD,¹ Håkan Arheden, MD, PhD.¹ ¹Department of Clinical Physiology, Lund University Hospital, Lund, Sweden, ²Department of Radiation Physics, Lund University Hospital, Lund, Sweden.

Introduction: Myocardial single photon emission computed tomography (SPECT) perfusion imaging has previously been used to estimate infarct size. Recently, delayed contrast enhanced magnetic resonance imaging (DE-MRI) has evolved as a validated tool to determine infarct size. Previous studies have shown a lower sensitivity for detection of subendocardial infarcts by SPECT compared to DE-MRI as well as a slight overestimation of infarct size by SPECT compared to measurements on explanted hearts.

Purpose: The present study was designed to evaluate SPECT as a tool to estimate acute as well as chronic infarct size in man, compared to DE-MRI, and to validate SPECT against phantom measurements.

Methods: Six patients with a first time myocardial infarction treated with successful primary percutaneous transluminal coronary angioplasty (PTCA) and ten patients with chronic myocardial infarction treated with coronary artery bypass grafting (CABG) were imaged using SPECT and DE-MRI to measure perfusion defect and infarct size, respectively. Imaging was performed one week after the acute setting or six months after CABG in the two populations. To validate SPECT measurements, different perfusion defect sizes were produced using an inflatable balloon in a thorax phantom.

Results: Infarct size was overestimated by SPECT compared to DE-MRI by 9 ± 2 ml, and 4 ± 12 ml, in acute (Figure 1a) and chronic (Figure 1b) infarction in man, respectively. In the phantom experiment, SPECT overestimated the perfusion defect by 3 ± 3 ml if the phantom perfusion defect was below or equal to 22 ml (Figure 1c). If the phantom defect size was larger than 22 ml, SPECT underestimated true size by 13 ± 12 ml (Figure 1d). Left ventricle wall volume was underestimated in all settings.

Conclusions: The present study demonstrates that SPECT overestimated absolute and relative infarct size in patients with acute and chronic infarction. The mismatch between SPECT and DE-MRI may be related to systematic differences between imaging modalities as shown by the phantom experiment but



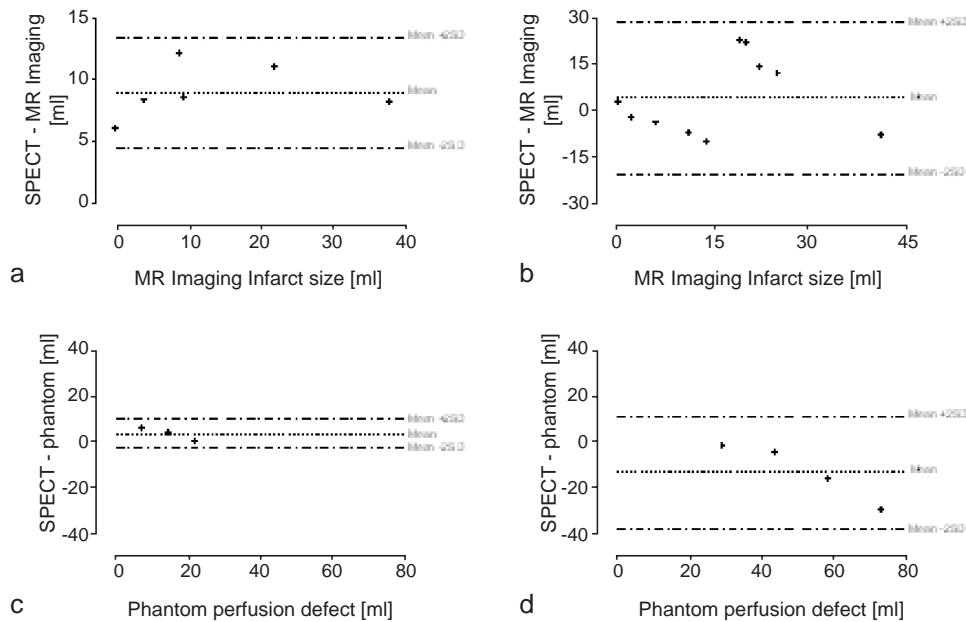


Figure 1. SPECT was found to overestimate infarct size by DE-MRI in the a) acute, and b) chronic settings, as well as c) in the phantom experiment if the perfusion defect size was below or equal to 22 ml. However, d) if the phantom defect size was larger than 22 ml, SPECT underestimated the perfusion defect.

could also be influenced by biological phenomena such as hypoperfused but viable myocardium or wall thinning due to hypofunctioning myocardium.

308. Evolution of Delayed Hyperenhancement Region Can Assess the Success of Myocardial Reperfusion Therapy Following Acute Myocardial Infarction

Mark Doyle, PhD, June Yamrozik, Geetha Rayarao, Ronald B. Williams, Maria Jaksec, Diane A. Vido, Robert W. W. Biederman, MD. *Allegheny General Hospital, Pittsburgh, PA, USA.*

Introduction: Assessment of the success of reperfusion therapy following myocardial infarction (MI) has chiefly relied on assessment of vessel patency or myocardial function. However, no quantitative means of judging success is agreed upon. Magnetic resonance imaging (MRI) assessment of ventricular function, when combined with gadolinium contrast to show the extent of delayed hyperenhancement (DHE) regions, has potential to provide a non-invasive quantitative index of reperfusion success.

Hypothesis: We hypothesized that the temporal evolution of DHE regions combined with a previously described wall thickening and DHE correlation index can be used to objectively judge reperfusion success post-MI.

Methods: Patients (n=11, 2 female) aged 38–69, post MI who received complete revascularization therapy by PTCA were recruited. MRI was performed Early (2.6 ± 1.2 days post MI) and Late (7.4 ± 1 week post MI). Images (GE CV/i) were obtained in the short axis orientation to assess function and DHE extent (Berlex, XX). The endocardial and epicardial borders were planimeted and data extracted at 100 points around the circumference of each slice to calculate end diastolic to end systolic wall thickening and record the DHE signal. For each slice we performed a correlation analysis to assess congruence of the DHE pattern and wall thickening at the Early time point. The EF was calculated using Simpson's rule. A 2 SD threshold was applied to the DHE signal to assess the extent of myocardium that had elevated DHE signal.

Results: At the Late time point, EF ranged from 38–68% (mean 55.2%). Linear regression analysis showed that the correlation of DHE and wall thickening, Early, was inversely related to EF at the Late time point, ($r=0.78$, $p<0.01$). The regression or progression of the extent of DHE from the early to Late time point increased the correlation with Late EF, $r=0.90$,

$P < 0.005$. The gap between the early time point prediction of EF and the EF achieved is attributable to the evolution of the extent of DHE.

Conclusions: Early post MI, those patients with a negative correlation of DHE with wall thickening are likely to beneficially remodel. At the Late time point, the progression of the extent of the DHE regions explains almost all the variation in the EF achieved at the Late time point. A linear combination of wall function and extent of DHE regions by MRI can be used to non-invasively assess the success of reperfusion quantitatively.

309. Defect Size Quantification After Acute Myocardial Infarction Using Contrast Enhanced MRI: Dependence of Acquisition and Analysis Parameters

Stephan G. Nekolla, Mira Hoernke, Tareq Ibrahim, Hubertus Buelow, Karin Schreiber, Markus Schwaiger. *Nuklearmedizinische Klinik, TU Muenchen, Muenchen, Germany.*

Introduction: As a wide range of acquisition parameters in contrast enhanced MRI (ceMRI) as well as analysis methods are available, this study investigates their influence on the quantitative delineation of defect size in patients after acute myocardial infarction.

Purpose: To develop a stable acquisition and analysis approach to quantify defect size after acute myocardial infarction.

Methods: In 29 patients (60 ± 15 y, 13M) with successful coronary stenting, ceMRI was performed within 7 ± 1 d. Using a 1.5 T system (Sonata, Siemens), fast inversion recovery (IR-TrueFISP) imaging with complete LV coverage was used (imaging matrix 256×128 , flip angle 60° , TR/TE: 2.3/1.4 ms, FOV 300–350 mm, slice thickness 8 mm). After contrast media injection (Gd-DTPA, 0.2 mmol/kg BW) for a total of 42 min data was taken every seven minutes. For every point, 4 inversion delays (TI) were used. LV contours were drawn manually and the regional signal intensity was automatically quantified in 1, 2 or 4 layers from endo- to epicardium and transferred into “polar maps.” Defect extent was determined using the thresholds in every layer and cumulated for total defect size. However, as normal myocardium shows up dark and defect areas are bright, conventional calibration is not directly applicable and three approaches were investigated: normalization to remote and defect areas and to the blood pool. Defect sizes were compared to

planimetric analysis using the 28 min p.i. scan with optimal darkening of the remote myocardial signal and coregistered SPECT using Tc-99m MIBI and previously established thresholds.

Results: Correlation between the planimetric defect extent assessment and the automated analysis was excellent (MR $22 \pm 13\%$ LV, MR $24 \pm 14\%$ LV resp.). Good agreement was found when comparing to SPECT defect sizes ($18 \pm 17\%$). Sensitivity analysis revealed that the remote approach using two layers gave the best overall performance when using proper myocardial nulling, i.e. increasing TI over time p.i. Here, individual differences averaged to $1\% \pm 5\%$ using a threshold of 200% between 20 and 40 min p.i. Using the defect area as reference, overestimation for times earlier than 20 min was found whereas the blood normalization resulted in severe overestimation for times later than 20 min and TI of less than 400 msec. For both defect and blood pool normalization, the statistical fluctuations were clearly larger as compared to remote normalization. In all cases, individually adjusted TI performed better than a fixed TI.

Conclusions: Quantitative assessment of infarct extent with MRI delayed enhancement imaging in patients after acute infarction showed a substantial variability due to different acquisition and analysis approaches. However, the use of remote normalization, two myocardial layers and a threshold of 200% allowed a reliable estimation of defect size. Although these findings warrant an investigation in a larger population with a reduced number of variables, the delineated technique provides a stable basement for this approach as a future reference technique itself.

310. Quantitative Assessment of Infarct Size by Contrast Enhanced Magnetic Resonance Imaging Early After Acute Myocardial Infarction: Comparison to Single Photon Emission Tomography

Tareq Ibrahim, MD,¹ Stephan G. Nekolla, PhD,² Mira Hörnke,² Hubertus P. Bülow, MD,² Karin Schreiber, MD,² Albert Schömig, MD,¹ Markus Schwaiger, MD.²
¹Deutsches Herzzentrum und 1. Medizinische Klinik des Klinikums Rechts der Isar, Technische Universität, München, Germany, ²Nuklearmedizinische Klinik, Technische Universität, München, Germany.

Introduction: Quantification of infarct size is important as a surrogate endpoint in evaluating new therapies



early after acute myocardial infarction (AMI). Contrast enhanced magnetic resonance imaging (ceMRI) represents a promising method to define irreversible tissue injury with high spatial resolution.

Purpose: The purpose of this study was to examine the time course of myocardial contrast enhancement after injection of Gd-DTPA in patients with reperfused AMI and to compare the extent with the size of perfusion defect determined by single photon emission tomography (SPECT).

Methods: We performed ceMRI and myocardial perfusion imaging by Tc99m-Sestamibi-SPECT in 33 patients with first AMI and successful coronary artery stenting 7±2 days after the acute event. CeMRI short axis slices (Siemens 1.5T, TrueFISP) of the entire left ventricle (LV, 12 slices) were continuously acquired over 42 min following Gd-DTPA bolus injection (0.2 mmol/kg) using variable inversion time in order to null normal myocardium. Based on a polar map approach, the extent of myocardial contrast enhancement (CE) was quantified as percent of the LV using a threshold >200% of remote myocardium and compared to coregistered SPECT perfusion defects based on a 50% count density threshold previously validated, peak creatinekinase (CK) and LV ejection fraction (EF).

Results: All infarcts were correctly localized by ceMRI. CE peaked at 14 min after contrast injection with 300% of remote myocardium, but remained at 280% at 42 min. CE extent varied from 18.3% LV at 14 min to 12.5% at 42 min. The mean difference of MRI contrast enhancement and SPECT perfusion defect remained below 2% LV between 21 and 42 min post contrast yielding the best correlation (r=0.91) at 28 min (Table 1).

Conclusions: Early after AMI, infarct size can be accurately assessed using ceMRI under standardized conditions. The extent of CE varies over time agreeing best with SPECT at 28 min. CeMRI appears suitable for serving as a surrogate endpoint assessing myocardial infarct size in-vivo.

311. Comparison of Snapshot and 3D Viability Techniques with Conventional 2-D Inversion-Recovery Gradient Echo Techniques for Viability Assessment

Giovanni Salanitri, MD,¹ Thomas Holly, MD,¹ Elizabeth Krupinski, PhD,² James C. Carr, MD,¹ Ai Zhang, PhD,³ YiuCho Chung, PhD,³ Frederick S. Pereles, MD.¹ ¹Radiology, Feinberg School of Medicine, Northwestern University, Chicago, IL, USA, ²Radiology, The University of Arizona Health Sciences Center, Tucson, AZ, USA, ³Siemens Medical Solutions, Chicago, IL, USA.

Introduction: The established standard for detection of delayed myocardial hyperenhancement in cardiac MR examinations has become the use of low flip angle gradient echo pulse sequences with an inversion recovery preparatory pulse (e.g. IR-TurboFLASH). By virtue of the requisite whole heart coverage necessary for viability examinations, this single slice per breath-hold, two-dimensional (2D) technique is relatively time consuming.

Purpose: This study compares conventional 2 D viability techniques with newer three-dimensional (3D) techniques as well as breathing independent snapshot methods to determine whether newer faster methods can be substituted for conventional MR viability imaging practices.

Methods: 30 consecutive patients with suspected myocardial infarction were evaluated at 1.5 T (Siemens Magnetom Sonata, Malvern PA) with three techniques: standard breath-held 2D IR TurboFLASH, breath-held 3D IR TurboFLASH with a partial Fourier acquisition, and a breathing-independent 2D snapshot balanced gradient echo technique. Two experienced blinded readers (one radiologist and one cardiologist) graded analogous short axis images of the cardiac base, mid-ventricle and apex on a 5 point scale for the transmural extent of myocardial hyperenhancement using a 14 segment model. Assessment of image quality was also performed using a five point scale.

Table 1. Time course of contrast enhancement and comparison to various parameters of infarct size.

Time after contrast injection	7 min	14 min	21 min	28 min	35 min	42 min
CE (% Remote)	277±64	299±69	297±84	293±76	289±81	280±73
CE Extent (% LV)	17.7±18	18.3±15	16.6±13	15.4±13	13.1±10	12.5±10
CE-SPECT (% LV)	2.5±13	3.1±9	1.4±9	-0.2±8	-0.7±7	-1.2±6
CE versus SPECT (r-value)	0.70	0.84	0.82	0.91	0.75	0.80
CE versus CK (r-value)	0.58	0.62	0.62	0.62	0.65	0.61
CE versus EF (r-value)	-0.40	-0.53	-0.58	-0.53	-0.38	-0.26

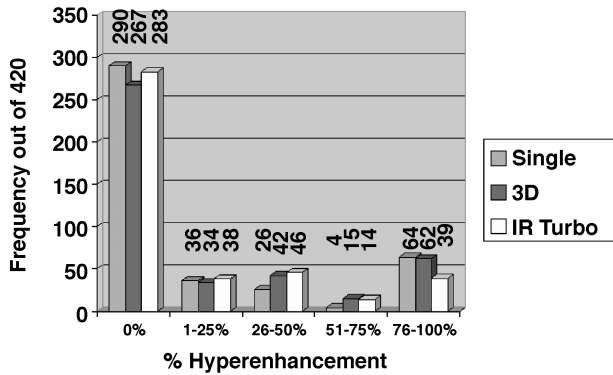


Figure 1. Distribution of ratings (0, 1, 2, 3, 4) within the three imaging categories does not differ significantly ($X^2=5.45$, $df=8$, $p>0.05$). (View this art in color at www.dekker.com.)

Results: Using a non-parametric Kruskal-Wallis test, no statistically significant differences in the presence and extent of hyperenhancement were detected in any segments as a function of method (Figure 1). There was a statistically significant difference in subjective image quality ratings with the snapshot technique being rated highest ($H=11.38$, $p=0.0034$). The second reader's data showed no significant differences from the first reader for any individual segments ($H=8.185$, $p=0.4156$).

Conclusions: Rapid MR viability imaging pulse sequences allow whole heart coverage in approximately 20 seconds or less using snapshot balanced gradient echo techniques and 3D gradient echo sequences. These rapid techniques are diagnostically comparable to conventional 2D viability sequences in the determination of the transmural extent of myocardial hyperenhancement.

SCALE for transmural extent of hyperenhancement: 0=0%, 1=1–25%, 2=26–50%, 3=51–75%, 4=76–100%. Total number of segments equals 420.

312. Using a TI Scout Sequence for Correlation with Standard Turbo-Flash Cardiac Viability Sequences: Effect on Reader Confidence

Christopher Chiccoskie, MD,¹ Edwin Wu, MD,² Elizabeth Krupinski, PhD,³ Scott Pereles, MD.¹ ¹Department of Radiology, Northwestern University, Northwestern Memorial Hospital, Chicago, IL, USA, ²Department of Medicine, Division of Cardiology, Northwestern Uni-

versity, Northwestern Memorial Hospital, Chicago, IL, USA, ³Department of Radiology, University of Arizona, Arizona Health Sciences Center, Tucson, AZ, USA.

Introduction: Delayed post-gadolinium 2D inversion recovery turbo-flash (TFL) imaging sequences are commonly used for the evaluation of myocardial viability. At our institution, a balanced gradient echo (True-FISP) variable TI scout (TI Scout) sequence is routinely performed 5 minutes after contrast infusion and immediately prior to TFL sequences to estimate the ideal inversion time (TI) for optimal nulling of signal intensity within the normal myocardium. This breath-held TI Scout sequence produces images of the myocardium at TI intervals of approximately 40 milliseconds throughout the entire cardiac cycle.

Purpose: The purpose of this study was to evaluate changes in reader confidence in interpretation of standard TFL cardiac viability sequences using the TI Scout sequence for direct correlation.

Methods: Two independent blinded readers retrospectively reviewed forty-nine consecutive examinations performed over a 5-month period for evaluation of cardiac viability. Short axis TFL and TI Scout images performed at the same mid-ventricle position were selected for review. Soft copy images were evaluated on a PACS workstation. TFL images only were reviewed first in randomized order. Each reader rated the images for the presence and transmural extent of myocardial hyperenhancement in each of six equiangular segments according to a 6-point ordinal scale, and graded confidence in the presence of myocardial hyperenhancement in each segment according to a 3-point ordinal scale. Two weeks later, each reader rated the TI Scout images only for the presence or absence of a suspected abnormality in each segment. Finally, each reader rated the TFL images in the same fashion as before using the TI Scout images for direct correlation, while blinded from the original readings.

Results: Agreement between the isolated TFL readings and isolated TI Scout readings for the presence of an abnormality was low ($kappa<0.50$) for all segments, with disagreement primarily due to myocardial hyperenhancement seen on TFL images that was not suspected on TI Scout images alone. Agreement between the isolated TFL readings and combined TFL and TI Scout readings was good ($kappa>0.50$) for all segments. Specifically, there was 85.5% agreement about the presence of myocardial hyperenhancement for all segments and 73.8% agreement about the degree of transmural extent for all segments. Reader confidence ratings were unchanged by correlative TI Scout images

in 61.8 % of cases. However, confidence was increased by correlation with the TI Scout images in 34.8% of all segments, significantly more than the 4.4% of all segments in which confidence ratings decreased (Kruskal–Wallis test, $H=14.18$, $p=0.0008$).

Conclusion: Correlation of a balanced gradient echo TI Scout sequence with standard 2D TFL cardiac viability sequences may be helpful to increase reader confidence of the presence of myocardial hyperenhancement in cases where enhancement is questionable.

313. Comparison Between Inversion Recovery TrueFISP and Inversion Recovery Turbo FLASH for the Assessment of Myocardial Viability

Stéphane Baldassarre, MD,¹ Olivier Cappelliez, MD,¹ Nathalie Gauquier, MD,¹ Jean Jacquy, MD,² Jacques Van Espen,¹ Luisa Divano, MD.¹ ¹MRI Unit, Chambor, Mons, Belgium, ²CHU Charleroi, Charleroi, Belgium.

Introduction: Reversible myocardial dysfunction can be identified by contrast-enhanced MRI before coronary revascularization (Kim et al., 2000). The inversion-recovery turboFLASH (IR-TFL) sequence gives the greatest difference in signal intensity between infarcted and normal myocardium (Simonetti et al., 2001). Inversion recovery trueFISP (IR-trueFISP) is described as a robust technique for infarct imaging. IR-trueFISP produces images with quality immune to heart rate variability or patient's breath holding ability (Chung et al., 2002), but it slightly underestimates the extent of myocardial infarction (Lee et al., 2003).

Purpose: To compare IR-trueFISP and IR-TFL sequences with respect to image quality and myocardial viability assessment.

Methods: Patient Imaging—we imaged 46 consecutive patients in a 1.5T clinical scanner (Siemens Symphony, Erlangen, Germany) for viability assessment. A series of contrast-enhanced images were acquired 15 minutes after intravenous contrast injection of a commercially available gadolinium-based contrast agent at a dose of 0.1 mmol per kilogram of body weight. The imaging protocol included vertical long axis views, horizontal long axis views and short axis views from the apex to the base of the left ventricle, using both IR-trueFISP and IR-TFL. Image analysis—For both imaging sequences, image quality was rated: good, sufficient, or insufficient. 43 patients with good

or sufficient image quality rating for both techniques were selected for comparison. We evaluated contrast-enhanced images using a model in which the left ventricle was divided in 17 segments (Cerqueira et al., 2002). A total of 86 contrast-enhanced left ventricles (731 segments), both IR-trueFISP and IR-TFL, were placed in a random order and analyzed by two observers who were unaware of the patient's identity and clinical data. Each segment was graded on a 3-point scale: 0=no hyperenhancement; 1=up to 75% hyperenhancement; 2=more than 75% hyperenhancement. The sum of all 17 segments score yielded the total hyperenhancement score (THS) (Lee et al., 2003).

Results: Observer agreement was almost perfect for image quality rating ($Kappa>0.81$ for both sequences). Image quality of IR-TFL sequence was insufficient for diagnostic purpose in 3 patients due to heart rate irregularity or inability to breath-hold (whereas it was rated "good" with IR-trueFISP). There was no statistically significant difference in image quality rating between IR-TFL and IR-trueFISP when those patients with insufficient image quality rating are rejected. Also, no statistically significant difference was found in hyperenhancement grading (for each segment individually and for THS) between IR-TFL and IR-trueFISP. Hyperenhancement (grade 1 and 2) visualized by IR-TFL was identified by trueFISP in 145 of 154 segments. Sensitivity and specificity of IR-trueFISP were 94.2% and 100% respectively. Positive and negative predictive values were 100% and 98.5% respectively. There were 9 false negative segments in 2 patients with very thin-walled scarred left ventricles. In two other segments (one patient) hyperenhancement was graded 1 with IR-TFL and 2 with IR-trueFISP.

Conclusions: IR-trueFISP produces an image quality that is comparable to IR-TFL. There was no statistically significant difference between the two techniques for grading hyperenhancement using a 3-point scale per segment or using THS per ventricle. Furthermore, IR-trueFISP shows high sensitivity and specificity. Therefore, IR-trueFISP appears as a valuable tool for assessment of myocardial viability despite cardiac arrhythmias or patient's inability to breath-hold.

REFERENCES

- Cerqueira, M. D., et al. (2002). *JCMR* 4(2):203–210.
- Chung, Y. C., et al. (2002). *JCMR* 4(1):12–13.
- Kim, R. J., et al. (2000). *NEJM* 343:1445–1453.
- Lee, D. C., et al. (2003). *JCMR* 5(1):79–80.
- Simonetti, O. P., et al. (2001). *Radiology* 218:215–223.

314. Detection of Silent Heart Disease in the Asymptomatic High Risk Diabetic Patient with Simultaneous Adenosine Stress Cardiac MRI and Myocardial Scintigraphy

Stephen R. Chen, MD,¹ Charles V. Voigt, MD,¹ Jerry A. Michel, MD,¹ Michael J. Lane, MD,² Scott R. Partyka, MD.² ¹Radiology, Brooke Army Medical Center, Fort Sam Houston, TX, USA, ²Radiology, South Texas Radiology Group, San Antonio, TX, USA.

Purpose: To investigate the incidence of silent myocardial ischemia/infarction in high risk diabetic patients with microalbuminuria and to compare adenosine stress cardiac MR (AS-CMR) and myocardial perfusion scintigraphy (SPECT). Both exams were performed with a single adenosine infusion to enable optimal comparison.

Method and Materials: 26 asymptomatic diabetic patients with microalbuminuria (urine albumin/creatinine) >1000 mg/gm were evaluated, normal level <30 mg/gm with IRB approval. All patients were screened for contraindications related to gadolinium (Opti-MARK, Tyco Healthcare/Mallinckrodt) enhanced MRI and adenosine infusion. The AS-CMR was performed with a 1.5T MR (Eclipse, Philips Medical Systems) with physiologic monitoring. Imaging protocol: Rest Tc-99m sestamibi (10 mCi) SPECT scan was obtained. The patient was then transferred to MRI where at the 3-minute point of a 6-minute IV infusion of adenosine (140 ug/kg/min), Tc-99m sestamibi (30 mCi) and gadolinium (0.05 mmol/kg) were injected into different veins simultaneously. Short axis left ventricle dynamic contrast perfusion AS-CMR exam was immediately performed during the initial gadolinium dose (3 cc/sec). An additional dose of gadolinium (0.05 mmol/kg) was injected after completion of the adenosine infusion. Post-contrast infarct avid images were obtained 10 minutes after the second gadolinium dose in the short, vertical long and horizontal long axis orientation. 20 minutes following the cessation of the adenosine infusion a repeat dynamic contrast-enhanced MRI was performed with gadolinium (0.05 mmol/kg) to simulate rest perfusion. The patient was then transferred to nuclear medicine and the stress SPECT images were obtained. The CMR and SPECT images were interpreted for myocardial ischemia and infarction separately by blinded fellowship trained BC radiologists.

Results: 19 patients completed all imaging. 15/19 (79%) patients were normal and 4/19 (21%) were abnormal. In three of the four abnormal exams, the

AS-CMR and SPECT results correlated (Patient A—lateral wall ischemia, Pt.B—inferior wall infarct, Pt.C inferior wall ischemia/infarct). In the fourth abnormal exam, the AS-CMR showed inferior ischemia, inferior–lateral infarct, and subendocardial anterior–septal infarct. However, the SPECT showed defects, which were interpreted as diaphragmatic, and chest wall attenuation artifacts.

Conclusion: The 45 minute AS-CMR and the 4-hour SPECT exams had similar diagnostic accuracy in detecting myocardial ischemia and/or infarction in asymptomatic diabetics with microalbuminuria. The utilization of the one time adenosine infusion for both the AS-CMR and SPECT exams allows for optimal comparison of the two modalities.

315. Quantification of Acute Myocardial Infarction by Delayed Enhancement MRI and QRS Scoring: A Comparison

Henrik Engblom,¹ Erik Hedstrom,¹ Galen S. Wagner, MD,² Olle Pahlm, MD, PhD,¹ Hakan Arheden, MD, PhD.¹ ¹Clinical Physiology, Lund University Hospital, Lund, Sweden, ²Duke University Medical Center, Durham, NC, USA.

Background: The distinction between areas of myocardial infarction (MI) and areas of viable myocardium is important for identification of patients who will benefit from revascularization therapy and to predict prognosis after acute MI. By using delayed enhancement MRI (DE-MRI) it is possible to distinguish infarcted myocardium from non-infarcted with high accuracy. Thus, DE-MRI has previously been shown valuable in evaluation of the diagnostic performance of 12-lead ECG for quantifying chronic, anterior MI in the left ventricle (LV).

Purpose: Our aim was to test the hypothesis that there is a strong correlation between MI size measured by DE-MRI and estimated by QRS scoring at the most common infarct locations, the anterior and inferior LV wall.

Methods: Twenty-two patients with single first time MI (all treated with primary PTCA) were examined by DE-MRI and the commonly available standard 12-lead ECG within 7 days of the acute event. A gadolinium-based contrast agent (Gd-DOTA, Guerbet, Gothia Medical AB, Billdal, Sweden) was injected intravenously (0.2 mmol/kg) 15–30 minutes



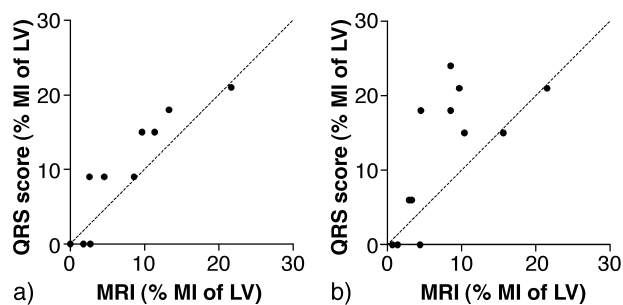


Figure 1.

before contrast enhanced images were acquired. To visualize the necrotic myocardium an inversion recovery turbo-FLASH technique was employed. Areas of necrosis were identified and quantified as a percentage of the LV mass from MR images by planimetric analysis. MR results were then compared to MI size estimated by QRS scoring based on previously established ECG criteria.

Results: MI size by DE-MRI measured $8 \pm 6\%$ (mean \pm SD) of the LV mass, and MI size by QRS scoring measured $11 \pm 8\%$. There was a stronger correlation between DE-MRI and QRS scoring for the anterior MIs ($r=0.93$, $p<0.0001$; $n=10$) than for the inferior MIs ($r=0.73$, $p<0.001$; $n=12$) (Figure 1). In 4 cases with inferior MI, MI size was significantly overestimated by QRS scoring, all with the majority of QRS points generated from lead aVL.

Conclusions: The results suggest that QRS scoring from the 12-lead ECG can be used to estimate size of acute MI, both in the anterior and inferior LV wall. In concordance with previous studies (Ideker et al., 1982; Roark et al., 1983) the performance of QRS scoring for anterior MI is superior to the performance in inferior MI. ECG criteria for lead aVL may have to be weighted differently in the future based on the MR observations in this study. Thus, DE-MRI is feasible for further development and optimization of QRS scoring.

REFERENCES

- Ideker, R. E., Wagner, G. S., Ruth, W. K., et al. (1982). Evaluation of a QRS scoring system for estimating myocardial infarct size. II. Correlation with quantitative anatomic findings for anterior infarcts. *Am. J. Cardiol.* 49:1604–1614.
- Roark, S. F., Ideker, R. E., Wagner, G. S., et al. (1983). Evaluation of a QRS scoring system for estimating

myocardial infarct size. III. Correlation with quantitative anatomic findings for inferior infarcts. *Am. J. Cardiol.* 51:382–389.

316. Assessment of Myocardial Viability Using Contrast Enhanced MRI—Comparison of Gd-DTPA and Gd-BOPTA

Thomas Schlosser, MD, Peter Hunold, MD, Kai-Uwe Waltering, MD, Sandra Massing, RT, Christoph U. Herborn, MD, Jörg Barkhausen, MD. *Radiology, University Hospital Essen, Essen, Germany.*

Introduction: Several studies demonstrated that contrast-enhanced magnetic resonance imaging (MRI) allows differentiation between reversible and irreversible ischemic injury. Much effort has been spent to find both optimum dose and time point for data acquisition after contrast injection. However, the effect of different contrast agents on contrast to noise ratios and the course of T1 values over time in damaged and normal myocardium has not been assessed yet.

Purpose: To compare Gadobenate Dimeglumine (Gd-BOPTA) and Gadopentate Dimeglumine (Gd-DTPA) for the assessment of myocardial viability in patients with chronic myocardial infarction (MI).

Methods: 15 patients with a history of MI were examined on two separate occasions with both agents (Gd-BOPTA, Multihance, Bracco S.p.A., Milan, Italy and Gd-DTPA Magnevist, Schering AG, Berlin, Germany) in randomised order. The minimum time between both examinations was 48 h.

Following the acquisition of cine MRI images to assess myocardial function, MRI was performed after the injection of contrast (0.2 mmol/kg). T₁ values of non-infarcted myocardium, infarcted myocardium and left ventricular cavity (LVC) were estimated based on steady state free precession images with incrementally increased inversion times acquired during a single breath-hold (Scheffler, 2001). This sequence was performed 1, 3, 5, 10 and 20 minutes after contrast injection. T₁-values were obtained using the following equation:

$$T1 = TI_{(min)} / \ln 2$$

where T₁(_{min}) is the inversion time of the image with the minimum signal intensity of the tissue.

15 min after injection of the contrast agent late enhancement MRI was performed using an segmented

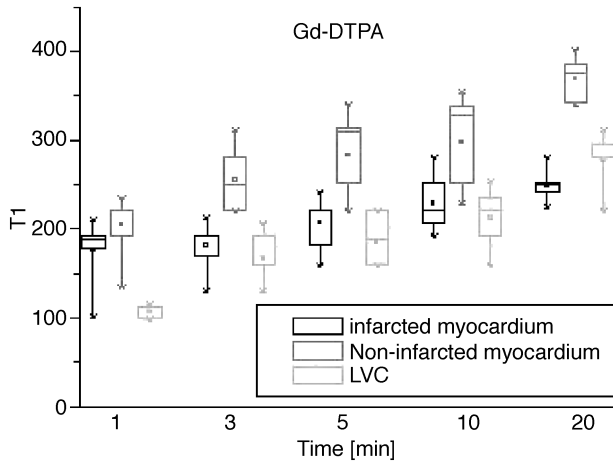


Figure 1. The course of T1 values over time in infarcted myocardium, non-infarcted myocardium and the LVC for Gd-DTPA and Gd-BOPTA. (View this art in color at www.dekker.com.)

inversion-recovery gradient-echo sequence (TR: 8 msec; TE: 4,3 msec; flip angle: 25°). Signal intensities and contrast-to-noise-ratios were measured in the non-infarcted myocardium, the infarcted myocardium and the LVC.

Results: Analysis of T1 values at all time points after contrast injection showed significant ($p < 0.05$) lower values for Gd-BOPTA data sets in the infarcted and non-infarcted myocardium compared to Gd-DTPA. The T1 values in the LVC were not significantly

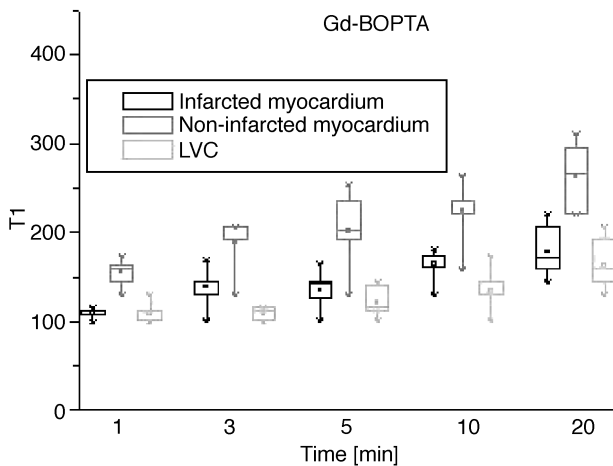


Figure 2. The course of T1 values over time in infarcted myocardium, non-infarcted myocardium and the LVC for Gd-DTPA and Gd-BOPTA. (View this art in color at www.dekker.com.)

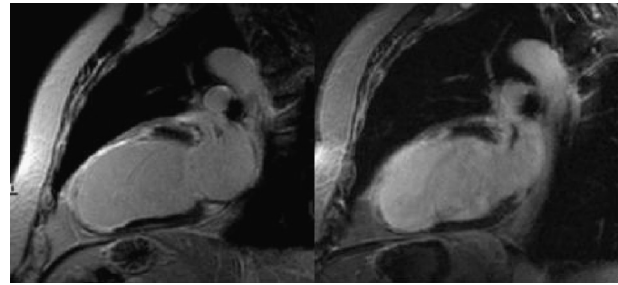


Figure 3. Contrast-enhanced MRI images in a patient after a large myocardial infarction in LAD territory using Gd-DTPA (left) and Gd-BOPTA (right).

different 1 min after contrast administration, however 3, 5, 10 and 20 min following injection they were significant ($p < 0.05$) lower for Gd-BOPTA (Figures 1 and 2).

Comparative analysis between measurements in the Gd-BOPTA data sets 15 minutes after injection and those obtained with Gd-DTPA demonstrated significantly higher SI in the infarcted myocardium and the LVC for Gd-BOPTA ($SI_{\text{infarct}} 58.6 \pm 10.9$ vs. 45.2 ± 13.3 , $p < 0.02$; $SI_{\text{LVC}} 69.8 \pm 18.5$ vs. 41.4 ± 9.0 , $p < 0.01$) whereas the SIs in the non-infarcted myocardium were not significantly different ($SI_{\text{noninfarct}} 12.7 \pm 7.2$ (Gd-BOPTA) vs. 9.3 ± 6.7 (Gd-DTPA)).

$CNR_{\text{infarct-noninfarct}}$ was significantly higher in the Gd-BOPTA data sets compared to Gd-DTPA (48.6 ± 14.2 vs. 34.5 ± 15.4 , $p < 0.04$), whereas $CNR_{\text{infarct-LVC}}$ was significantly higher in Gd-DTPA enhanced images (5.2 ± 8.5 vs. -10.9 ± 17.9 , $p < 0.02$; Figure 3).

Conclusion: 15 minutes after contrast injection CNR between infarcted and normal myocardium was higher in the Gd-BOPTA data sets, but Gd-DTPA permitted better differentiation between the infarcted myocardium and the LV cavity. This may help to detect subendocardial infarction, because 15 minutes after injection of Gd-BOPTA the LV cavity was still isointense or slightly hyperintense compared to the infarcted tissue. In order to distinguish between the infarcted tissue and the LVC, late-enhancement studies using Gd-BOPTA might benefit from a longer delay after contrast injection. However, to improve workflow in cardiac MRI a more rapid clearing contrast agent appears advantageous.

REFERENCE

Scheffler (2001). *Magn. Reson. Med.* Apr. 45:720–723.

317. Can CMR Reduce the Need for Invasive Coronary Angiography in Patients with New-Onset Congestive Heart Failure?

Szilard Voros, MD,¹ Brian J. Schietinger, MD,¹ Craig H. Meyer, PhD,² Frederick H. Epstein, PhD,³ Walter J. Rogers, PhD,³ Christina M. Bove, MD,¹ Jennifer K. Hunter, RN,¹ John M. Christopher, BA, RTRMR,³ Christopher M. Kramer, MD.¹ ¹Cardiology, University of Virginia, Charlottesville, VA, USA, ²Biomedical Engineering, University of Virginia, Charlottesville, VA, USA, ³Radiology, University of Virginia, Charlottesville, VA, USA.

Introduction: Many patients with new-onset CHF undergo invasive coronary angiography to exclude coronary artery disease (CAD) as the underlying cause. A non-invasive method to identify patients who do not require such invasive evaluation would be desirable.

Purpose: We hypothesized that a comprehensive CMR examination including imaging of LV size and function, scar, and coronary arteries could identify those patients requiring invasive assessment.

Methods: We studied 14 patients (9 men; mean age 49±15 years) with new-onset CHF with no history of CAD, MI, or evidence of acute ischemia, using a 1.5T clinical imaging system (Siemens Sonata 1.5T). Gd-DTPA (0.1 mM/kg) was infused iv prior to scanning. For volumetric and functional analysis, breath-hold steady-state free precession (SSFP) cine imaging was performed in 8–10 short axis slices, covering the heart from base to apex. For delayed enhancement scar imaging (DE), breath-held turboFLASH inversion recovery imaging was done in the same slices, 10–20 minutes after contrast (Simonetti et al., 2001). Inversion time was chosen to null normal myocardial signal. CMRA was done using a 3D, SSFP-based fat-suppressed breath-hold sequence (TE 1.5 ms, flip angle 65°, 92×256×16 matrix, FOV 197×350×37, 2.1×1.4×2.3 mm voxel size, trigger delay 350–450 ms). Presence or absence of CAD was defined clinically based on invasive coronary angiography (n=12) and/or radionuclide imaging. Volumetric data was compared between patient groups by unpaired t-test. Analysis of DE and CMRA was performed by investigators blinded to clinical data. Data are presented as mean±S.D.

Results: Overall, 4 of 14 patients (29%) had CAD. CMR imaging was complete in all 14, except for CMRA in one. Mean study duration was 54±12 minutes. Volumetric parameters did not differentiate between those with and without CAD (EDV: 211±20 mL vs. 187±78 mL; ESV 144±30 mL vs. 119±59



Figure 1.

mL; EF 32±10% vs. 36±12% and LV mass 198±38 grams vs. 206±96 grams, respectively, p=NS for all). DE was not present in 8 patients and none of these had CAD. Of the 6 patients with DE, all 6 had subendocardial DE in a coronary distribution and 4 of these patients had CAD (mean % DE: 4.39±1.9%). Of the 2 patients with DE but no obstructive CAD, one had an embolic infarct due to a hypercoagulable state and the other had myocarditis. The sensitivity and negative predictive value of DE were 100% and the specificity and positive predictive value 80% and 63.7%, respectively. In addition to subendocardial DE, 2 patients (1 with CAD and one without) had midwall DE (McCrohon et al., 2003) (see Figure 1 for example of patient with apical scar from CAD and midwall DE in the basal septum).

The proximal coronary arteries were well-visualized in most patients (quality on a 4-point scale and visualized length were 3.1±0.9 and 1.7±0.6 cm for the LMCA, 2.6±0.6 and 5.4±1.9 cm for the LAD, 2.2±0.9 and 4.3±2.0 cm for the LCx and 2.7±0.6 and 7.1±4.4 cm for the RCA). Of the 4 patients with CAD, CMRA identified the lesion in one; 2 had distal lesions in segments not visualized by CMRA and one lesion was not seen in a visualized segment.

Based on evidence of DE and/or CMRA-identified lesions, 6 patients would have required further invasive workup, sparing 8 (57%).

Conclusions: In this preliminary study, a comprehensive CMR examination was quite useful in excluding CAD in well over half of patients with new-onset CHF. The absence of DE or CAD on CMRA identifies patients who may not require referral for coronary angiography.

REFERENCES

McCrohon, J. A., et al. (2003). *Circulation* 108:54–59.
Simonetti, O. P., et al. (2001). *Radiology* 218:215–223.

318. Diagnostic Value of Adenosine Stress MRI in 92 Patients Compared to Tl-201-SPECT and Coronary Angiography for the Detection of Coronary Artery Disease and Myocardial Scar Tissue

Thorsten Dill,¹ Okan Ekinci,¹ Jochen Hansel,¹ Matthias Rau,¹ Alexander Kluge,² Georg F. Bachmann,² Christan W. Hamm.¹ ¹Cardiology, Kerckhoff-Heart Center, Bad Nauheim, Germany, ²Radiology, Kerckhoff-Heart Center, Bad Nauheim, Germany.

Introduction: Contrast enhanced magnetic resonance imaging of myocardial perfusion during adenosine infusion (stress MRI) is a new technique for detection of myocardial ischemia in CAD.

Purpose: In this study, the diagnostic value of this method for detecting hemodynamically relevant coronary artery stenoses was assessed and compared to 201-Tl-SPECT myocardial scintigraphy (SPECT) and x-ray coronary angiography findings.

Methods: 92 (9y, 64 male) with suspected CAD underwent \square consecutive patients (pts.) (63 adenosine stress MRI (Siemens Sonata, 1.5 T), SPECT and x-ray angiography on the following day.

MRI: After bolus injection of 0.1 mmol/kg bw Gd-DTPA (Magnevist, Schering), dynamic acquisition of 60 \times 3 short axis images was performed at rest and during

4 minutes of adenosine injection (140 μ g/kg bw). For detection of myocardial scar tissue (delayed enhancement) an inversion recovery TSE sequence was used. Myocardial segments on MRI and SPECT images were assigned to corresponding coronary arteries. Results were compared to invasive angiography findings.

Results: Angiography revealed relevant stenosis in 121 vessels of 71/92 pts. (77.2%). Hypoperfusion was detected during adenosine infusion in 58/92 pts. (63.0%) in stress MRI and 63/92 (68.5%) in SPECT. The sensitivity of stress MRI was 87.2% (SPECT: 84%), the specificity 97.1% (SPECT: 84%). Correlation analysis: stress MRI/angiography: $r=0.783$, $p<0.001$; SPECT/angiography: $r=0.532$, $p=0.001$; stress MRI/SPECT $r=0.491$, $p=0.002$. Myocardial scar tissue was detected by SPECT in 29/92 pts (31.5%) compared to 41/92 pts (44.6%) on MRI. 28/29 scar tissue findings in SPECT were reproducible by MRI but 12/41 scar tissue findings on MRI were missed by SPECT.

Conclusion: Adenosine stress MRI and SPECT scintigraphy show similar sensitivity. However, stress MRI has significantly higher specificity (97%) in comparison to SPECT (84%). There is better correlation between stress MRI results and angiography findings than between SPECT and angiography. Adenosine stress MRI has higher diagnostic value for detection of coronary artery stenoses than SPECT. The detection of myocardial scar tissue is superior to SPECT.

Request Permission or Order Reprints Instantly!

Interested in copying and sharing this article? In most cases, U.S. Copyright Law requires that you get permission from the article's rightsholder before using copyrighted content.

All information and materials found in this article, including but not limited to text, trademarks, patents, logos, graphics and images (the "Materials"), are the copyrighted works and other forms of intellectual property of Marcel Dekker, Inc., or its licensors. All rights not expressly granted are reserved.

Get permission to lawfully reproduce and distribute the Materials or order reprints quickly and painlessly. Simply click on the "Request Permission/Order Reprints" link below and follow the instructions. Visit the [U.S. Copyright Office](#) for information on Fair Use limitations of U.S. copyright law. Please refer to The Association of American Publishers' (AAP) website for guidelines on [Fair Use in the Classroom](#).

The Materials are for your personal use only and cannot be reformatted, reposted, resold or distributed by electronic means or otherwise without permission from Marcel Dekker, Inc. Marcel Dekker, Inc. grants you the limited right to display the Materials only on your personal computer or personal wireless device, and to copy and download single copies of such Materials provided that any copyright, trademark or other notice appearing on such Materials is also retained by, displayed, copied or downloaded as part of the Materials and is not removed or obscured, and provided you do not edit, modify, alter or enhance the Materials. Please refer to our [Website User Agreement](#) for more details.

[Request Permission/Order Reprints](#)

Reprints of this article can also be ordered at

<http://www.dekker.com/servlet/product/DOI/101081JCMR120028313>